SEVEN
EDITORA
2025

CONTEMPORARY ISSUES IN ENGINEERING AND ENVIRONMENTAL SCIENCES

LEONARDO BETEMPS KONTZ, JANDER LUIS FERNANDES MONKS,
BERNARDO DOS SANTOS VAZ, CARLOS EDUARDO SCHAEDLER,
DANIEL RICARDO ARSAND, GIANI MARIZA BRITZIUS BARWALD,
MARCELO PESKE HARTWIG, PABLO MACHADO MENDES,
RICARDO LEMOS SAINZ, RICARDO PERAÇA TORALLES

EDITORA CHEFE
Profº Me. Isabele de Souza Carvalho

EDITOR EXECUTIVO
Nathan Albano Valente

ORGANIZADORES DO LIVRO
Leonardo Betemps Kontz
Jander Luis Fernandes Monks
Bernardo dos Santos Vaz
Carlos Eduardo Schaedler
Daniel Ricardo Arsand
Giani Mariza Britzius Barwald
Marcelo Peske Hartwig
Pablo Machado Mendes
Ricardo Lemos Sainz
Ricardo Peraça Toralles

PRODUÇÃO EDITORIAL
Seven Publicações Ltda

EDIÇÃO DE ARTE
Evellyn Thais de Souza

EDIÇÃO DE TEXTO
Stephanie Caroline Meyer de Quadros

BIBLIOTECÁRIA
Bruna Heller

IMAGENS DE CAPA
Evellyn Thais de Souza

Todos os manuscritos foram previamente submetidos à avaliação cega pelos pares, membros do Conselho Editorial desta Editora, tendo sido aprovados para a publicação com base em critérios de neutralidade e imparcialidade acadêmica.

A Seven Publicações Ltda é comprometida em garantir a integridade editorial em todas as etapas do processo de publicação, evitando plágio, dados ou resultados fraudulentos e impedindo que interesses financeiros comprometam os padrões éticos da publicação.
Situações suspeitas de má conduta científica serão investigadas sob o mais alto padrão de rigor acadêmico e ético.

Dados Internacionais de Catalogação na Publicação (CIP)
(Câmara Brasileira do Livro, SP, Brasil)

C761

Contemporary Issues in Engineering and Environmental Sciences [recurso eletrônico] / Leonardo Betemps Kontz ... [et al.]. – São José dos Pinhais, PR: Editora Seven, 2025.
Dados eletrônicos (1 PDF).

ISBN 978-65-6109-329-3

1. Engenharia. 2. Sustentabilidade. 3. Tecnologia. I. Kontz, Leonardo Betemps. II. Monks, Jander Luis Fernandes. III. Vaz, Bernardo dos Santos. IV. Schaedler, Carlos Eduardo. V. Título.

CDU 62

Bruna Heller - Bibliotecária - CRB10/2348

Índices para catálogo sistemático:

1 Engenharia 62

DOI: 10.56238/livrosindi202579-001

Seven Publications Company
CNPJ: 43.789.355/0001-14
editora@sevenevents.com.br
São José dos Pinhais/PR

ORGANIZERS

Leonardo Betemps Kontz

Jander Luis Fernandes Monks

Bernardo dos Santos Vaz

Carlos Eduardo Schaedler

Daniel Ricardo Arsand

Giani Mariza Britzius Barwald

Marcelo Peske Hartwig

Pablo Machado Mendes

Ricardo Lemos Sainz

Ricardo Peraça Toralles

AUTHORS

Marcelo Peske Hartwig
PhD in Sciences from the Luiz de Queiroz College of Agriculture – University of São Paulo (USP) Full Professor at the Federal Institute of Education, Science and Technology Sul-Rio-grandense – Pelotas Campus, in the programs of Environmental Management Technology, Environmental Sanitation Technology, and the Master's Program in Environmental Engineering and Sciences.

Jéssica Etcheverria do Prado Hartwig
Bachelor's Degree in Environmental Management Technology from the Federal Institute of Education, Science and Technology Sul-Rio-grandense – Pelotas Campus (IFSUL). Master's Degree from the Graduate Program in Environmental Engineering and Sciences at the Federal Institute of Education, Science and Technology Sul-Rio-grandense – Pelotas Campus (IFSUL). Doctoral Candidate in the Graduate Program in Environmental Sciences at the Federal University of Pelotas (UFPel).

Silvana Pereira Rödel
Bachelor's Degree in Geography from the Federal University of Pelotas (UFPel) and Master's Degree in Environmental Engineering and Sciences from the Federal Institute of Education, Science and Technology Sul-Rio-grandense – Pelotas Campus.

Fábio Pereira dos Santos de Castro
Bachelor's Degree in Environmental Management Technology from the University Pitágoras / UNOPAR. Master's Degree from the Graduate Program in Environmental Engineering and Sciences at the Federal Institute of Education, Science and Technology Sul-Rio-grandense – Pelotas Campus (IFSUL).

Pedro José Sanches Filho
PhD in Analytical Chemistry
Retired Professor in the Master's Program in Environmental Engineering and Sciences at the Federal Institute of Education, Science and Technology Sul-Rio-grandense (IFSul).

Jander Luis Fernandes Monks
PhD in Agroindustrial Science and Technology
Professor in the Master's Program in Environmental Engineering and Sciences at the Federal Institute of Education, Science and Technology Sul-Rio-grandense (IFSul).

Mauricio Campesato Padilha
Bachelor's Student in Chemical Engineering at the Federal Institute of Education, Science and Technology Sul-Rio-grandense (IFSul).

Daniela Härter Hörnke
Master's Student in Environmental Engineering and Sciences in the Master's Program in Environmental Engineering and Sciences at the Federal Institute of Education, Science and Technology Sul-Rio-grandense (IFSul).

Carlos Eduardo Schaedler
PhD in Crop Protection
Professor in the Master's Program in Environmental Engineering and Sciences at the Federal Institute of Education, Science and Technology Sul-Rio-grandense (IFSul).

Ricardo Peraça Toralles
PhD in Agroindustrial Science and Technology
Professor in the Master's Program in Environmental Engineering and Sciences at the Federal Institute of Education, Science and Technology Sul-Rio-grandense(IFSul).

Daniel Ricardo Arsand
PhD in Chemistry
Professor in the Master's Program in Environmental Engineering and Sciences at the Federal Institute of Education, Science and Technology Sul-Rio-grandense(IFSul).

Susane Beatriz Seus
Master in Environmental Engineering and Sciences

Bernardo dos Santos Vaz
PhD in Animal Science
Professor in the Master's Program in Environmental Engineering and Sciences at the Federal Institute of Education, Science and Technology Sul-Rio-grandense(IFSul).

Suzana de Moura Pereira
Biologist, Master in Biology of Continental Aquatic Environments, Master in Environmental Engineering and Sciences, PhD in Ecology and Evolution of Biodiversity.

Aleccia Rodrigues Macedo
Master's Student in Environmental Engineering and Sciences in the Master's Program in Environmental Engineering and Sciences at the Federal Institute of Education, Science and Technology Sul-Rio-grandense(IFSul).

Gladimir da Silva
Master's Student in Environmental Engineering and Sciences in the Master's Program in Environmental Engineering and Sciences at the Federal Institute of Education, Science and Technology Sul-Rio-grandense(IFSul).

Pablo Machado Mendes
PhD in Food Science and Technology
Professor in the Master's Program in Environmental Engineering and Sciences at the Federal Institute of Education, Science and Technology Sul-Rio-grandense(IFSul).

Thábata Bierhals Hartwig
Master's Student in Environmental Engineering and Sciences in the Master's Program in Environmental Engineering and Sciences at the Federal Institute of Education, Science and Technology Sul-Rio-grandense(IFSul).

Daniela Harter Hornke
Master's Student in Environmental Engineering and Sciences in the Master's Program in Environmental Engineering and Sciences at the Federal Institute of Education, Science and Technology Sul-Rio-grandense(IFSul).

Gilberto Cardoso Xavier
Master's Student in Environmental Engineering and Sciences in the Master's Program in Environmental Engineering and Sciences at the Federal Institute of Education, Science and Technology Sul-Rio-grandense(IFSul).

João Pedro da Silva Viana
Bachelor's Student in Civil Engineering course at the School of Engineering of FURG - Federal University of Rio Grande Foundation.

Juliana da Fonseca Teixeira
Bachelor's Student in Business Civil Engineering at the School of Engineering of FURG - Federal University of Rio Grande.

Ingrid Telles Moraes
Bachelor's Student in Civil Engineering course at the School of Engineering of FURG - Federal University of Rio Grande Foundation.

Alessandra Buss Tessaro
Professor at the School of Engineering of FURG - Federal University of Rio Grande Foundation.

Ricardo Lemos Sainz
PhD. Doctorate in Agroindustrial Science and Technology.
Professor in the Master's Program in Environmental Engineering and Sciences at the Federal Institute of Education, Science and Technology of S Sul-Rio-grandense (IFSul).

Rubinei de Servi Ferraz
Master's Student in Environmental Engineering and Sciences in the Master's Program in Environmental Engineering and Sciences at the Federal Institute of Education, Science and Technology Sul-Rio-grandense(IFSul).

Giani Mariza Britzius Barwald
PhD in Agricultural Biotechnology
Professor in the Master's Program in Environmental Engineering and Sciences at the Federal Institute of Education, Science and Technology Sul-Rio-grandense (IFSul).

Leonardo Betemps Kontz
PhD in Production and Systems Engineering.
Professor in the Master's Program in Environmental Engineering and Sciences at the Federal Institute of Education, Science and Technology Sul-Rio-grandense(IFSul).

Edi Ramson Bergmann
Master's Student in Environmental Engineering and Sciences in the Master's Program in Environmental Engineering and Sciences at the Federal Institute of Education, Science and Technology Sul-Rio-grandense (IFSul).

PRESENTATION

The Graduate Program in Engineering and Environmental Sciences proudly launches its first book under the theme ***Contemporary Issues in Engineering and Environmental Sciences***, challenging readers, in each chapter, to reflect on the many possibilities for managing environments and transforming raw materials while promoting environmental sustainability.

We live in an era in which engineering and environmental sciences do not merely diagnose the impacts of human activity, but fundamentally contribute to safeguarding the survival and quality of life of future generations. This volume brings together a collection of studies that exemplify this mission, seamlessly navigating between technological innovation, resource management, and the rigorous monitoring of our ecosystems.

Within these pages, readers will encounter a multidisciplinary and practice-oriented approach to urgent contemporary challenges. The book invites us to rethink the concept of "waste," transforming environmental liabilities into valuable assets. It showcases ingenuity in the valorization of by-products, whether through the incorporation of glass powder to produce more sustainable concrete or through the conversion of biomass from invasive species, such as Annoni grass, into sources of reducing sugars for bioenergy production.

Responsibility throughout the life cycle of materials is also reflected in laboratory and industrial management practices. The authors present low-cost and highly efficient solutions, including the use of solar evaporation for the treatment of liquid chemical waste and the phytotoxicological assessment of soils impacted by fish waste disposal, ensuring that their return to the environment occurs in a safe and responsible manner.

Beyond remediation and reuse, this book delves into the complexity of environmental diagnostics. Chapters dedicated to the detection of micropollutants, such as bisphenol A in aquatic organisms, and to the analysis of soil contamination by heavy metals derived from wood preservation processes draw attention to silent risks that demand constant vigilance.

Finally, the volume does not overlook the macroscale of territorial and water resources management. In the context of climate change, the analysis of intense rainfall events for peak flow estimation becomes an indispensable tool for disaster prevention and the planning of resilient drainage systems.

Readers are therefore invited to explore these chapters not only as academic contributions, but as a compendium of solutions. May this reading inspire new ideas and strengthen the technical and ethical commitment required to build an environmentally balanced future.

Enjoy your reading.

PhD. Jander Luis Fernandes Monks
Coordinator of the Master's Program in Engineering and Environmental Sciences

PhD. Leonardo Betemps Kontz
Deputy Coordinator of the Master's Program in Engineering and Environmental Sciences

SUMMARY

PREFACE

The contemporary challenges faced by society demand integrated, scientifically grounded, and ethically responsible responses from engineering and environmental sciences. In this context, the Graduate Program in Engineering and Environmental Sciences of the Federal Institute of Education, Science and Technology Sul-Rio- grandense (IFSul) presents this volume as its first collective editorial endeavor, reflecting the maturity, diversity, and interdisciplinary strength of the research developed within the program.

This book brings together contributions from faculty members, graduate students, and collaborators whose work addresses critical issues related to environmental diagnostics, sustainable resource management, technological innovation, and the mitigation of anthropogenic impacts. The chapters illustrate how engineering tools and environmental sciences converge to propose solutions that are both technically robust and environmentally responsible, aligned with global sustainability agendas and regional realities.

A distinctive feature of this volume is its emphasis on methodological rigor combined with applied relevance. The chapters not only advance theoretical understanding but also offer reproducible methodologies, low-cost solutions, and innovative approaches suitable for real-world applications in urban, rural, industrial, and laboratory contexts. This balance reinforces the role of graduate education as a driving force for knowledge generation, technological advancement, and societal transformation.

By fostering dialogue between engineering disciplines and environmental sciences, this book underscores the importance of interdisciplinary collaboration in addressing complex environmental problems. It also reflects the institutional commitment of the Graduate Program to academic excellence, social responsibility, and the training of professionals capable of contributing meaningfully to sustainable futures.

We hope that this volume will serve not only as a scientific reference, but also as a source of inspiration for researchers, students, professionals, and policymakers. May the ideas and solutions presented here encourage critical reflection, innovation, and continued engagement in the pursuit of environmentally balanced and resilient societies.

Leonardo Betemps Kontz

Jander Luis Fernandes Monks

INTRODUCTION

Leonardo Betemps Kontz, Jander Luis Fernandes Monks

Contemporary society faces increasingly complex environmental challenges resulting from climate change, accelerated urbanization, intensification of productive systems, and the growing pressure on natural resources. In this context, engineering and environmental sciences play a strategic role that extends beyond environmental diagnosis, encompassing the design, evaluation, and implementation of technically sound and socially responsible solutions aimed at sustainable development.

Addressing such challenges requires integrated and interdisciplinary approaches, supported by methodological rigor and empirical evidence. Environmental problems such as hydrological extremes, waste generation and management, soil and water contamination, and the sustainable competitiveness of productive systems cannot be adequately understood or mitigated through isolated disciplinary perspectives. Instead, they demand the convergence of engineering principles, environmental sciences, analytical chemistry, geotechnologies, and strategic management frameworks.

This volume is situated within this interdisciplinary and applied perspective. Developed from research conducted within the Graduate Program in Engineering and Environmental Sciences at the Federal Institute of Education, Science and Technology Sul-Rio-grandense (IFSul), the book brings together contributions from faculty members, graduate students, and collaborators. Collectively, these studies reflect the scientific maturity of the program and its commitment to generating knowledge that is both academically robust and directly applicable to real-world environmental challenges.

OBJECTIVES OF THE VOLUME

The primary objective of this book is to present and critically discuss theoretical, methodological, and technological approaches to contemporary issues in engineering and environmental sciences. Specifically, the volume aims to:

Demonstrate the application of quantitative and qualitative methods for environmental diagnosis and engineering design;

Explore strategies for the valorization of residues and biomass within the framework of circular economy principles;

Assess analytical and experimental techniques for the characterization of complex environmental matrices;

Highlight the role of modeling, geotechnologies, and monitoring tools in environmental planning and decision-making processes;

Integrate technical and strategic perspectives related to sustainability, innovation, and the competitiveness of productive systems.

SCOPE AND METHODOLOGICAL APPROACHES

The scope of this book encompasses multiple analytical scales, ranging from laboratory-based studies to watershed and territorial assessments, and from material-level analyses to system-level evaluations. The methodological approaches adopted across the chapters include hydrological modeling, physicochemical and chromatographic analyses, experimental assays, ecotoxicological bioassays, geospatial analysis, and conceptual frameworks derived from management and strategic studies applied to environmental and agro-industrial systems.

This methodological diversity underscores the inherently interdisciplinary nature of contemporary environmental engineering and reinforces the importance of combining classical methods with emerging technologies to produce reliable, reproducible, and policy-relevant scientific knowledge.

STRUCTURE OF THE BOOK

The volume is organized into ten chapters, structured to guide the reader from environmental diagnosis to the development of technical and strategic solutions.

Chapter 1 addresses the analysis of intense rainfall events and the estimation of peak flows, emphasizing hydrological modeling as a fundamental tool for urban and rural planning and for the mitigation of flood risks under changing climatic conditions.

Chapter 2 examines the influence of sample preparation methods on the chromatographic characterization of pyroligneous liquid, comparing liquid–liquid extraction and lyophilization and highlighting the implications of methodological choices for analytical reliability.

Chapter 3 focuses on the valorization of biomass from invasive species, analyzing the production of reducing sugars from Annoni grass as a strategy for bioenergy generation and environmental management.

Chapter 4 investigates the environmental implications of wood preservation processes, with particular attention to chemically treated materials and the associated risks of soil and environmental contamination.

Chapter 5 is dedicated to the assessment of emerging micropollutants in aquatic ecosystems, reinforcing the importance of continuous environmental monitoring and risk evaluation.

Chapter 6 presents low-cost and efficient solutions for the treatment of liquid chemical waste, emphasizing solar evaporation as an appropriate technology for laboratory and institutional contexts.

Chapter 7 evaluates the phytotoxicity of soils affected by the disposal of fish-processing residues, employing bioassays as tools for environmental assessment and management.

Chapter 8 explores the incorporation of glass waste into cementitious materials, assessing its effects on mechanical performance and its potential to reduce environmental impacts in the construction sector.

Chapter 9 addresses the conversion of agro-industrial residues, specifically grape pomace, into biochar through pyrolysis, situating this approach within the broader context of bioenergy and circular economy strategies.

Finally, Chapter 10 expands the technical focus of the volume by examining sustainability-driven competitiveness in agro-food systems, with particular emphasis on olive oil production, integrating concepts of innovation, territorial identity, and strategic management.

SCIENTIFIC CONTRIBUTION AND RELEVANCE

By integrating empirical research, methodological innovation, and strategic analysis, this book contributes to advancing the field of engineering and environmental sciences. The chapters offer reproducible methodologies, empirically grounded results, and conceptual frameworks that may inform future research, professional practice, and public policy development.

This volume is intended to serve as a reference for researchers, graduate students, practitioners, and decision-makers seeking scientifically rigorous and practically applicable insights into contemporary environmental challenges. Ultimately, it aims to support the development of resilient, sustainable, and environmentally responsible systems across diverse contexts.

CHAPTER 1:
DESIGN PEAK FLOW BY INTENSE RAINFALL ANALYSIS

Marcelo Peske Hartwig, Jéssica Etcheverria do Prado Hartwig, Silvana Pereira Rödel

ABSTRACT

This chapter presents a detailed methodology for determining the maximum design flow, integrating traditional hydrological techniques with Geographic Information System (GIS) tools in a case study of the Arroio Moreira/Fragata sub-basin, in the city of Pelotas - RS. The study's rationale highlighted how surface modifications and urban imperviousness can alter hydrological functioning, correlating flow management. To address the lack of direct streamflow data, the methodology used rainfall data from the same hydrological region obtained via the HidroWeb platform (ANA). To fill gaps in the annual maximum daily precipitation series, the Regional Weighting Method was employed, with data consistency validated through the Double-Mass curve method. The statistical analysis of extreme events was conducted using the Gumbel Method, which allowed for the estimation of maximum rainfall associated with different return periods, while the Robaina and Peiter rainfall disaggregation technique was applied to convert daily precipitation into short-duration intensities, essential for plotting Intensity-Duration-Frequency (IDF) curves. The use of geotechnologies, such as Landsat 8 satellite imagery and SRTM altimetric data, was fundamental for delimiting the 171.941 km^2 drainage area and calculating critical physiographic parameters, such as the time of concentration (Tc ≈ 290 min) using the Kirpich Equation. Furthermore, land use and land cover mapping allowed for the determination of a weighted average runoff coefficient (C) of 0.272. By integrating these variables into the Rational Method, the study resulted in a maximum design flow of 179.23 m^3/s for a 5-year return period. The work concludes that this methodological integration offers precise technical support for the design of hydraulic structures and for resilient environmental planning against extreme events in small watersheds.

Keywords: Peak Discharge; Hydrology; Extreme Events.

1 INTRODUCTION

Superficial modifications to the natural characteristics of a watershed alter its hydrological functioning, with greater expression, in the expansion of the urban perimeter, which promotes surface impermeabilization, increased local temperature, increased evapotranspiration, reflecting in high rainfall indices that cause urban and rural floods, as a consequence of the excess and velocity of the surface runoff produced by the reduction of soil infiltration capacity.

The dimensioning of hydraulic structures in urban or agricultural areas for water use, capture systems, water reuse, or for systems of protection against extreme events is of great importance, because it integrates the watershed management system for the utilization and management of water resources, essential for the planning of conservation,

environmental preservation, and protection, but it primarily encounters barriers in how to calculate the design flow rate that will be adopted for the calculations of these systems due to the numerous variables existing in a natural and anthropized system.

Currently, alternatives are sought for the control of flood peaks by installing hydraulic structures for containment, storage, and distribution in watersheds, which meet the Sustainable Development Goals (SDGs). These goals are directly related to the calculation and management of peak flows and their applications. An example is SDG 6 (Clean Water and Sanitation), where flow dimensioning and management prevents contamination from floods, protects water resources, and improves water availability and quality.

These peak flow controls are also addressed by SDG 11, which aims for the pursuit of sustainable cities and communities where resilient drainage systems and pluvial infrastructures reduce urban risks, improve safety and quality of life. The calculation of peak flows can aid in the development of storage systems for controlling and mitigating these peaks, resulting in smoother discharges at the outlet section, preventing floods in urban and agricultural areas, and the stored but undischarged volume will serve as a reservoir for treated water supply.

A relationship can be established with SDG 13, which addresses action against global climate change, because it includes the analysis of flows and scenarios of rainfall intensification to adopt adaptation measures and protection planning against extreme events. The construction of storage reservoirs can help balance the region's temperature, since water is a natural temperature regulator. In these locations, a vegetal system of surface protection would be present that would work against erosion, control of regional temperatures, and accentuated runoff.

The increase in impermeabilization causes surface runoff to achieve high velocities and volume increases in very short time intervals. Flow peaks occur more frequently and at greater magnitudes in urban areas, in comparison with forest or rural areas. In addition, floods occur more frequently, making the watershed more sensitive to both moderate and weak precipitations (WATTS; HAEKE, 2003).

The study of maximum flow rates in watersheds facing intense rainfall is associated with SDG 15 (Life on Land), which protects terrestrial life by aiming to reduce floods and erosion with the purpose of protecting soil and terrestrial habitats through watershed management with nature-based solutions (wetlands, green corridors, permanent preservation areas (app), legal reserve) that promote ecological restoration (FAO, 2017).

One of the problems for the dimensioning of these structures, in all aspects previously addressed, is the obtaining of the data that will be used to reach the maximum design flow rate result. The most adequate process is the obtaining of the flow rate data measured directly in the river channel at measuring stations, since these represent all surface phenomena until resulting in surface runoff and flow rate, such as infiltration, accumulation, retention, evapotranspiration, and water velocity, from the most distant point of the watershed until it reaches the main channel and thus the watershed outlet section.

When we do not possess data from fluviometric stations, specifically at the outlet section of the studied watershed, statistical treatment techniques are used for the transformation of pluviometric data into flow rate.

The maximum flow rate can be estimated based on precipitation series obtained at pluviometric stations in the region under analysis, using methods that represent the main processes of transforming precipitation into flow rate, such as the Gumbel Method for determining the design rain and the Intensity-Duration-Frequency (IDF) curve, to estimate, as a function of the time of concentration (Tc), the rainfall intensity that will be applied in the equation, and subsequently applying the Rational Method, which encompasses all the processes involved at the moment the rain precipitates in the watershed into just one coefficient for calculating flow rates at the outlet section of a basin.

Rainfall precipitation, among the hydrological elements, is what most interferes with human life, since it is configured as the main input of water into the hydrological system, making other variables such as flow rate and infiltration strongly linked to its occurrence (SOUZA, 2013). In addition to these, evapotranspiration, surface runoff velocity, accumulation, retention, among others, can be associated. All these variants directly interfere with the flow rate result at the outlet section of a basin, which means that not all precipitation occurring in the watershed will reach the outlet section of the watershed.

Precipitation is the climatic variable with the greatest variability across diverse time scales. For this reason, the study of extreme events of annual maximum daily precipitation (Pdma) is related to severe damage to human activities in almost all regions of the world, due to its potential to cause soil water saturation, surface runoff, and erosion (TAMMETS and JAAGUS, 2013), as well as in rural and agricultural areas.

According to Bueno et al. (2019), watersheds are units that present essential aspects for conducting quantitative and qualitative studies of water, as well as the management of

water resources, as they comprise the entire natural catchment area for this resource originating from rain, providing surface runoff to the main channel.

The adoption of the watershed as a planning unit was done to assign a greater environmental basis for management, so that the political-administrative units become responsible for executing coordinated and integrated actions with a technical basis to defend common interests (SILVA, 2005).

From this perspective, in Brazil, the fundamental territorial unit for water resources management, established through the National Water Resources Policy – PNRH (BRASIL, 1997), are the watersheds.

According to Santana (2003), the size and limits of the watershed are important for determining water resource parameters such as annual total and flood potential, for evaluating how, when, and where to apply management measures for controlling water quality, quantity, or regime. The size of a watershed is an essential consideration in hydrological behavior, being one of the most difficult parameters to model.

Through the utilization of geotechnology tools (cartography, remote sensing, GPS, and Geographic Information Systems – GIS), it is possible to delimit and evaluate watershed divides obtained from elevation data, among the most utilized of which are those from the Shuttle Radar Topography Mission – SRTM (FARR et al., 2007). The use of automatic techniques allows for the efficient delimitation of basin divides with minimal operator interference (TORRES, 2007).

Geotechnologies are tools that can expedite and facilitate monitoring and management in watersheds, with updated and more precise information to determine the surface elements that interfere with the calculation of the maximum design flow rate, such as the determination of land use and cover, slope, soil map, water system, area, perimeter, among others, which allows inferring a series of data related to surface runoff and the runoff coefficient.

The utilization of satellite (LANDSAT) and altimetric (SRTM) images allows for the establishment of these relationships in a computational environment that can be constantly supplied, providing rapid responses, facilitating decision-making for adequate watershed management. This makes it possible to identify areas sensitive to flooding, erosion risk, contamination risks, identification of locations for urban/rural development, among other information that allows for seeking the protection and conservation of the natural environment and the reduction and control of sanitary and atmospheric emissions.

GIS allows the researcher to use a computerized database containing information from diverse sources. The information is spatially distributed, with each element having a geographic coordinate of natural characteristics, such as vegetation, hydrology, soil, climate, among others, and economic, political, and social aspects, presenting a thematic division into subsystems integrating a GIS. GIS also allows data crossing, by operating on a series of spatial operators (Boolean, algebraic, and geometric operations), making it possible to relate a certain phenomenon of reality with the selected spatial location (CAMPOS, et al., 2015; SOUSA; PAULA, 2019; PEREIRA; CABRAL, 2021).

GIS has become increasingly utilized in land use planning, as it is a tool with a high capacity for information storage as well as a great capacity for data manipulation. Its use has represented greater speed and effectiveness in micro-watershed regions, generating maps that assist in the study and planning of these areas (NARDINI, 2009).

The objective of this chapter is to present a methodology for determining the maximum design flow rate in all its calculation stages, starting from the acquisition and treatment of precipitation data using the Gumbel Method up to the result of the maximum flow rate using the Rational Method in a case study in the Moreira/Fragata watershed in the municipality of Pelotas – RS.

2 STUDY AREA

The present study was developed in the Moreira/Fragata Watershed, located in the southern region of the state of Rio Grande do Sul. The choice of the area is due to its importance for the urban and rural water system due to the high presence of flooded areas, considered a natural filter for surface water, drinking water supply, as well as the growing pressure of land use and occupation and the high susceptibility to extreme events in its lowest part, due to presenting a characteristic of flat and naturally flooded relief.

According to Santos et al (2020), the Moreira/Fragata Watershed is inserted into the large Coastal Hydrographic Basin of the RS state hydrographic system, more specifically in the Mirim – São Gonçalo Hydrographic Basin, it has an area of 171.941 km^2, and encompasses three municipalities: Pelotas, Capão do Leão, and Morro Redondo.

To characterize the space delimited by the Moreira/Fragata Watershed, a Landsat 8 satellite scene from 03/12/2025 with 30x30m resolution was used, obtained through Earth Explore, available in the United States Geological Survey-USGS system, along with spatial analysis tools (landscape ecology metrics) to illustrate the arrangement of the basin, which

comprises distinct environments, referenced through the geodetic reference system - WGS 84 UTM Zone 22S.

The delimitation of the study area was carried out using SRTM (Shuttle Radar Topography Mission) images from the year 2000, with altimetric information of the region. With pre-processing, the image was corrected and the pixel size was standardized, pixels without data were removed, negative values were corrected, pixels without data were filled, and spurious depressions were removed. With this information, the Digital Elevation Model (DEM) was obtained, and with this, the digital procedure for automatic watershed detection was performed, where the coordinate of the outlet section of the Arroio Moreira/Fragata is indicated and the system traces the water divide (watershed boundary).

The total area of the Moreira/Fragata sub-basin is 171.941 km^2. The slope used was calculated on average, by the ratio between the difference in altitude highest elevation of 286.00 meters and lowest elevation of 3.79 meters and the thalweg length of 26,809.44 meters.

The Arroio Moreira/Fragata, the main river, presents a geometric drop of 285 m, covering an extension of 37.9 km, flowing into the Lagoa do Fragata.

Figure 1. Location Map of the Moreira/Fragata Watershed.

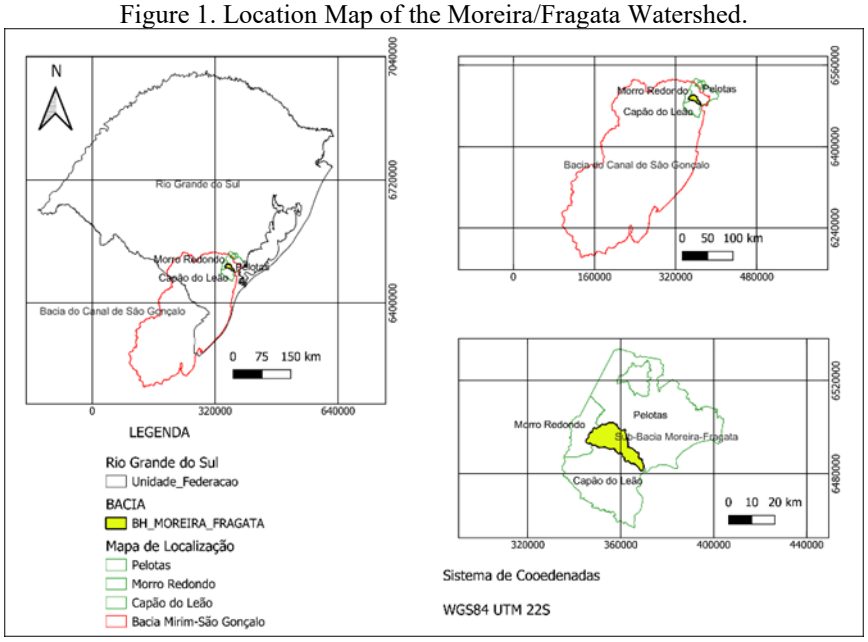

The classification of land use and land cover was performed based on Landsat 8 satellite images, through unsupervised classification. The defined classes were forest,

pasture, cultivation, exposed soil, urbanization, water, and wetland in vector form using the segmentation procedure. The classification was performed with the OTB (OrfeoToolbox Processing Provider) tool, using the “Segmentation” function and the “Meanshift” algorithm with processing in “Vector” mode (Figure 2). With the classified image, the areas occupied by each established use (Table 1) were calculated in order to calculate the runoff coefficient.

Figure 2. Land Use and Land Cover Map developed digitally.

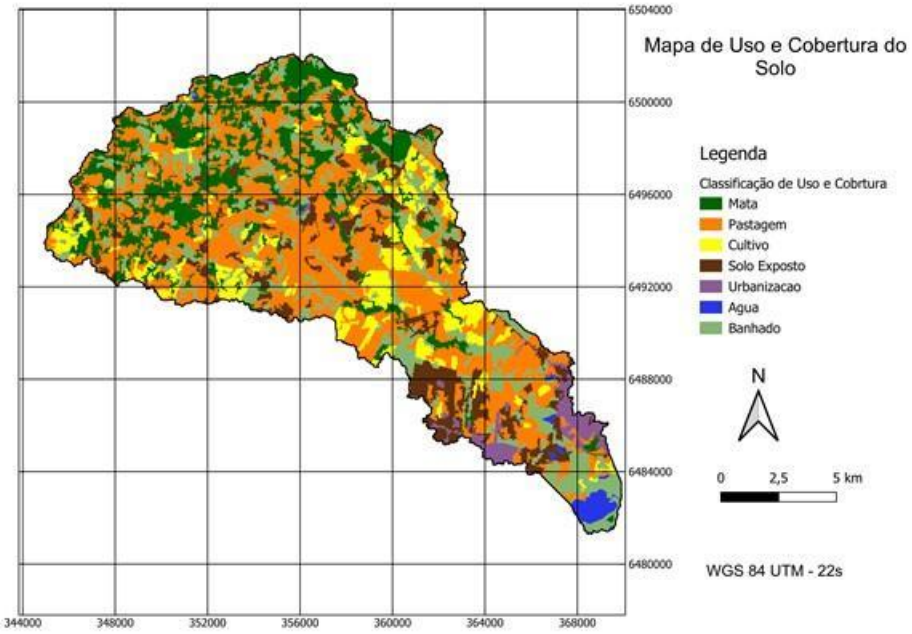

Table 1. Characterization of land use and land cover of the Moreira/Fragata Watershed.

Uso e Ocupação	Área (km²)	Percentual (%)
Mata	39,102	19,36
Pastagem	79,464	39,35
Cultivo	20,448	10,13
Solo Exposto	21,312	10,55
Urbanização	5,673	2,81
Água	2,355	1,17
Banhado	3,587	3,587

3 ACQUISITION OF PLUVIOMETRIC DATA AND GAP FILLING

Pluviometric precipitation is a random natural phenomenon, meaning it does not have a homogeneous distribution in space-time. Knowledge of this information becomes an important tool for various socio-environmental studies, such as urban planning and prevention against natural disasters. This information can be used provided that the pluviometric series have quality and density, and meet satisfactory statistical and geostatistical parameters (SALGUEIRO e MONTENEGRO, 2008). In addition to the mentioned characteristics, having complete and dense series also condition and facilitate watershed management in the search for resilient regions, improving water use and distribution, soil and water conservation, and the prevention of future events related to intense rainfall, among others.

The objective of a rainfall measurement station is to obtain a time series, without gaps, of precipitations over the years, or to study the variation of rain intensities throughout storms. In any case, there may be periods without information, voids, or gaps in the

observations, due to problems with the recording equipment and/or with the station operator, incorrect filling in the field notebook, wrong sum of the number of measuring cylinders when the precipitation is high, value estimated by the observer for not being at the sampling location, growth of vegetation or other obstruction near the observation post, equipment damage, mechanical problems in the graphic recorder, among others.

The acquisition of good quality rainfall data is quite difficult, so it is rare to find a reliable series of pluviometric or pluviographic data that possess complete series and consistency in their data. To analyze the consistency of the data, it is necessary to have a good knowledge of the acquisition methods, the equipment used, the installation sites, and also the personality of the observers.

The filling of gaps or voids are techniques that enable the construction of a new set of data by means of punctual sets of previously known data, thus allowing for. The inclusion of this filled pluviometric data must translate information as close as possible to reality, considering the great importance for the socio-environmental scope, for urban planning, natural disaster forecasting, energy generation, agriculture, tourist activities, and water resource management as a whole (BIER; FERRAZ, 2017; HUANG; WANG; XUE, 2015; MELLO; KOLHS; OLIVEIRA, 2017).

There are several approaches to filling gaps in pluviometric data series, each with its advantages and disadvantages, as highlighted by Vieira et al. (2018), which include the Regional Weighting, Linear Regression, Multiple Regression, and Potential Regression, as well as the use of Neural Networks and Geostatistical Techniques, such as Kriging. This chapter does not intend to exhaust the subject; in this sense, we will use only the Regional Weighting method.

It should be noted that the performed filling is not a new datum, but rather an estimate of the missing data (ARAÚJO et al, 2023). When filling faulty data in a historical series, Vieira et al. (2018) emphasize the importance of not altering the main characteristics, such as variability, seasonal movements, and correlations with data from other series, to which one wishes to associate them when inserting the estimates. Thus, when a gap is supplemented by means of estimates, the result may bring uncertainties. However, in the assessment using statistically treated data, in the case of gaps, the certainty of the analysis is enhanced.

For the acquisition of hydrological precipitation data in Brazil, the online platform HidroWeb is used, where data is analyzed free of charge by means of the Hidro software (SGH/ANA/2018), belonging to the National Water and Basic Sanitation Agency (ANA),

as presented in Figure 3, one of the pluviometric observation stations whose data was used to fill gaps in the Moreira/Fragata Watershed (Sub-basin).

The HidroWeb Portal is an integral tool of the National Water Resources Information System (SNIRH) and offers access to the database that contains all the information collected by the National Hydrometeorological Network (RHN), gathering data on river levels, flows, rainfall, climatology, water quality, and sediments. It is an important tool for society and public and private institutions, as the data collected by the hydrometeorological stations are essential for water resource management and various economic sectors, such as energy generation, irrigation, navigation, and industry, in addition to the design, maintenance, and operation of small and large hydraulic infrastructure, such as dams, urban pluvial drainage, and even culverts and roofs. The data available on the HidroWeb Portal refer to the conventional collection of hydrometeorological data, meaning daily records made by observers and measurements taken in the field by hydrology technicians and hydrologist engineers (AGÊNCIA NACIONAL DE ÁGUAS, 2025).

According to Araújo et al. (2023), based on the analyses of the three gap filling methods considered in their work and the validation through the Double Mass, it was found that Regional Weighting (PR) and Multiple Regression (RM) presented the best results. According to the same author, these approaches proved to be more adequate for filling gaps in precipitation data in the Southwest Planning Region of Mato Grosso. Their results reinforce the effectiveness of these techniques in overcoming the limitations of incomplete data and providing reliable estimates of pluviometric conditions in this specific region of the country.

Figure 3. Example of formatting and acquisition of pluviometric data in the HIDRO software (ANA).

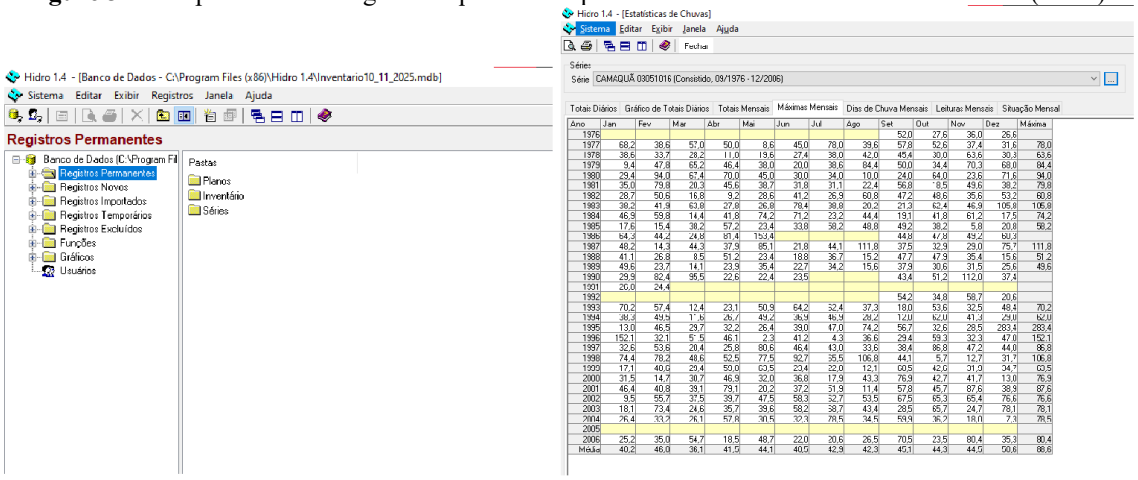

For the calculation of gap filling using the Regional Weighting Method (PR), three stations must be selected that have at least ten years of continuous data and are located within a maximum distance of 130 km from each other.

According to Tucci (2020), the selected stations must not only be close enough to estimate precipitation, but also located in climatological and geomorphological regions similar to the station to be filled. The Regional Weighting Method (PR) is commonly used to fill missing data in series of maximum daily precipitation on a monthly or annual basis.

For a station that presents gaps, these are filled using the following equation of the Regional Weighting Method:

$$Px = \frac{1}{3} \times \left(\frac{Mx}{Ma} \times Pa + \frac{Mx}{Mb} \times Pb + \frac{Mx}{Mc} \times Pc\right) \qquad \text{Eq 1}$$

Px = precipitation of the station with the gap to be filled (mm);

Mx = mean of the station with the gap (mm);

Ma, Mb, Mc = mean of the neighboring stations without gaps (mm);

Pa, Pb, Pc = precipitation of the neighboring stations corresponding to the same year of the gap (mm).

For the analysis in the sub-basin of Arroio Moreira/Fragata, data from four rainfall observation stations in a hydrologically similar region of the State of Rio Grande do Sul were used, with the 20 most recent years of annual maximum daily precipitation (Pdma) observations, in which the Cordeiro de Farias Station presented gaps.

Table 2 presents the compilation of precipitation data, where the gaps to be filled using the Regional Weighting Method are shown.

The development of the equation for the 1991 gap at the Cordeiro de Farias station is carried out using the values indicated in Table 2 as follows:

$$P_{1991} = \frac{1}{3} \times \left[\left(\frac{98{,}20}{90{,}00} \times 91{,}70\right) + \left(\frac{98{,}20}{89{,}43} \times 87{,}70\right) + \left(\frac{98{,}20}{88{,}25} \times 76{,}00\right)\right]$$

$$P_{1991} = 93{,}64mm$$

The results for the year 1991 are presented in Table 3. Subsequently, the procedure will be applied to all gaps in the Cordeiro de Farias station throughout the years. Once all gaps have been filled, the mean value for this station must be recalculated.

Table 2. Maximum daily data for each year with gaps at the Cordeiro de Farias station.

Anos	Estações (máximas diárias anuais)			
	Cordeiro de Farias	Pelotas	Camaquã	Rio Grande -Regatas
	03152016	03152014	03051016	03252024
1986	85,00	105,80	106,80	82,20
1987	88,20	105,40	111,80	118,00
1988	93,40	76,40	51,20	59,00
1989	74,20	52,80	49,60	50,00
1990	114,60	78,20	80,40	80,30
1991		91,70	87,70	76,00
1992		105,80	100,80	77,00
1993		80,00	70,20	118,00
1994	130,60	97,40	62,00	67,90
1995		91,40	183,40	121,50
1996		97,80	152,10	98,20
1997		92,90	86,80	80,30
1998	66,90	101,40	106,80	66,60
1999		99,80	63,50	67,30
2000		82,20	76,90	92,50
2001	105,10	66,60	87,60	60,20
2002	128,50	69,80	76,60	118,30
2003	83,70	125,60	78,10	103,80
2004		92,40	78,50	122,40
2005	110,00	83,80	86,80	118,00
2006		92,90	80,40	75,80
Médias	98,20	90,00	89,43	88,25

Table 3. Maximum daily data for each year with gaps filled at the Cordeiro de Farias station.

Anos	Estações (máximas diárias anuais)			
	Cordeiro de Farias	Pelotas	Camaquã	Rio Grande -Regatas
	03152016	03152014	03051016	03252024
1986	85,00	105,80	106,80	82,20
1987	88,20	105,40	111,80	118,00
1988	93,40	76,40	51,20	59,00
1989	74,20	52,80	49,60	50,00
1990	114,60	78,20	80,40	80,30
1991	**93,64**	91,70	87,70	76,00
1992	**103,93**	105,80	100,80	77,00
1993	**98,56**	80,00	70,20	118,00
1994	130,60	97,40	62,00	67,90
1995	**145,44**	91,40	183,40	121,50
1996	**127,66**	97,80	152,10	98,20
1997	**95,34**	92,90	86,80	80,30
1998	66,90	101,40	106,80	66,60
1999	**84,50**	99,80	63,50	67,30
2000	**92,35**	82,20	76,90	92,50
2001	105,10	66,60	87,60	60,20
2002	128,50	69,80	76,60	118,30
2003	83,70	125,60	78,10	103,80
2004	**107,74**	92,40	78,50	122,40
2005	110,00	83,80	86,80	118,00
2006	**91,33**	92,90	80,40	75,80
Médias	100,99	90,00	89,43	88,25

After completing the gap-filling process (Table 3) and calculating the mean of the station with missing data, the records must be verified through consistency analysis. This method is employed to assess the homogeneity of rainfall records, that is, to detect anomalies in the rain gauge station, which may be due to relocation, instrument conditions, or changes in the observation method.

The method consists of constructing a double cumulative curve, in which the accumulated annual maximum daily precipitations of the rain gauge station with filled gaps are related to the accumulated mean of the annual maximum daily precipitations of all stations in the region, including the one with gaps, considered homogeneous from a meteorological perspective. Consistency in the data series will be verified when a linear trend is observed between the intersection of these accumulated maxima, evaluated through the adjustment of the regression equation and the coefficient of determination (r^2).

Table 4 provides the accumulated values of the analyzed stations and the mean of these accumulations, which are used to construct the Double Cumulative curves, or the Double Mass Method, as presented in Figures 5, 6, 7, and 8.

Table 4. Accumulated values from the four rain gauge stations and the mean among the observation posts.

Anos	Estações (Acumulados)				Médias
	Cordeiro de Farias 03152016	Pelotas 03152014	Camaquã 03051016	Rio Grande -Regatas 03252024	
1986	85,00	105,80	106,80	82,20	94,95
1987	173,20	211,20	218,60	200,20	200,80
1988	266,60	287,60	269,80	259,20	270,80
1989	340,80	340,40	319,40	309,20	327,45
1990	455,40	418,60	399,80	389,50	415,83
1991	549,04	510,30	487,50	465,50	503,08
1992	652,97	616,10	588,30	542,50	599,97
1993	751,53	696,10	658,50	660,50	691,66
1994	882,13	793,50	720,50	728,40	781,13
1995	1027,56	884,90	903,90	849,90	916,57
1996	1155,23	982,70	1056,00	948,10	1035,51
1997	1250,57	1075,60	1142,80	1028,40	1124,34
1998	1317,47	1177,00	1249,60	1095,00	1209,77
1999	1401,97	1276,80	1313,10	1162,30	1288,54
2000	1494,32	1359,00	1390,00	1254,80	1374,53
2001	1599,42	1425,60	1477,60	1315,00	1454,41
2002	1727,92	1495,40	1554,20	1433,30	1552,71
2003	1811,62	1621,00	1632,30	1537,10	1650,51
2004	1919,36	1713,40	1710,80	1659,50	1750,76
2005	2029,36	1797,20	1797,60	1777,50	1850,41
2006	2120,69	1890,10	1878,00	1853,30	1935,52

It can be observed in Figures 4 to 7 that the adjustment of the double mass curves at all stations demonstrated consistency through the linear trend of the lines, with an r^2 value close to one (1.0), indicating an excellent fit.

Figure 4. Double cumulative curve of the Cordeiro de Farias station and the mean, indicating consistency through the linearity of the points.

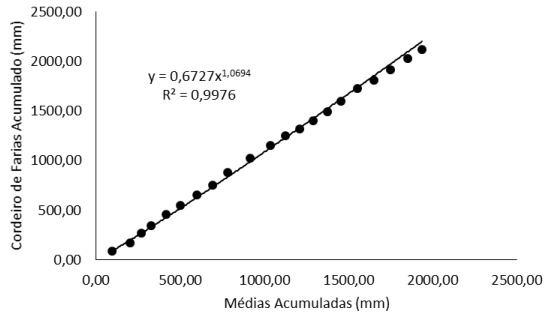

Figure 5. Double cumulative curve of the Pelotas station and the mean, indicating consistency through the linearity of the points.

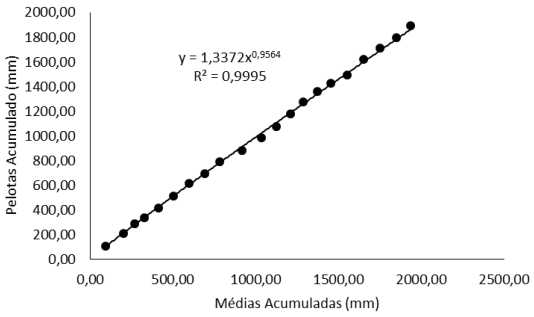

Figure 6. Double cumulative curve of the Camaquã station and the mean, indicating consistency through the linearity of the points.

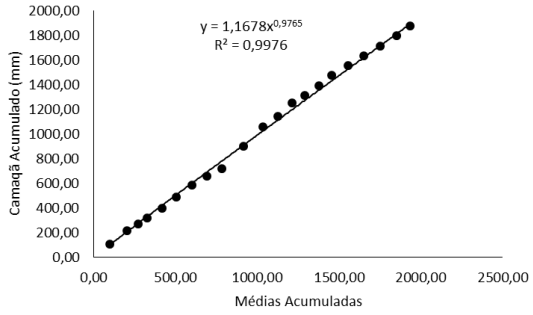

Figure 7. Double cumulative curve of the Rio Grande – Regatas station and the mean, indicating consistency through the linearity of the points.

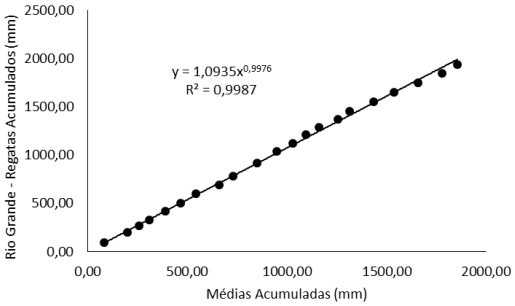

If the points do not align along a straight line, it indicates a lack of consistency, which must be corrected.

A change in slope is one of the occurrences that determines two or more lines. It represents a typical example of systematic errors, changes in observation conditions, or modifications in the physical environment, such as climatic variations.

To consider the existence of a change in slope, it is common practice to require the occurrence of at least five successive points aligned according to the new trend.

The change in slope in the double mass analysis line is the only error that can be corrected. Figure 8 illustrates the change in slope in a double mass analysis and its identifiers for applying the correction of this slope.

Figure 8. Variables of the slope adjustment equation for the desired trend line.

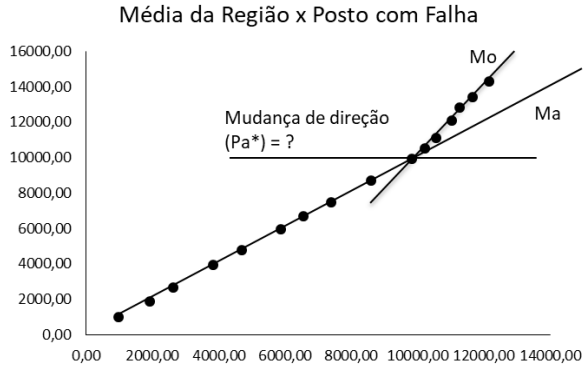

Since the gap-filling in the sub-basin of Arroio Moreira/Fragata at the Ponte Cordeiro de Farias station resulted in a linear trend, it was not necessary to apply the correction equation for changes in slope. If the application of the equation had been required, it is demonstrated below:

$$Pc = Pa + \left[\left(\frac{Ma}{Mo}\right) \times (Pa - Pa^{*})\right] \qquad \text{Eq 2}$$

Pc = Value of the point to be corrected (mm);

Ma = Slope coefficient of the desired trend;

Mo = Slope coefficient of the trend to be corrected;

Pa = Accumulated value to be corrected (mm);

Pa = Value of the coordinate corresponding to the intersection of the two trends (mm).

The slope coefficient of the line is obtained from the exponent of the variable "X" in a power equation when adding the trend line to the double mass curve.

When the new trend of the line is calculated, the value of Pa* must be repeated in the column of the new results.

Since no inconsistency was identified in the double mass analysis after the gap-filling process, the next step is to apply the Gumbel analysis to calculate the recurrence interval of the annual maximum daily series.

4 CALCULATION OF RECURRENCE INTERVALS USING THE GUMBEL METHOD

The Gumbel method plays a crucial role in the transformation of rainfall data into design flows, as it allows the estimation of extreme rainfall events associated with different return periods, being essential for the safe sizing of hydraulic structures in river basins. The Gumbel Method is a statistical frequency analysis technique that belongs to Extreme Value Theory, and it is used to estimate the probable maximum rainfall associated with a given return period (Tr). This method also enables the calculation and plotting of the intensity–duration–frequency (IDF) curve for heavy rainfall events.

The Gumbel method has the advantages of requiring few parameters, ease of calculation, appropriate application in hydrology, and acceptance by technical standards, governmental manuals, and classical literature.

The Gumbel method is based on the principle that the largest annual rainfall (or another annual extreme value) can be treated as a random variable that follows a probability distribution, allowing the estimation of future extreme events based on historical data. In the case of rainfall data, the highest daily precipitation of each year (Pdma) is used to obtain probabilities associated with different return periods.

The principle of the method lies in obtaining a fault-free series of pluviometric data consisting of the maximum daily precipitation of each year over a minimum of 10 years of observations, calculating the mean and standard deviation of the series, fitting this series to a Gumbel distribution—which mathematically describes the behavior of extreme events—and using this distribution to estimate the rainfall value corresponding to any desired return period (Tr).

The adjustment of the Gumbel distribution is carried out through equations for calculating a reduced variable (b) for each year observed, as well as the calculation of the return period (Tr) as a function of the reduced variable for each year. Additionally, by

means of tabulation, a reduced variable (Yn) and a standard deviation (σn) are obtained as functions of the number of observations (n), which are then used in the calculation of the reduced variable (b).

$$b = \frac{\sigma_n}{\sigma_x} \times \left[x - \left(\underline{x} - \sigma_x \times \frac{y_n}{\sigma_n}\right)\right] \qquad \text{Eq 3}$$

b = Reduced variable of the Gumbel distribution for calculating the return period (Tr);

σn = Standard deviation as a function of the number of observations (tabulated);

σx = Standard deviation of the series of maximum daily data for each year;

x = Observation of the maximum annual daily rainfall;

$\overline{x}$= Mean of the maximum rainfall values in the data series;

yn = Reduced variable as a function of the number of observations (tabulated).

Table 5. Reduced variable (yn) and standard deviation (σn) as a function of the number of observations (Gumbel, 1958).

n	yn	σn	n	yn	σn	n	yn	σn
8	0,4843	0,9043	35	0,5403	1,1285	64	0,5533	1,1793
9	0,4902	0,9288	36	0,541	1.1313	66	0,5538	1,1814
10	0,4952	0,9497	37	0,5418	1,1339	68	0,5543	1,1834
11	0,4996	0,9676	38	0,5424	1,1363	70	0,5548	1,1854
12	0,5035	0,9833	39	0,5430	1,1388	72	0,5552	1,1873
13	0,507	0,9972	40	0,5436	1,1413	74	0,5557	1,1890
14	0,51	1,0095	41	0,5442	1,1436	76	0,5561	1,1906
15	0,5128	1,0206	42	0,5448	1,1458	78	0,5565	1,1923
16	0,5157	1,0316	43	0,5453	1,148	80	0,5569	1,1938
17	0,5181	1,0411	44	0,5458	1,1499	82	0,5572	1,1953
18	0,5202	1,0493	45	0,5463	1,1519	84	0,5576	1,1967
19	0,522	1,0566	46	0,5468	1,1538	86	0,558	1,198
20	0,5236	1,0628	47	0,5473	1,1557	88	0,5583	1,1994
21	0,5252	1,0696	48	0,5477	1,1574	90	0,5586	1,2007
22	0,5268	1,0754	49	0,5481	1,159	92	0,5589	1,2020
23	0,5283	1,0811	50	0,5485	1,1607	94	0,5592	1,2032
24	0,5296	1,0864	51	0,5489	1,1623	96	0,5595	1,2044
25	0,5309	1,0915	52	0,5493	1,1638	98	0,5598	1,2055
26	0,5320	1,0961	53	0,5497	1,1653	100	0,5600	1,2065
27	0,5332	1,1004	54	0,5501	1,1667	150	0,5646	1,2253
28	0,5343	1,1047	55	0,5504	1,1681	200	0,5672	1,236
29	0,5353	1,1086	56	0,5508	1,1696	250	0,5688	1,2429
30	0,5362	1,1124	57	0,5511	1,1708	300	0,5699	1,2479
31	0,5371	1,1159	58	0,5515	1,1721	400	0,5714	1,2545
32	0,538	1,1193	59	0,5518	1,1734	500	0,5724	1,2588
33	0,5388	1,1226	60	0,5521	1,1747	750	0,5738	1,2651
34	0,5396	1,1255	62	0,5527	1,1770	1000	0,5745	1,2685

After calculating the reduced variable, the recurrence period is determined according to the following equation:

$$Tr = \frac{1}{1 - e^{-e^{-b}}} \qquad \text{Eq 4}$$

Tr = Return period (years);

b = Reduced variable.

Using the results from Table 3, we will calculate the return period (Tr) based on the averages of the annual maximum daily precipitation from the four observed stations. To do so, we must follow the procedures of probability analysis by ordering the averages in descending order, assigning a rank number to each, and only then calculating the reduced variable (b) and, finally, the return period (Tr). A total of 21 average precipitation observations and standard deviations were analyzed, with the parameters yn and σn extracted from Table 5. The calculations are presented in Tables 6 and 7.

Table 6. Annual daily maximums (mm) at the four observation stations.

Anos	Estações (máximas diárias anuais)				Médias
	Cordeiro de Farias 03152016	Pelotas 03152014	Camaquã 03051016	Rio Grande - Regatas 03252024	
1986	85,00	105,80	106,80	82,20	**94,95**
1987	88,20	105,40	111,80	118,00	**105,85**
1988	93,40	76,40	51,20	59,00	**70,00**
1989	74,20	52,80	49,60	50,00	**56,65**
1990	114,60	78,20	80,40	80,30	**88,38**
1991	**93,64**	91,70	87,70	76,00	**87,26**
1992	**103,93**	105,80	100,80	77,00	**96,88**
1993	**98,56**	80,00	70,20	118,00	**91,69**
1994	130,60	97,40	62,00	67,90	**89,48**
1995	**145,44**	91,40	183,40	121,50	**135,43**
1996	**127,66**	97,80	152,10	98,20	**118,94**
1997	**95,34**	92,90	86,80	80,30	**88,84**
1998	66,90	101,40	106,80	66,60	**85,43**
1999	**84,50**	99,80	63,50	67,30	**78,78**
2000	**92,35**	82,20	76,90	92,50	**85,99**
2001	105,10	66,60	87,60	60,20	**79,88**
2002	128,50	69,80	76,60	118,30	**98,30**
2003	83,70	125,60	78,10	103,80	**97,80**
2004	**107,74**	92,40	78,50	122,40	**100,26**
2005	110,00	83,80	86,80	118,00	**99,65**
2006	**91,33**	92,90	80,40	75,80	**85,11**
Médias	100,99	90,00	89,43	88,25	

Table 7. Calculation of recurrence periods (Tr) for each daily maximum in each observed year.

Anos	Médias (mm)	Ordem	Ordenados	b	Tr (anos)
1986	94,95	1	135,43	3,3562	29,18
1987	105,85	2	118,94	2,2764	10,25
1988	70,00	3	105,85	1,4194	4,65
1989	56,65	4	100,26	1,0533	3,40
1990	88,38	5	99,65	1,0135	3,29
1991	87,26	6	98,30	0,9251	3,06
1992	96,88	7	97,80	0,8923	2,97
1993	91,69	8	96,88	0,8323	2,83
1994	89,48	9	94,95	0,7058	2,57
1995	135,43	10	91,69	0,4923	2,19
1996	118,94	11	89,48	0,3473	1,97
1997	88,84	12	88,84	0,3054	1,92
1998	85,43	13	88,38	0,2753	1,88
1999	78,78	14	87,26	0,2023	1,79
2000	85,99	15	85,99	0,1190	1,70
2001	79,88	16	85,43	0,0822	1,66
2002	98,30	17	85,11	0,0614	1,64
2003	97,80	18	79,88	-0,2812	1,36
2004	100,26	19	78,78	-0,3532	1,32
2005	99,65	20	70,00	-0,9277	1,09
2006	85,11	21	56,65	-1,8017	1,00
Média =	92,17				
n =	21				
σn =	1,0628				
σx =	16,2337				
yn =	0,5236				

By numerically equating b and Tr, as an example, in the first and second rows we will have:

$$b = \frac{1{,}0628}{16{,}2337} \times \left[\left(135{,}43 - \left(92{,}17 - \left(16{,}2337 \times \frac{0{,}5236}{1{,}0628}\right)\right)\right)\right] = 3{,}3562$$

$$b = \frac{1{,}0628}{16{,}2337} \times \left[\left(118{,}94 - \left(92{,}17 - \left(16{,}2337 \times \frac{0{,}5236}{1{,}0628}\right)\right)\right)\right] = 2{,}2764$$

⋮

$$Tr = \frac{1}{\left(1 - e^{-e^{-3{,}3562}}\right)} = 29{,}18\ anos$$

$$Tr = \frac{1}{\left(1 - e^{-e^{-2,2764}}\right)} = 10,25\ anos$$

⋮

After the calculations, a logarithmic line is plotted between the ordered values of annual maximum daily mean precipitation and the return periods (Tr), along with the generated logarithmic equation and the coefficient of determination (r^2) (Figure 9). Since the calculated return periods are relative to the sample period and dependent on the reduced variable b, they do not result in integer values. As the design of hydraulic structures or protection systems against extreme events requires predetermined integer Tr values, the logarithmic equation generated by the line is used to determine precipitation values for Tr of 2, 5, 10, 25, 50, and 100 years.

Figure 9. Linearization of one-day maximum precipitation using the Gumbel method.

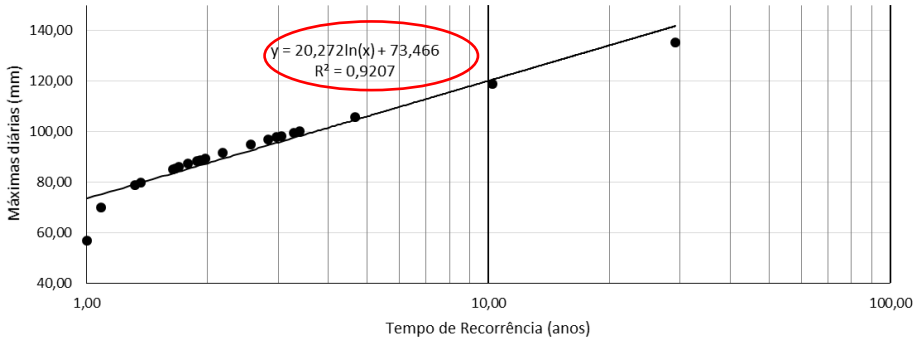

For a return period (Tr) of 2 years, we obtain the following annual maximum daily precipitation:

$$Y = 20,272 \cdot Ln(2) + 73,466 = 87,52\ mm$$

The Pdma values for the other return periods (Tr) are presented in Table 9.

Precipitation values are observed over a single day, even after being adjusted using the Gumbel method. This means that the collection of rainfall data is not carried out at exact 24-hour intervals, making it necessary to apply corrections for 24-hour rainfall and subsequently for shorter time intervals. This procedure is referred to as the rainfall disaggregation function.

Rain gauge stations generally do not measure rainfall over short durations. In most Brazilian municipalities, the data available from these stations consist of daily rainfall, annual maximum rainfall, and sometimes monthly rainfall. However, the main methods for

calculating design discharge require short-duration rainfall intensity, for example 1 hour, 30 minutes, 20 minutes, or 10 minutes, depending on the type of project.

Disaggregation allows the estimation of IDF (Intensity–Duration–Frequency) curves, which are fundamental in hydrology and are used in urban drainage, culvert design, dams, channeling, and flood control. Without disaggregation, it would not be possible to construct these curves in most localities.

The analytical form of the disaggregation technique is found in the work of Robaina and Peiter (1992), whose objective was to test the performance of a rainfall disaggregation model, aimed at generating mean daily maximum precipitation for durations shorter than 24 hours.

The disaggregation function of Robaina and Peiter (1992) was developed when the authors tested the performance of a model designed to estimate intense rainfall with durations shorter than 24 hours in the State of Rio Grande do Sul, using rainfall data collected by rain gauges. The function was conceived based on the assumption that there should exist a mathematical expression defining the relationship between the annual maximum precipitation for any given duration and the annual precipitation for the 24-hour period.

$$f(t) = 0{,}00008 \times t + 0{,}14 \times ln(1 + 0{,}33 \times t) \qquad \text{Eq. 5}$$

Where the duration time (t) must be expressed in minutes (min).

The disaggregation function allows the calculation of a transformation coefficient for precipitation values over the desired time intervals, by simply inserting the time in minutes into the variable t of the equation.

Table 8. Conversion values using the disaggregation function at different durations.

Durações (h)	Durações (min)	Coeficiente de conversão
0,25 h	15	0,2509
0,5 h	30	0,3368
1 h	60	0,4297
2h	120	0,5281
6 h	360	0,6988
8 h	480	0,7484
10 h	600	0,7891
12 h	720	0,8241
24 h	1440	0,9784

Table 9. Calculation of precipitation for the determined return periods (Tr) and disaggregation of one-day rainfall.

Durações (h)	Durações (min)	Coeficiente de conversão	Tempos de recorrência (Tr) determinados						
			2	5	10	25	50	100	500
			Precipiatções calculadas pela equação de reta com os Tr determinados ( )						
			87,52	106,09	120,14	138,72	152,77	166,82	199,45
0,25 h	15	0,2509	21,96	26,62	30,14	34,80	38,33	41,85	50,04
0,5 h	30	0,3368	29,48	35,73	40,47	46,72	51,46	56,19	67,18
1 h	60	0,4297	37,61	45,59	51,63	59,61	65,64	71,68	85,70
2h	120	0,5281	46,22	56,03	63,45	73,26	80,68	88,10	105,33
6 h	360	0,6988	61,16	74,14	83,96	96,94	106,76	116,58	139,38
8 h	480	0,7484	65,50	79,40	89,92	103,82	114,33	124,85	149,27
10 h	600	0,7891	69,06	83,71	94,80	109,46	120,55	131,63	157,38
12 h	720	0,8241	72,12	87,43	99,01	114,31	125,89	137,47	164,36
24 h	1440	0,9784	85,63	103,80	117,55	135,73	149,47	163,22	195,14

Using the logarithmic equation generated from the Gumbel distribution, the maximum daily precipitation is calculated for each estimated return period (Tr). With this precipitation value, the disaggregation coefficient is applied to the stipulated time intervals, as shown in Table 9, thereby creating a sequence of duration intervals and their respective rainfall values.

Calculation of the one-day maximum rainfall with return periods (Tr) of 2 and 5 years and its position in Table 9:

$$Y = 20{,}272 * LN(2) + 73{,}466 = 87{,}52mm$$

$$Y = 20{,}272 * LN(5) + 73{,}466 = 106{,}09mm$$

⋮

Calculation of the disaggregation of the one-day maximum rainfall for durations of 24 hours and 12 hours, computed using the disaggregation function and indicated in Table 9:

$$P_{24h;2anos} = 87{,}52 \times 0{,}9784 = 85{,}63mm$$

$$P_{12h;2anos} = 87{,}52 \times 0{,}8241 = 72{,}12mm$$

⋮

The calculations were carried out until Table 9 was completed, so that it becomes possible to calculate precipitation intensity and subsequently plot the IDF curves.

5 CALCULATION OF INTENSITY–DURATION–FREQUENCY (IDF) CURVES

The characterization of intense precipitation, whether in liquid or solid form, is always conditioned by hydrological factors such as **Duration**, corresponding to the time considered for the rainfall event which, in the case of river floods, may be on the order of

hours or days, and in the case of hydraulic structures, hours or minutes **Intensity**, which corresponds to the ratio between the precipitation depth and its duration, and **Frequency**, generally expressed as an occurrence within a given number of years.

Precipitation intensity is given by the ratio between the volume or maximum depth of rainfall and the time over which it occurred. Precipitation intensity has an inverse relationship between the amount of rainfall in an event and the duration of that precipitation within the same event.

$$i = \frac{P}{t} \qquad \text{Eq 6}$$

i = precipitation intensity (mm/h or mm/min);

P = maximum precipitation observed (mm);

t = duration of occurrence (h or min).

The intensity will be greater when a high volume of rainfall occurs within a short time interval. Short durations are considered to be those between 10 and 30 minutes, during which the maximum precipitation peak is reached quickly, and, in a watershed, there is no time for infiltration, resulting in the entire precipitated volume being converted into surface runoff.

The IDF curve is the mathematical relationship between a probable maximum precipitation event that may occur within a given time interval, during a statistical period of occurrence. It allows the estimation of maximum rainfall intensity for different durations and return periods, based on historical series.

The IDF curve expresses the magnitude (mm/h or mm/min) of extreme precipitation for different time scales and probability levels. This magnitude allows the identification of whether a precipitation event has the potential to cause disturbances in a region or watershed.

To obtain the flood volume or the maximum design discharge, it is necessary, after determining the physiographic characteristics of the basin, to establish the precipitation intensity for a given duration. This is carried out through the disaggregation of the maximum one-day rainfall events recorded during the year and their frequency of occurrence, defined by the return periods (Tr) under analysis, as well as their temporal distribution, obtained from data collected at different stations within the same hydrological region.

The calculation of rainfall intensities is performed using Table 9, based on the ratio between precipitation adjusted by the correction factors obtained from rainfall

disaggregation (Table 8). With these results, the Intensity–Duration–Frequency curves are plotted.

Table 10. Calculation of rainfall intensities for durations shorter than 24 hours.

Durações (min)	Intensidades e tempos de recorrência (Tr)						
	2	5	10	25	50	100	500
15	1,46	1,77	2,01	2,32	2,56	2,56	3,34
30	0,98	1,19	1,35	1,56	1,72	1,72	2,24
60	0,63	0,76	0,86	0,99	1,09	1,09	1,43
120	0,39	0,47	0,53	0,61	0,67	0,67	0,88
360	0,17	0,21	0,23	0,27	0,30	0,30	0,39
480	0,14	0,17	0,19	0,22	0,24	0,24	0,31
600	0,12	0,14	0,16	0,18	0,20	0,20	0,26
720	0,10	0,12	0,14	0,16	0,17	0,17	0,23
1440	0,06	0,07	0,08	0,09	0,10	0,10	0,14

As an example, four precipitation intensity curves (mm/min) indicated in Table 9 were plotted, corresponding to the sub-basin of Arroio Moreira/Fragata, using the same durations applied in the disaggregation of the one-day maximum rainfall into intervals shorter than 24 hours (Figures 10, 11, 12, and 13). On the X-axis, the durations (min) are presented, and on the Y-axis, the intensities (mm/min), with a power-type trend line.

Figure 10. IDF for a 2-year return period

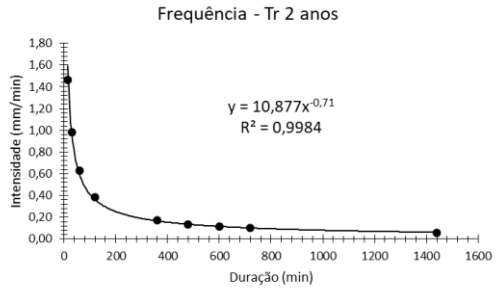

Figure 11. IDF for a 5-year return period.

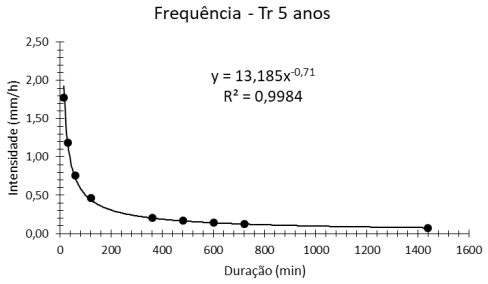

Figure 12. IDF for a 10-year return period.

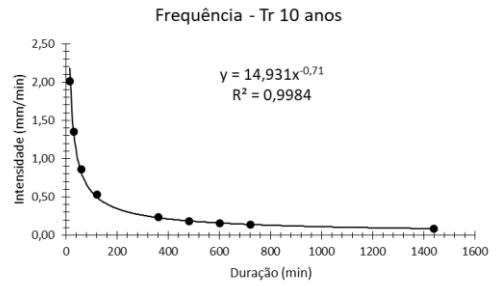

Figure 13. IDF for a 50-year return period.

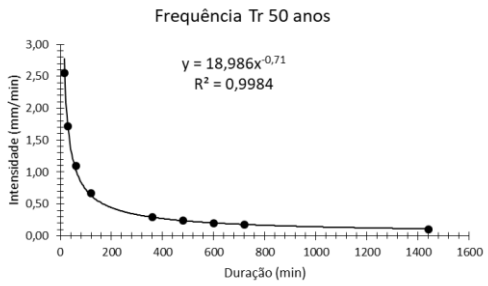

For the use of IDF curves in hydraulic structure design, a return period is chosen that is appropriate for the type of structure to be constructed. For simpler urban structures such as culverts, storm sewers, gutters, and others intended to contain extreme events, it is

common to adopt return periods between 5 and 10 years, which, in the case of IDF curves, are represented by frequency.

Another criterion is associated with the size of the study basin, which must be such that, at the time of precipitation, rainfall occurs uniformly across the entire basin area. In this way, the rainfall duration is considered equal to the basin's concentration time.

CONCENTRATION TIME (TC)

The time of concentration (Tc) of a watershed is the time required for the rainfall at the most distant point of the basin to reach its outlet. In other words, it is the elapsed time after the onset of precipitation during which the entire basin is simultaneously contributing to the discharge at the outlet section.

The calculation of Tc is fundamental in a hydraulic project, as it defines the critical rainfall duration for the estimation of floods caused by extreme events.

For the calculation of the time of concentration (Tc), there are several equations, all of which meet the intended purpose. In this case, the Kirpich Equation will be used.

$$Tc = 57 \times \left(\frac{L^3}{H}\right)^{0,385} \qquad \text{Eq 7}$$

Tc = time of concentration (min);

L = length of the main channel (km);

H = elevation difference between the most distant point and the outlet (m).

For the calculation of the time of concentration (Tc), it is necessary to obtain the length or extent of the thalweg (L) and the elevation difference between the most distant point and the outlet. Geoprocessing is a tool that enables the determination of the physiographic characteristics of a basin, as well as other coefficients that will be used in the calculation of the maximum design discharge by the Rational Method.

Geoscience plays an essential role in this context by improving the determination of method parameters such as land use and occupation data, slope, thalweg length, soil maps, among others, which make the estimation of the runoff coefficient more accurate. Digital terrain models (DTM) enhance the calculation of the time of concentration, and remote sensing techniques increase the reliability of precipitation and landscape change analyses (SILVA; TUCCI; MENDES, 2020).

For the calculation of the time of concentration in the Moreira/Fragata sub-basin, located in the region of Pelotas, RS, which presents a thalweg length of 26,809.44 meters, a maximum elevation of 286.00 meters, and a minimum elevation of 3.79 meters.

$$Tc = 57 \times \left(\frac{26{,}80944^3}{286{,}00 - 3{,}79}\right)^{0{,}385} = 289{,}79\ ou\ 4{,}83\ h$$

With the result of Tc and using it as the rainfall duration, the precipitation intensity can be obtained from the IDF curves shown in Figures 10, 11, 12, and 13. For the Arroio Moreira/Fragata sub-basin, the curve with a 5-year return period (Figure 11) will be used to determine the precipitation intensity (mm/min) when the rainfall duration is equal to Tc.

Figure 14. Graphical identification of rainfall intensity on the IDF curve.

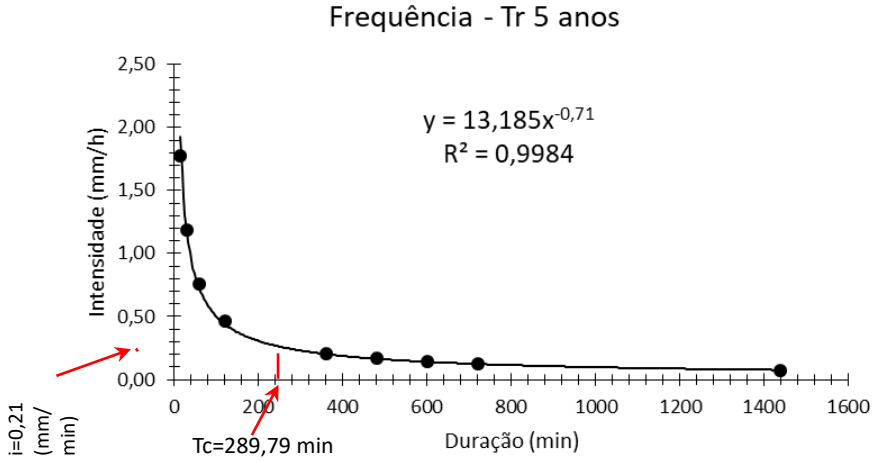

The intensity can be obtained by intersecting the time of concentration (Tc) on the Duration axis (min) with the precipitation curve, then projecting onto the precipitation intensity axis (mm/min) to estimate the value to be used in the Rational Method equation. In this case, the estimated rainfall intensity was 0.21 mm/min.

Another way to determine it is by using the regression equation generated through the insertion of the trend line, which allows for greater accuracy in the result, applying the Tc value to the X variable.

$$i = 13{,}185 \cdot 289{,}79^{-0{,}71} = 0{,}23\ mm/min$$

It can be observed that the results obtained from both processes were very similar; therefore, both methodologies are suitable for determining rainfall intensity in hydraulic structure design projects.

6 SURFACE RUNOFF COEFFICIENT (C)

The surface runoff coefficient (C), also referred to as the runoff or defluvium coefficient, is a dimensionless number that ranges between zero (0) and one (1), indicating the fraction of rainfall that is converted into surface runoff (JÚNIOR, 2015).

$$C = \frac{Escamento\ superficial}{Precipitação} \qquad \text{Eq 8}$$

The closer the value is to zero (0), the lower the surface runoff and the greater the infiltration; conversely, the closer it is to one (1), the higher the surface runoff and the lower the infiltration.

The surface runoff coefficient is directly related to the slope of the watershed, the soil type, and the type of land cover present in the area.

"Impermeable areas tend to exhibit higher surface runoff coefficients than vegetated areas; steeper slopes result in higher C values; rough surfaces with vegetation present lower C values; and wetter soils tend to promote surface runoff over shorter time intervals, generating higher C values.

An accurate estimation of the surface runoff coefficient enables more efficient and safer designs, reducing effects that contribute to increased environmental impacts in the face of extreme events.

Watersheds usually present more than one type of land cover, soil type, and slope; therefore, these aspects must be taken into consideration. In this case, a weighted average calculation of surface runoff is performed, where each variable is treated according to its area of occupation.

The estimation of the surface runoff coefficient (C) involves the use of tables based on surface characteristics, soil types, and slopes; however, these values may contain a degree of subjectivity depending on the designer's experience.

Modern techniques, such as the use of remote sensing and Geographic Information Systems (GIS), have been employed to estimate more accurate values of C, as they can easily express the correlation between slope, land use, and soil type.

$$\underline{C} = \frac{C_1 \times A_1 + C_2 \times A_2 + C_3 \times A_3}{At} \ldots \qquad \text{Eq 9}$$

"C1 = runoff coefficient of Area 1 as a function of slope, soil type, and vegetation cover; C2 = runoff coefficient of Area 2 as a function of slope, soil type, and vegetation cover; C3 = runoff coefficient of Area 3 as a function of slope, soil type, and vegetation cover; A1 = Area 1 of the watershed;

A2 = Area 2 of the watershed;

A3 = Area 3 of the watershed;

At = Total area of the watershed.

Table 11. Runoff coefficient (C) according to topography, land cover, and soil type (Daker, 1983).

Cobertura do Solo	Tipo de Solo	Plana 0–2,5%	Suavemente ondulada 2,5–5%	Ondulada 5–10%	Fortemente ondulada 10–20%	Amorrada 20–40%	Montanhosa 40–100%
Culturas anuais	Argiloso	0,5	0,6	0,68	0,76	0,85	0,95
	Franco	0,44	0,52	0,59	0,66	0,73	0,81
	Arenoso	0,4	0,48	0,54	0,61	0,67	0,75
Culturas permanentes	Argiloso	0,48	0,56	0,61	0,67	0,72	0,77
	Franco	0,34	0,41	0,46	0,52	0,56	0,64
	Arenoso	0,31	0,38	0,43	0,48	0,53	0,59
Pastagens limpas	Argiloso	0,31	0,38	0,43	0,48	0,53	0,59
	Franco	0,27	0,33	0,37	0,42	0,47	0,5
	Arenoso	0,25	0,3	0,34	0,38	0,42	0,46
Capoeiras	Argiloso	0,22	0,26	0,29	0,32	0,37	0,41
	Franco	0,19	0,23	0,25	0,28	0,32	0,35
	Arenoso	0,17	0,21	0,23	0,26	0,29	0,33
Matas	Argiloso	0,15	0,18	0,2	0,22	0,25	0,28
	Franco	0,13	0,16	0,18	0,2	0,23	0,24
	Arenoso	0,12	0,14	0,16	0,18	0,2	0,22

Table 12. C value for rural areas (Tucci, 2004).

Tipo de área	C
1 Topografia	
terreno plano, declividade de 0,2-0,6 m/km;	0,30
terreno, declividade de 3-4 m/km;	0,20
morros, declividade de 30-50 m/km;	0,10
2 Solo	
argila impermeável;	0,10
permeabilidade média;	0,20
arenoso;	0,40
3 Cobertura	
áreas cultivadas;	0,10
árvores.	0,20

Table 13.C value adopted by the São Paulo City Hall (Tucci, 2004).

Zonas	C
Edificação muito densa: Partes centrais, densamente construída de uma cidade com ruas e calçadas pavimentadas	0,70 – 0,95
Edificação não muito densa: Partes adjacente ao centro, de menor densidade de habitações, mas com ruas e calçadas pavimentadas	0,60 – 0,70
Edificações com poucas superfícies livres: Partes residenciais com construções cerradas, ruas pavimentadas	0,50 – 0,60
Edificações com muitas superfícies livres Partes residenciais com ruas macadamizadas ou pavimentadas	0,25 – 0,50
Subúrbios com alguma edificação Partes de arrabaldes e subúrbios com pequena densidade de construção	0,10 – 0,25
Matas, parques e campos de esportes Partes rurais, áreas verdes, superfícies arborizadas, parques ajardinados, campos de esportes sem pavimentação	0,05 – 0,10

Table 14. C value (Tucci, 2004)

Superfície	C	
	Intervalo	Valor esperado
Pavimento:		
Asfalto;	0,70 – 0,95	0,83
Concreto;	0,80 – 0,95	0,88
Calçadas;	0,75 – 0,85	0,80
Telhado;	0,75 – 0,95	0,85
Cobertura – grama solo arenoso:		
Plano (2%);	0,05 – 0,10	0,08
Médio (2 – 7%);	0,10 – 0,15	0,13
Alta (7%);	0,15 – 0,20	0,18
Grama – solo pesado:		
Plano (2%);	0,13 – 0,17	0,15
Médio (2 – 7%);	0,18 – 0,22	0,20
Alta (7%).	0,25 – 0,35	0,30

Table 15. Correction factor of C (Tucci, 2004).

Tempo de retorno (anos)	Cf
2 a 10	1,00
25	1,10
50	1,20
100	1,25

Using data from the Arroio Moreira/Fragata sub-watershed, we obtained the different classes of land use and land cover, the thalweg length, and the elevation difference. Subsequently, the average slope of the sub-watershed was calculated, and finally, the weighted average surface runoff coefficient was determined.

$$declividade\ (\%) = \frac{286{,}00 - 3{,}79}{26809{,}44} \times 100 = 1{,}05\%$$

The soil present in the region of the Arroio Moreira/Fragata sub-basin is classified as Planosol, with a sandy loam texture, which is considered medium.

With this information, we can, in a simplified manner, determine the average surface runoff coefficient of the basin by initially constructing a table that cross-references these data and associates Tables 11, 12, 13, and 14 to obtain the tabulated C value for each type of land cover. Thus, it is possible to calculate the weighted average C coefficient as described below.

Table 16. Determination of the surface runoff coefficient (C) for each land use and occupation.

Uso e Ocupação	Área (km^2)	Declividade (%)	Solo	C (Tabelado)
Mata	39,102	1,05	Médio	0,13
Pastagem	79,464	1,05	Médio	0,27
Cultivo	20,448	1,05	Médio	0,34
Solo Exposto	21,312	1,05	Médio	0,40
Urbanização	5,673	1,05	Médio	0,83
Água	2,355	1,05	Médio	0,00
Banhado	3,587	1,05	Médio	0,00

$$\underline{C} = \frac{(39{,}102 \times 0{,}13) + (79{,}464 \times 0{,}27) + (20{,}448 \times 0{,}34) + (21{,}312 \times 0{,}40) + (5{,}673 \times 0{,}83) + (2{,}355 \times 0) + (3{,}587 \times 0)}{171{,}941}$$

$$\underline{C} = 0{,}272$$

7 RATIONAL METHOD FOR PEAK DISCHARGE CALCULATION

The calculation of the design peak flow is important for flood control, sizing of culverts, storm sewers, pumping systems, channels, pipelines, spillways, levees, and other hydraulic structures.

The calculation of peak discharge in small watersheds using the Rational Method is one of the simple and rapid approaches to manage the planning and design of drainage systems capable of preventing floods and reducing environmental impacts in both urban and rural areas (CHOW, MAIDMENT, MAYS, 1988).

The basic principles of the Rational Method are to consider the duration of the design storm equal to the basin's time of concentration (Tc), to adopt a single surface runoff coefficient (C) estimated based on the watershed characteristics, and to note that the method does not evaluate the flood volume or the temporal distribution of discharges.

$$Q_{max} = \frac{C.I.A}{3{,}6} \qquad \text{Eq 10}$$

Q = Design peak discharge (m^3/s).

I = Average rainfall intensity over the basin, with duration equal to the basin's time of concentration (mm/h).

A = Drainage area of the basin (km^2).

C = Runoff coefficient.

In this way, the integration of hydrology, geotechnologies, and environmental planning strengthens the capacity for protection, prevention, and control of hydrological impacts, simultaneously meeting engineering technical requirements and global socio-environmental gobals.

With the variables already obtained, we can insert them into the equation for calculating the design peak discharge using the Rational Method as follows:

Rainfall intensity (I) = 0.23 mm/min

Sub-basin area (A) = 171.941 km²

Surface runoff coefficient (C) = 0.272

Return period (Tr) = 5 years.

Since we are using a return period of 5 years, it is not necessary to correct the surface runoff coefficient, according to the coefficients in Table 15. If the adopted return period is greater than 10 years, the calculated C must be multiplied by Cf from Table 15.

$$Q_{Máx} = \frac{(0{,}272 \times 1) \times (0{,}23 \times 60) \times 171{,}941}{3{,}6} = 179{,}23\ \frac{m^3}{s}$$

In the equation, the surface runoff coefficient is multiplied by 1 because Cf for a return period (Tr) of 2 to 10 years has this value (Table 15). The rainfall intensity is multiplied by 60 to convert from mm/min to mm/h.

8 CONCLUSION

Using the Rational Method to calculate the design peak discharge for the Arroio Moreira/Fragata sub-watershed, a Qmax of 179.23 m³/s was obtained.

When hydraulic structure calculations are carried out, this value should be used for the design, such as spillways, channels, pumping stations, pipelines, among others.

REFERENCES

AGÊNCIA NACIONAL DE ÁGUAS – ANA. SNIRH – Sistema Nacional de Informações sobre Recursos Hídricos: HidroWeb – Apresentação. Brasília: ANA, [s.d.]. Disponível em: https://www.snirh.gov.br/hidroweb/apresentacao. Acesso em: 21 nov. 2025.

ARAÚJO, A. R. A. et al. Análise de métodos de preenchimento de falhas em dados pluviométricos para a Região de Planejamento Sudoeste de Mato Grosso, Brasil. Revista Brasileira de Geografia Física, v. 16, n. 4, p. 1104–1114, 2023.

BIER, A. A.; FERRAZ, S. E. T. Comparação de metodologias de preenchimento de falhas em dados meteorológicos para estações no sul do Brasil. Revista Brasileira de Meteorologia, v. 32, n. 2, p. 215–226, 2017.

BRASIL. Lei nº 9.433, de 08 de janeiro de 1997. Institui a Política Nacional de Recursos Hídricos, cria o Sistema Nacional de Gerenciamento de Recursos Hídricos e dá outras providências. Diário Oficial da União, Brasília, DF, 9 jan. 1997.

BUENO, G. E. S. et al. A qualidade da água na microbacia hidrográfica do ribeirão Santo Antônio para o abastecimento humano no município de Iporá (GO). Itinerarius Reflections, v. 15, n. 3, 2019.

CAMPOS, S. et al. Caracterização morfométrica da microbacia do rio Bauru/SP obtida por técnicas de geoprocessamento. InterEspaço: Revista de Geografia e Interdisciplinaridade, v. 1, n. 3, p. 222–234, 2015.

CHOW, V. T.; MAIDMENT, D. R.; MAYS, L. W. Applied Hydrology. New York: McGraw-Hill, 1988.

ELY, D. F. et al. Análise de métodos para o preenchimento de falhas aplicados em séries de dados pluviométricos do Estado do Paraná (Brasil). Raega – O Espaço Geográfico em Análise, v. 51, p. 122–142, 2021. DOI: https://doi.org/10.5380/raega.v51i0.72944.

FAO – Food and Agriculture Organization of the United Nations. Watershed Management and Ecosystem Services. Rome: FAO, 2017.

FARR, T. G. et al. The Shuttle Radar Topography Mission. Reviews of Geophysics, v. 45, n. 2, 2023. Disponível em: http://www.agu.org/pubs/crossref/2007/2005RG000183.shtml. Acesso em: nov. 2025.

JÚNIOR, A. R. B. Elementos de Hidrologia Aplicada. Ouro Preto: UFOP, 2015. p. 92–155.

MELLO, Y. R.; KOHLS, W.; OLIVEIRA, T. M. N. Uso de diferentes métodos para o preenchimento de falhas em estações pluviométricas. Boletim de Geografia, v. 35, n. 1, p. 112–121, 2017. DOI: http://dx.doi.org/10.4025/bolgeogr.v35i1.30893.

NARDINI, R. C. Determinação do conflito de uso e ocupação do solo em áreas de preservação permanente da Microbacia do Ribeirão Água-Fria, Bofete (SP), visando a conservação dos recursos hídricos. 2009. Dissertação (Mestrado em Ciências Agronômicas) – Universidade Estadual Paulista, Botucatu, 2009.

PEREIRA, M. D. R.; CABRAL, J. B. P. Perda de solo no alto curso das bacias hidrográficas dos ribeirões Taquaruçu Grande e Taquaruçuzinho, Palmas (TO). Revista Brasileira de Geografia Física, v. 14, n. 1, 2021.

ROBAINA, A. D.; PEITER, M. X. Modelo de desagregação e de geração de chuvas intensas no RS. In: CONGRESSO BRASILEIRO DE ENGENHARIA AGRÍCOLA, 21.; SIMPÓSIO DE ENGENHARIA AGRÍCOLA DO CONE SUL, 1., 1992, Santa Maria. Anais... Santa Maria: Sociedade Brasileira de Engenharia Agrícola, 1992. p. 746–753.

SALGUEIRO, J. H. P. B.; MONTENEGRO, S. M. G. L. Análise da distribuição espacial da precipitação na bacia do rio Pajeú em Pernambuco segundo método geoestatístico. Revista Tecnológica, Fortaleza, v. 29, n. 2, p. 174–185, 2008.

SANTANA, D. P. Manejo Integrado de Bacias Hidrográficas. Sete Lagoas: Embrapa Milho e Sorgo, 2003. (Documentos, 30).

SILVA, A. L. M. Direito do Meio Ambiente e dos Recursos Naturais. 784 p., 2005.

SILVA, J. L.; TUCCI, C. E. M.; MENDES, C. A. B. Aplicações de geotecnologias na hidrologia e no manejo de bacias hidrográficas. Revista Brasileira de Recursos Hídricos, v. 25, p. 1–12, 2020.

SOUSA, F. R. C.; PAULA, D. P. Análise de perda do solo por erosão na bacia hidrográfica do Rio Coreaú (Ceará-Brasil). Revista Brasileira de Geomorfologia, v. 20, n. 3, 2019.

SOUZA, V. A. S. et al. Análise de chuvas intensas por meio da desagregação de precipitações diárias de Jaru e Machadinho d'Oeste (RO), Brasil. Revista Verde de Agroecologia e Desenvolvimento Sustentável, v. 8, n. 1, p. 80–85, jan./mar. 2013.

SANTOS, G. B. et al. Análise da qualidade das águas do Arroio Moreira/Fragata (RS) através de métodos estatísticos. Revista Ibero-Americana de Ciências Ambientais, v. 11, n. 4, p. 217–226, 2020. DOI: http://doi.org/10.6008/CBPC2179-6858.2020.004.0019.

TAMMETS, Tiina; JAAGUS, Jaak. Climatology of precipitation extremes in Estonia using the method of moving precipitation totals. Theoretical and Applied Climatology, v. 111, n. 3–4, p. 623–639, 2013.

TORRES, T. G. Geotecnologias na geração do divisor de bacias hidrográficas: um instrumento para a Política de Recursos Hídricos. 2007. Dissertação (Mestrado) – Universidade Federal de Mato Grosso do Sul, Campo Grande, 2007.

TUCCI, C. E. M. Hidrologia: ciência e aplicação. 2. ed.; 2. reimpr. Porto Alegre: Ed. Universidade/UFRGS; ABRH, 2001.

TUCCI, C. (org.). Hidrologia: ciência e aplicação. 3. ed. Porto Alegre: Editora da Universidade da UFRGS; ABRH, 2004.

UN – United Nations. Transforming Our World: The 2030 Agenda for Sustainable Development. New York: United Nations, 2015.

VIEIRA, S. A. et al. Metodologia de imputação de dados hidrometeorológicos para análise de séries históricas para avaliação de impactos das mudanças climáticas – Bacia do Rio dos Sinos, RS, Brasil. Revista Brasileira de Climatologia, n. 23, p. 189–204, 2018. DOI: https://doi.org/10.5380/abclima.v23i0.562119.

WATTS, L. F.; HAWKE, R. M. The effects of urbanization on hydrologic response: a study of two coastal catchments. Journal of Hydrology (NZ), v. 42, n. 2, p. 125–143, 2003.

CHAPTER 2:
LYOPHILIZATION VERSUS LIQUID–LIQUID EXTRACTION IN THE CHROMATOGRAPHIC ANALYSIS OF PYROLIGNEOUS LIQUID

Giani Mariza Britzius Barwald, Fábio Pereira dos Santos de Castro, Pedro José Sanches Filho

ABSTRACT

The use of biomass is a growing alternative for the reuse of agro-industrial residues. In this context, lignocellulosic biomasses can be converted by pyrolysis to obtain charcoal, gas, and bio-oil or pyroligneous liquid (PL), which presents a predominantly aqueous matrix. Several techniques have been applied to characterize its composition and, thus, evaluate its use; therefore, the aim of this study was to evaluate liquid–liquid extraction (LLE) and lyophilization (LYO) combined with gas chromatography coupled to mass spectrometry (GC/MS) to characterize the compounds that constitute the pyroligneous liquid obtained from peach pits. The pyroligneous liquid characterized was obtained on an industrial scale, operating within a temperature range of 500 °C. For LLE, 1.0 mL of pyroligneous liquid were extracted with dichloromethane (DCM), dried with Na_2SO_4 and evaporated to 0.5 mL. For lyophilization, 200 µL were frozen for 24 hours and lyophilized for 24 hours under a pressure of 218 µm Hg and a temperature of −58 °C. The samples from both methods were derivatized with 30 µL of N-methyl-N-(trimethylsilyl)-trifluoroacetamide (MSTFA) and analyzed by gas chromatography. The samples prepared by LYO showed a predominance of 39.57% acids, 35.02% alcohols and 17.27% phenols, whereas those obtained by LLE presented 39.1% phenolic compounds, 25.4% acids and 20.7% alcohols. The preparation method using the LYO technique proved to be efficient and reproducible, allowing a reduction in the use of organic solvent and resulting in less waste generation.

Keywords: Agroindustrial waste; Extraction; Liquid Pyrolysis; Sample preparation; Thermoconversion.

1 INTRODUCTION

The use of lignocellulosic biomass has emerged as a sustainable alternative for the valorization of agro-industrial waste. Among these residues, peach stones, generated in large quantities by the fruit-processing industry, constitute a recalcitrant material whose improper disposal can lead to environmental impacts. Their thermochemical conversion, particularly through pyrolysis, yields charcoal, gases and a bio-oil composed of an oily fraction and an aqueous fraction known as pyroligneous liquid.

Pyroligneous liquid is a chemically complex matrix containing hundreds of oxygenated compounds derived from the thermal degradation of cellulose, hemicellulose and lignin. This complexity demands suitable analytical approaches for proper characterization, especially gas chromatography coupled with mass spectrometry (GC/MS). However, sample preparation plays a crucial role in analytical performance due to the high polarity and hydrophilic nature of the matrix.

In this context, two methods are commonly employed for preparing samples for GC/MS: liquid–liquid extraction (LLE) and lyophilization (LYO). LLE uses organic solvents to extract target compounds but shows limitations when dealing with highly polar analytes. Lyophilization, in turn, removes water by sublimation, preserving thermally sensitive compounds and broadening the chemical profile detectable by GC/MS.

Therefore, the aim of this study was to compare LLE and LYO as sample preparation strategies for the aqueous phase of the pyroligneous liquid obtained from peach-stone pyrolysis, evaluating their influence on the qualitative and quantitative characterization of compounds by GC/MS.

2 THEORETICAL FRAMEWORK

2.1 LIGNOCELLULOSIC BIOMASS AND AGRO-INDUSTRIAL WASTE GENERATION

Lignocellulosic biomasses are among the main renewable alternatives for the valorization of agro-industrial waste due to their wide availability and potential for generating high-value bioproducts (KHAN et al., 2023). Their structure is predominantly composed of cellulose, hemicellulose and lignin, whose proportions vary among plant species and determine the thermal behavior of the biomass during conversion processes (LU; WU, 2012; VAN de VELDEN et al., 2010).

Peach stones, generated on a large scale by the food industry, represent a recalcitrant residue with slow natural degradation, justifying the growing interest in their use as a feedstock for thermochemical processes (KHAN et al., 2023). Studies indicate that lignocellulosic materials from agricultural residues such as shells, pits, and fibers, present an adequate composition for pyrolysis and carbonization (MORAES et al., 2012).

2.2 PYROLYSIS: PRINCIPLES AND PRODUCTS

Pyrolysis is a thermocatalytic process that promotes the thermal decomposition of biomass in the absence of oxygen, generating three main fractions: gases, bio-oil and charcoal (ARAZO et al., 2017). Carbonization occurs at lower temperatures (up to 400 °C), whereas pyrolysis operates at higher temperatures and produces a broader diversity of volatile products (ARAZO et al., 2017).

The liquid fraction obtained from pyrolysis consists of an oily phase (bio-oil) and an aqueous phase known as pyroligneous extract or pyroligneous liquid (PESENTI, 2021). This aqueous phase may contain more than 200 compounds—mostly oxygenated—derived

from the thermal breakdown of hemicellulose, cellulose and lignin (BETEMPS et al., 2017; SANCHES FILHO et al., 2017; ZHOU et al., 2023).

Its constituents include carboxylic acids (such as acetic and lactic acids), lignin-derived phenols (catechol, guaiacol, cresols), aldehydes, ketones and polyoxygenated alcohols (DIAS, 2021; SONG et al., 2014). The diversity and complexity of this matrix highlight the need for robust and selective analytical methodologies.

2.3 AQUEOUS PHASE OF BIO-OIL: COMPOSITION AND ANALYTICAL CHALLENGES

The aqueous phase of bio-oil, also known as pyroligneous liquor, is characterized by high concentrations of oxygenated compounds, strong polarity and pronounced acidity (PESENTI, 2021; DIAS, 2021). Such attributes create significant analytical challenges, particularly due to: the incompatibility between hydrophobic solvents and the highly polar matrix; the low volatility of many analytes, which complicates GC/MS detection e; the presence of highly polar compounds, such as sugars and hydroxylated acids, which often exhibit low recovery in classical extraction methods (BETEMPS et al., 2017; SANCHES FILHO et al., 2020).

The literature shows that lignin-derived compounds are preferentially extracted by organic solvents, whereas hemicellulose- and cellulose-derived compounds are better recovered using gentle water-removal techniques such as lyophilization (RUIZ-MATUTE et al., 2011; ZHOU et al., 2023).

2.4 SAMPLE PREPARATION METHODS FOR GC/MS

2.4.1 Liquid–Liquid Extraction (LLE)

Liquid–liquid extraction is widely applied for preparing samples destined for chromatographic characterization of the aqueous phase of bio-oil, typically employing solvents such as dichloromethane (DCM) (SANCHES FILHO et al., 2020; BETEMPS et al., 2017). The technique is based on the partition coefficient of analytes between the aqueous and organic phases. However, several authors highlight significant limitations of LLE in pyroligneous liquids: solvent saturation due to the high organic load (BETEMPS et al., 2017); low extraction efficiency for highly polar compounds (SANCHES FILHO et al., 2020); analyte losses during solvent evaporation, particularly for volatile phenols (BRIDGWATER, 2012) e analytical discrimination against less hydrophobic compounds.

Despite these limitations, LLE is particularly efficient for extracting lignin-derived phenols—such as guaiacol, cresols and catechol, widely reported in pyrolysis products from peach stones (MORAES et al., 2012; FARRAPEIRA et al., 2021).

2.4.2 Lyophilization (LYO)

Lyophilization has gained prominence as a sample preparation technique for GC/MS due to its ability to remove water from the matrix via sublimation, avoiding thermal and chemical degradation (BALDACONI, 2021). According to Sanches Filho et al. (2020), this method enhances the recovery of: short-chain carboxylic acids, polyoxygenated alcohols, sugars and sugar-derived compounds e thermally sensitive analytes.

During lyophilization, water transitions directly from solid to gas without passing through the liquid phase, decreasing the loss of volatiles and minimizing secondary reactions such as oxidation or condensation (RUIZ-MATUTE et al., 2011).

Studies involving different types of biomass have demonstrated that lyophilization yields a more representative chemical profile of the original aqueous phase, providing broader and less selective chromatographic fingerprints (SANCHES FILHO et al., 2020; DE SOUSA et al., 2025).

2.5 GAS CHROMATOGRAPHY–MASS SPECTROMETRY (GC/MS)

GC/MS is one of the most widely used techniques for the characterization of bio-oils and their aqueous fractions due to its high sensitivity and ability to identify compounds through mass spectra (BETEMPS et al., 2017; SANCHES FILHO et al., 2017). However, its performance depends strongly on sample preparation, since low-volatility or highly polar analytes need to be derivatized to increase their thermal stability and chromatographic response.

Derivatization with MSTFA is a well-established approach for enhancing the detection of acids, phenols and sugars (BETEMPS et al., 2017; SANCHES FILHO et al., 2020). The identification of compounds is typically performed by comparing retention times and mass spectra with NIST and WILEY libraries, considering similarity indices above 80% as acceptable (FARRAPEIRA et al., 2021).

3 MATERIALS AND METHODS

3.1 REAGENTS

The solvent used for the extraction of the aqueous phase was chromatographic-grade dichloromethane (DCM). For sample derivatization, N-methyl-N-(trimethylsilyl)trifluoroacetamide (MSTFA) was employed. A mixture of phenolic standards (phenol, o-cresol, p-cresol, m-cresol, vanillin, 2-methoxyphenol, 2-ethylphenol, 3-ethylphenol, 4-ethylphenol, 2-methoxy-4-vinylphenol) was also used. All reagents were purchased from Supelco – Sigma Aldrich.

3.2 PYROLIGNEOUS LIQUID PRODUCTION AND SEPARATION

Peach stones, a by-product of fruit processing, were obtained from local suppliers in the city of Pelotas, Rio Grande do Sul (RS), Brazil. The almond was separated from the lignified endocarp using a mechanical lathe. The endocarp was ground in a knife mill and sieved in a vibrating mesh system. Particles smaller than 2 mm were dried at 105 °C for one hour.

For pyrolysis, 20 g of dried endocarp were placed inside a steel reactor. The heating operation was conducted over 6 hours, with a ramp of 30 °C min^{-1} until reaching 500 °C, using nitrogen (35 mL min^{-1}) as carrier gas.

3.3 TREATMENT OF THE AQUEOUS PHASE (AP)

To analyze the compounds present in the pyroligneous liquid by gas chromatography, two sample preparation methods were compared: liquid–liquid extraction (LLE) with DCM and lyophilization (LYO).

3.3.1 Liquid–Liquid Extraction (LLE)

A 1.0 mL aliquot of pyroligneous liquid (PL) was submitted to liquid–liquid extraction in a test tube with 5 mL of DCM. The extraction was performed three times. The combined organic phases were dried over sodium sulfate (Na_2SO_4) and evaporated to 1.0 mL. A 200 µL aliquot of this extract was transferred to a vial, derivatized with 30 µL of MSTFA, and the final volume was adjusted to 1 mL with DCM (SANCHES FILHO et al., 2020). Figure 1 shows the process performed for the analysis of the sample treated by LLE. The process consisted of extraction with DCM; separation of the solvent from the sample

by decantation; drying to eliminate aqueous residues; derivatization and analysis by GC/MS.

Figure 1. Stages of the liquid–liquid extraction process (LLE).

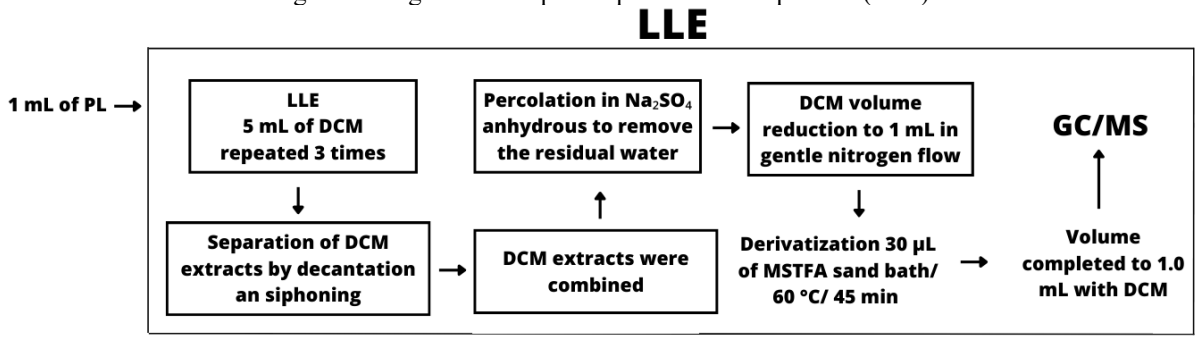

3.3.2 Lyophilization (LYO)

For lyophilization, a Liotop L101 freeze dryer was used. A 200 µL aliquot of PL previously frozen in an ultra-low-temperature freezer was placed directly in a vial and lyophilized for 24 hours under 218 µm Hg and −58 °C. Figure 2 shows the process performed for the analysis of the sample by LYO. The process consisted of freezing the pyroligneous liquid; lyophilization; derivatization and analysis by GC/MS.

Figure 2. Stages of the lyophilization process (LYO).

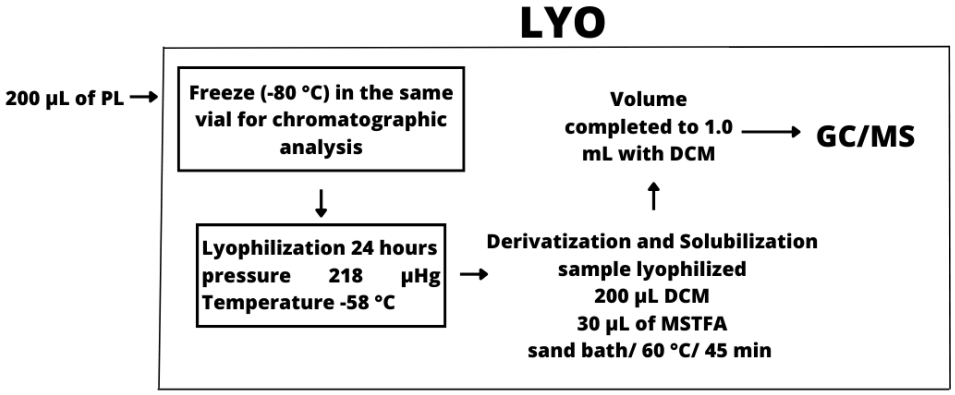

3.3.3 Analytical Procedure

Blank analyses were carried out in parallel with each extraction method: 1.0 mL of distilled water for LLE and 200 µL of pre-frozen distilled water for LYO. Limits of detection (LOD) and quantification (LOQ) were estimated based on repeated injections of these blanks, calculated using 3- and 10-fold the standard deviation of the blank signal divided by the slope of the analytical curve (BETEMPS et al., 2017; BRITO et al., 2003).

Corrections were applied for analytes with recovery below 70%. Blanks were subjected to the same steps as real samples.

Method recovery was evaluated following Sanches Filho et al. (2020). Fresh samples were prepared under the same experimental conditions but fortified with 100 mg L^{-1} of the phenolic standard mixture. Recoveries were calculated according to Equation 1:

$$\text{Recovery}(\%) = ((ACF - ACNF)/CAA) * 100 \quad \text{eq. 01}$$

Where: ACF = analyte concentration in the fortified sample; ACNF = analyte concentration in the non-fortified sample; CAA = added analyte concentration.

Precision was evaluated by the relative standard deviation (%RSD) of triplicates.

3.4 GC/MS ANALYSIS

A 1 µL aliquot of each extract, fortified and non-fortified, was injected in split mode (1:20) in a Shimadzu QP2010 Ultra GC/MS equipped with an RTX-5MS column (30 m × 0.25 mm × 0.25 µm).

Injector and interface temperatures were maintained at 280 °C, and ion source temperature at 200 °C. The oven temperature program was as follows: initial temperature of 60 °C (held for 5 min); increase of 8 °C min^{-1} to 160 °C; followed by 3 °C min^{-1} to 300 °C, with a final hold of 15 min. Analyses were performed in SCAN mode (70 eV).

Compound identification was performed through comparison of retention times and mass spectra with the NIST and WILEY libraries, accepting matches with similarity above 80%. Relative percentages were calculated from the integrated peak areas.

For quantification of fortified samples, analytical curves (10–200 mg L^{-1}) of the phenolic standard mixture were constructed. Chromatographic precision was assessed using %RSD from five consecutive injections of a 20 mg L^{-1} derivatized phenolic standard solution.

4 RESULTS AND DISCUSSION

The merit figures summarized in Table 1 show that the lyophilization (LYO) method exhibited superior performance compared to liquid–liquid extraction (LLE). Correlation coefficients (R) ranged from 0.959 to 0.995, indicating excellent linearity for all analytes. LOD and LOQ values were adequate for the concentration ranges typically found in the aqueous phase of bio-oils, ensuring reliable detection of phenolic compounds.

Chromatographic precision was satisfactory, with %RSD values between 1.7% and 5.4%, meeting the requirements for GC/MS analyses (BRITO et al., 2003).

Table 1: Merit figures for the chromatographic method and comparative recoveries of LYO and LLE.

Analyte	a	b	r	RSD %	ER%	LD mg L^{-1}	LQ mg L^{-1}	LYO	Rsd %	LLE	Rsd %
Phenol	25,332	35,124	0,989	2,9	3,9	0,12	0,4	44,8	17,3	32,3	20,1
o-cresol	60,252	110,287	0,976	3,1	4,2	0,1	0,33	74,1	4,0	68,9	19,3
p-cresol	48,105	102,357	0,974	2,5	2,7	0,13	0,43	92,8	19,5	73,9	18,7
m-cresol	47,362	108,349	0,995	1,7	3,7	0,11	0,36	94,2	20,7	64,6	17,5
2-ethyl phenol	49,951	112,304	0,991	3,1	2,9	0,12	0,4	92,5	20,5	79,2	18,8
4-ethyl phenol	49,157	101,997	0,969	2,9	4,8	0,09	0,3	96,2	11,9	80,3	18,7
2- methoxy-phenol	63,485	123,524	0,992	2,6	2,5	0,57	1,88	100,7	5,6	76,3	15,6
3-ethyl phenol	48,751	106,249	0,968	3,2	3,8	0,23	0,76	117,2	13,7	80,2	19,3
2methoxy-4vinyl phenol	22,851	17,258	0,976	4,9	5,4	0,15	0,5	92,3	14,3	95,3	19,2
Vanilin	33,254	49,325	0,959	4,1	4,6	0,12	0,40	118,4	12,7	99,2	12,3

Recoveries obtained via LYO were above 70% for most analytes, confirming the efficiency of this method in preserving compounds during sample preparation. Only phenol showed lower recovery (44.8%), which can be attributed to its high volatility and low molar mass, factors that enhance losses during sublimation.

Other phenolic compounds, such as cresols, guaiacols and syringols, presented recoveries between 74.1% and 118.4%. Recoveries higher than 100% are common in complex matrices such as pyroligneous liquids, often resulting from matrix effects that enhance analytical response. These findings align with the work of Sanches Filho et al. (2020), who also reported recoveries between 60.6% and 124.3% when applying LYO to aqueous phases of bio-oils derived from rice husk.

In contrast, LLE showed lower and more variable recovery values. Phenol again exhibited the lowest recovery (32.3%), reinforcing the vulnerability of this compound to losses during handling. Recoveries for the remaining analytes ranged from 64.6% to

99.2%, though with greater variability in %RSD, likely due to multiple extraction steps, drying with inorganic salts and evaporation of the solvent.

According to Betemps et al. (2017) and Sanches Filho et al. (2020), LLE commonly results in: solvent saturation due to high organic content, limited extraction of highly polar compounds, analyte losses during solvent evaporation e, analytical discrimination caused by hydrophilic matrices.

Overall, the results confirm that LYO is the most suitable method for chromatographic characterization of the aqueous phase of pyroligneous liquids. It provides higher and more consistent recoveries, better preservation of volatile and oxygenated compounds and reduced analytical discrimination, features especially relevant for highly hydrophilic matrices.

Figure 3. Distribution of chemical classes (LYO).

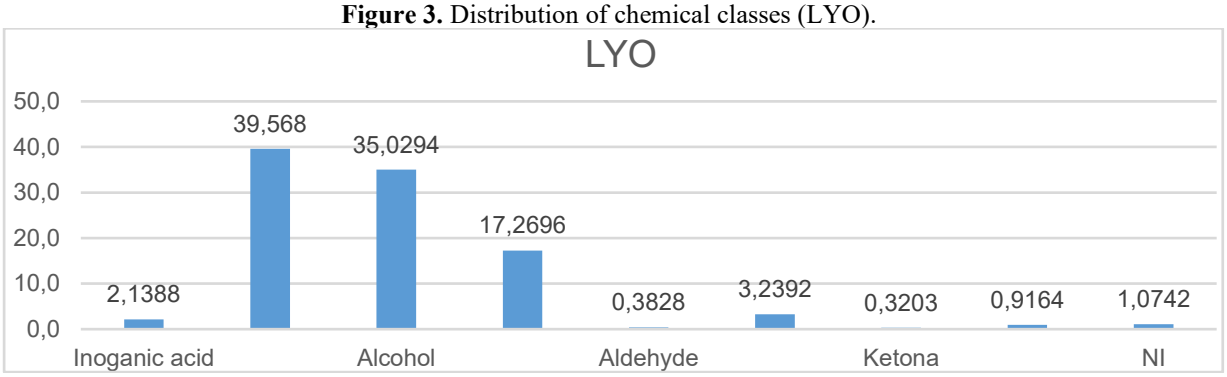

Samples prepared via LYO exhibited a predominance of carboxylic acids (39.57%), followed by polyoxygenated alcohols (35.02%) and phenols (17.27%) (Figure 3). This profile indicates that lyophilization favors the recovery of hydrophilic and highly oxygenated compounds, consistent with mild water removal by sublimation. This mechanism minimizes losses of volatile analytes and reduces the risk of secondary reactions.

The high proportion of acids reflects typical behavior of aqueous phases of bio-oils, commonly enriched with acetic, glycolic, lactic and butanoic acids (DIAS, 2021; ZHOU et al., 2023). The expressive presence of alcohols, including diols and triols, indicates extensive degradation of cellulose and hemicellulose, forming compounds such as glycerol, ethylene glycol and furfuryl alcohols (SONG et al., 2014).

Phenols, although less abundant in LYO samples, remain important markers of lignin decomposition. Their lower relative abundance indicates partial loss of volatile phenolic compounds during sublimation, a trend also observed in other LYO-based studies.

Additionally, the presence of sugars (3.24%) demonstrates the ability of lyophilization to preserve thermally sensitive carbohydrates and oligosaccharides.

Figure 4 shows that in the liquid-liquid extraction method, there was a predominance of phenols (39.1%), followed by acids (25.4%) and alcohols (20.7%). This behavior is in agreement with the literature on bio-oils from fast pyrolysis and agricultural waste pyrolysis (Betemps et al., 2017; Sanches Filho et al., 2017), in which phenolic compounds exhibit high affinity for organic solvents such as dichloromethane (DCM), justifying their predominance.

Figure 4. Distribution of chemical classes (LLE)

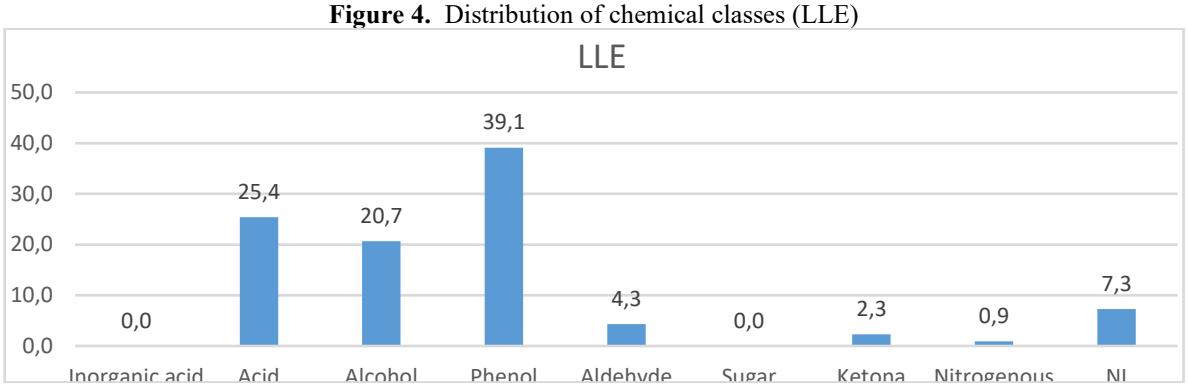

Extraction with DCM favors the transfer of relatively less polar compounds, especially phenols derived from lignin degradation (such as guaiacol, cresols, and catechol), explaining the significant increase of this class compared to LYO. Studies show that phenols are more efficiently recovered by chlorinated solvents, which have an intermediate affinity for oxygenated aromatic molecules (Bridgwater, 2012; Moraes et al., 2012).

On the other hand, the lower values for acids and alcohols reflect the limitation of LLE in extracting highly hydrophilic and polar compounds. This occurs due to the saturation of the organic solvent and the low partition of very polar compounds into the organic phase, as already described in similar methodologies applied to the aqueous phase of bio-oils (Betemps et al., 2017; Sanches Filho et al., 2020).

Another relevant aspect is the near absence of sugars and inorganic acids, indicating that the solvent is not capable of extracting such compounds, which reinforces the low efficiency of LLE in the integral recovery of the components of the aqueous fraction.

The comparison between Figures 3 and 4 reveals clear trends: LYO preferably recovers highly oxygenated compounds, such as acids, alcohols, and sugars, due to the gentle removal of water and the absence of solvent manipulation steps, which can cause

losses or discrimination. In contrast, LLE favors phenolic compounds due to the affinity of these compounds for dichloromethane but loses a significant portion of the more hydrophilic compounds.

Thus, the class distribution obtained by LYO is more representative of the original composition of the pyroligneous liquor, while LLE provides a more selective, yet limited, chemical spectrum. These results reaffirm what has already been observed in studies on the characterization of the aqueous phase of bio-oils: methods without the use of solvents (such as LYO) tend to preserve greater chemical diversity, while extractive techniques introduce selectivity and potential losses (Sanches Filho et al., 2020; Zhou et al., 2023).

Table 2. Results by the LYO method, with a similarity greater than 80% and an area greater than 1%.

	Name	*RT (start)*	*RT (end)*	*% Area*	*Function*
1	Butanoic acid	27.800	27.940	1,16	Acid
2	Glycerol	23.730	23.850	1,27	Alcohol
3	Benzoic acid	22.350	22.475	1,67	Acid
4	Phosphoric acid	23.610	23.730	1,68	Acid
5	Deoxyribopyranose	33.215	33.360	1,97	Sugar
6	5-Hydroxy-n-valeric acid	25.275	25.440	2,94	Acid
7	2-Hidroxi propanoic	15.315	15.470	3,07	Acid
8	1,2-Etanodiol	10.920	11.115	3,39	Alcohol
9	2-Hidroxi butanoic	18.235	18.440	4,33	Acid
10	2,6-Dimethoxyphenol	27.195	27.380	4,39	Phenol
11	Butanoic acid	22.200	22.350	6,90	Acid
12	1,2,5 pentanotriol	30.340	30.530	9,18	Alcohol
13	2-Hydroxi etanoic	15.985	16.175	9,75	Acid
14	1,2-Benzenediol	24.730	24.900	10,28	Phenol
15	Tetrahydro-2-furanylmethanol	18.865	18.945	17,93	Alcohol

The semiquantitative analysis of the organic fraction obtained by the LYO method revealed the presence of 15 compounds with an area greater than 1% and similarity above 80%, highlighting a set formed by carboxylic acids, polyoxygenated alcohols, lignin-derived phenols, and sugars or their pyrolysis products, reflecting the typical chemical pattern of bio-oils obtained from the pyrolysis of lignocellulosic biomass. The predominance of these compounds is associated with the thermal decomposition of hemicellulose, cellulose, and lignin, which originate highly oxygenated and hydrophilic

molecules, which tend to concentrate in the aqueous phase after condensation. This behavior is widely described in recent studies on the characterization of the aqueous phase of bio-oils (Zhou et al., 2023).

Carboxylic acids constituted the most expressive class in the sample, including structures such as short-chain acids and hydroxylated acids. The literature shows that this class can represent significant fractions of the aqueous phase, being responsible for properties such as high acidity, corrosivity, and thermal instability. Acids such as acetic, lactic, glycolic, and butanoic are widely reported in biomass pyrolysis and play a central role in the reactivity of the matrix, in addition to presenting potential in bioconversion routes (Dias, 2021).

The presence of polyoxygenated alcohols, including diols, triols, and furanic derivatives, indicates intense participation in the degradation of structural carbohydrates, especially cellulose and hemicellulose. Compounds such as glycerol, ethylene glycol, and furanic alcohols are frequently identified in the aqueous phase of bio-oil and have technological relevance as chemical intermediates. This class is also associated with the high solubility of the fraction and the strongly hydrophilic character observed in matrices originating from the fractionation of bio-oils (Song et al., 2014).

The phenols observed in the sample, including catechol, guaiacol, and syringol in their derivatized forms, are classic markers of lignin degradation. These compounds appear in a lower proportion than acids but are structurally important due to their high reactivity and potential added value. Studies show that phenolic compounds recovered from the aqueous phase can be used as antioxidants or chemical intermediates in bioproducts, reinforcing the importance of this class for the integral utilization of bio-oils (Zhou et al., 2023).

The detection of sugars and derived oligosaccharides, frequently converted during derivatization, indicates that lyophilization was effective in preserving thermally sensitive molecules, such as: levoglucosan, glucose, and pyranose derivatives, which frequently degrade or are not extracted by traditional methods like LLE. Studies show that derivatization processes, when combined with gentle drying techniques like LYO, increase the efficiency of carbohydrate detection in GC-MS analyses, which reinforces the role of lyophilization as a strategic analytical tool for the characterization of bio-oils (Ruiz-Matute et al., 2011).

Thus, the results obtained demonstrate that the LYO method provides a broader chemical profile and is richer in highly oxygenated compounds, highlighting its suitability

for qualitative and semiquantitative analyses of aqueous phases of pyroligneous liquors, and confirming its potential as an efficient and sustainable alternative compared to conventional sample preparation techniques (De Sousa et al., 2025).

The semiquantitative composition obtained by the LLE method shows that the pyroligneous liquor derived from the pyrolysis of peach stones has a complex chemical profile, mainly consisting of phenols, carboxylic acids, alcohols, in addition to smaller proportions of aldehydes and ketones. This set of compounds is characteristic of bio-oils obtained from lignocellulosic biomass, reflecting the thermal degradation of the three structural biopolymers: lignin, hemicellulose, and cellulose. The predominance of phenols and acids observed in the sample is consistent with the thermal behavior of fruit endocarps of the Prunus genus, widely reported in the specialized analytical pyrolysis literature (Farrapeira et al., 2021).

Table 3- Results by the LLE method, with a similarity greater than 80% and an area greater than 1%.

	Name	*RT (start)*	*RT (end)*	%Area	Function
1	(2-methylpropanol	5.103	2226589	7,1	Alcohol
2	Butanoic acid	5.490	1657781	5,3	Acid
3	3-Hydroxy-2-butanone	5.551	368710	1,2	Ketona
4	Butanoic acid, 4-hydroxy-	6.559	392571	1,3	Acid
5	(2-methylbutanol	6.758	452226	1,5	Alcohol
6	2-Butenoic acid, tert	7.428	394661	1,3	Acid
7	Butanoic acid, 2-oxo-,	9.321	2151116	6,9	Acid
8	phenol	14.443	1701377	5,5	Phenol
9	Pentanoic acid, 4-oxo-,	18.277	414583	1,3	Acid
10	4-methylphenol	18.430	583101	1,9	Phenol
11	Silane, trimethyl[(tetrahydrofurfuryl)oxy]-	18.853	3234914	10,4	Alcohol
12	2,4-Hexadienoic acid, tert-butyldimethylsilyl ester, (E,E)-	20.755	1572596	5,0	Acid
13	2-Methoxyphenol trimethylsilyl ether	21.699	1053277	3,4	Phenol
14	Benzoic acid trimethylsilyl ester	22.323	1697115	5,4	Acid
15	3-Trimethylsilyloxy-2-methylpyran-4-one	23.697	788112	2,5	Acid
16	1,2-Benzenediol bis(trimethylsilyl) ether	24.730	3883006	12,5	Alcohol
17	Benzaldehyde, 3-methoxy-4-hydroxi]-	27.031	406711	1,3	Aldehydo
18	2,6-Dimethoxyphenol, trimethylsilyl ether	27.212	3859543	12,4	Phenol

19	Benzaldehyde, 3-methoxy-4-[(trimethylsilyl)oxy]-	30.826	1141416	3,7	Acid
20	4'-Hydroxy-3'-methoxyacetophenone,	32.965	458481	1,5	Ketona
21	1,3,5-Tris(trimethylsiloxy)benzene	35.563	749624	2,4	Acid
22	1,7-Di(3-ethylphenyl)-2,2,4,4,6,6-hexamethyl-1,3,5,7-tetraoxa-2,4,6-trisilaheptane	36.608	526475	1,7	Phenol
23	(4-Hydroxy-3-methoxyphenyl)ethylene glycol tris(trimethylsilyl) ether	36.962	683812	2,2	Phenol
24	3-Vanilpropanol, bis(trimethylsilyl)-	37.531	785578	2,5	Alcohol

The class of phenols was the most representative, highlighting 1,2-benzenediol bis(trimethylsilyl) ether (12.5%), 2,6-dimethoxyphenol TMS (12.4%), phenol (5.5%), 4-methylphenol (1.9%), in addition to vanillyl and guaiacyl derivatives. These compounds derive directly from lignin degradation, especially from the guaiacyl (G) and syringyl (S) units, which are predominant in angiosperms. Previous studies showed that bio-oils obtained from peach stones have high levels of catechol, syringol, and guaiacol, in line with the results observed here (Moraes et al., 2012).

The second most expressive class was that of carboxylic acids, with compounds such as butanoic acid (5.3%), 2-oxo-butanoic acid (6.9%), benzoic acid TMS (5.4%), and 2,4-hexadienoic acid TMS (5.0%). These products are formed predominantly by the degradation of hemicellulose and secondary oxidation reactions of intermediate compounds. The significant presence of acids is typical of crude bio-oils, contributing to their high acidity, corrosivity, and chemical instability, characteristics discussed in studies on the pyrolysis of lignocellulosic materials (Bridgwater, 2012).

Alcohols also appeared in relevant proportions, especially 2-methylpropanol (7.1%), 2-methylbutanol (1.5%), in addition to polyoxygenated alcohols derived from thermal rearrangement processes of carbohydrates. The presence of furanoid TMS compounds, such as trimethyl[(tetrahydrofurfuryl)oxy]silane (10.4%), indicates the expressive participation of hemicellulose, since furan derivatives are classic products of the thermal degradation of pentoses. These results are consistent with studies that identified furan oxides and oxygenated alcohols as relevant constituents in bio-oils obtained under similar pyrolysis conditions (Shen; Gu, 2009).

The fraction of aldehydes and ketones occurred in lower percentages but includes important compounds such as 3-hydroxy-2-butanone (1.2%), hydroxyacetophenones (1.5%), and methoxylated benzaldehydes, which are structural derivatives of lignin and

carbohydrate dehydration and rearrangement reactions. Although less abundant, these compounds contribute significantly to the reactivity, instability, and characteristic odor of bio-oils. Works on the pyrolysis of peach stones and other aromatic biomasses also point to phenol aldehydes as recurrent constituents of the chromatographic profile (Farooq et al., 2018).

Overall, the profile presented confirms that the analyzed pyroligneous liquor is strongly influenced by lignin degradation, with phenols as the predominant class, followed by acids and alcohols derived from hemicellulose and cellulose. This pattern is widely recognized in GC-MS and GC×GC-TOFMS studies applied to peach stone bio-oil, which frequently highlight syringol, guaiacol, catechol, and furanic derivatives as majority peaks. Thus, the results in Table 3 show that the chemical composition obtained is typical of bio-oils derived from lignocellulosic fruit residues (Farrapeira et al., 2021; Moraes et al., 2012).

5 CONCLUSIONS

The comparison between sample preparation methods showed that lyophilization (LYO) outperforms liquid–liquid extraction (LLE) for GC/MS characterization of the aqueous phase of pyroligneous liquid. LYO provided higher and more consistent recoveries, enhancing the detection of organic acids, polyoxygenated alcohols, sugars and low-molecular-weight phenols. Water removal by sublimation helped reduce losses of volatile compounds and minimized analytical discrimination typical of highly hydrophilic matrices.

Although LLE is a traditional and widely applied method, its performance was limited by solvent saturation, low extraction efficiency for highly polar compounds and analyte loss during solvent evaporation. Still, it remained consistent with literature trends in recovering lignin-derived phenols.

Overall, LYO stands out as a more robust, reproducible and environmentally friendly strategy, significantly reducing solvent consumption and waste generation. Its results indicate a chemical profile more representative of the original matrix, reinforcing its suitability for studies aiming to better understand the composition and behavior of aqueous phases of bio-oils derived from lignocellulosic biomass.

REFERENCES

ARAZO, R. O. et al. Bio-oil production from dry sewage sludge by fast pyrolysis in an electrically-heated fluidized bed reactor. Sustainable Environment Research, v. 27, n. 1, p. 7–14, 2017.

BALDACONI, A. Efeito da secagem por liofilização e do método de extração de bioativos do abacate e sua influência na atividade antioxidante. 2021. Trabalho de Conclusão de Curso (Tecnologia em Processos Químicos) – Universidade Tecnológica Federal do Paraná, Toledo, 2021. Disponível em: http://repositorio.utfpr.edu.br/jspui/handle/1/26796.

BETEMPS, G. R. et al. Chromatographic characterization of bio-oil generated from rapid pyrolysis of rice husk in stainless steel reactor. Microchemistry Journal, v. 134, p. 218–223, 2017. DOI: 10.1016/j.microc.2017.06.007.

BRIDGWATER, A. V. Review of fast pyrolysis of biomass and product upgrading. Biomass & Bioenergy, v. 38, p. 68–94, 2012.

BRITO, N. M. et al. Validação de métodos analíticos: estratégia e discussão. Pesticidas: Revista de Ecotoxicologia e Meio Ambiente, v. 13, p. 129–146, 2003. DOI: 10.5380/pes.v13i0.3173.

DE SOUSA, E. M. et al. Characterization of the aqueous phase from pyrolysis of açaí seeds and fibers (Euterpe oleracea Mart.). Energies, v. 18, n. 14, p. 3820, 2025. DOI: 10.3390/en18143820.

DIAS, I. A. Estabilidade físico-química da fase aquosa resultante do fracionamento do bio-óleo. 2021. Dissertação (Mestrado em Química) – Universidade Federal do Paraná, Curitiba, 2021.

FAROOQ, M. et al. Characterization and optimization of bio-oil from pyrolysis of lignocellulosic biomass. Energy Conversion and Management, v. 165, p. 628–639, 2018.

FARRAPEIRA, R. O. et al. GC×GC in the characterization of bio-oil from Brazilian biomasses. Brazilian Journal of Analytical Chemistry, v. 8, n. 31, p. 66–81, 2021.

KHAN, M. Z. et al. Agricultural waste management strategies for environmental sustainability. Environmental Pollution, v. 316, p. 120–128, 2023.

LU, G.; WU, S. Analytical pyrolysis studies of corn stalk and its three main components by TG-MS and Py-GC/MS. Journal of Analytical and Applied Pyrolysis, v. 97, p. 8–11, 2012. DOI: 10.1016/j.jaap.2012.04.010.

MARTINS, A. F. et al. Caracterização dos produtos líquidos e do carvão da pirólise de serragem de eucalipto. Química Nova, v. 30, p. 873–878, 2007. DOI: 10.1590/S0100-40422007000400021.

MORAES, M. S. A. et al. Qualitative analysis of bio-oils of agricultural residues obtained through pyrolysis using comprehensive two dimensional gas chromatography with time-of-flight mass spectrometric detector. Journal of Analytical and Applied Pyrolysis, v. 98, p. 51–64, 2012. DOI: 10.1016/j.jaap.2012.05.007.

PESENTI, M. C. Caracterização química do extrato pirolenhoso obtido a partir de Eucalyptus grandis e testes alelopáticos da fração destilada. 2021. Dissertação (Mestrado) – Universidade Tecnológica Federal do Paraná, Curitiba, 2021.

RUIZ-MATUTE, A. I. et al. Derivatization of carbohydrates for GC and GC–MS analyses. Journal of Chromatography B, v. 879, p. 1226–1240, 2011. DOI: 10.1016/j.jchromb.2010.11.013.

SANCHES FILHO, P. J. et al. Application of the SARA method for determination of hydrocarbons by GC/qMS in bio-oil obtained by fast pyrolysis of rice husk. Microchemical Journal, v. 135, p. 226–238, 2017. DOI: 10.1016/j.microc.2017.08.015.

SANCHES FILHO, P. J. et al. Use of lyophilization as analytical strategy for chromatographic characterization of aqueous phase of bio-oil produced by rice husk pyrolysis. Microchemical Journal, v. 152, 104457, 2020. DOI: 10.1016/j.microc.2019.104457.

SHEN, D.; GU, S. The mechanism for thermal decomposition of cellulose and its main products. Bioresource Technology, v. 100, p. 6496–6504, 2009.

SONG, J. et al. Separation of chemical groups from bio-oil aqueous phase via sequential processes for upgrading. OSTI – U.S. Department of Energy, 2014. Disponível em: https://www.osti.gov/servlets/purl/1356890.

SPOKAS, K. A. et al. Qualitative analysis of volatile organic compounds on biochar. Chemosphere, v. 85, n. 5, p. 869–882, 2011. DOI: 10.1016/j.chemosphere.2011.06.108.

VALADÃO, L. S et al. Chromatographic characterization of pyroligneous liquid obtained from carbonization of peach stone. Revista Ibero-Americana de Ciências Ambientais, v. 10, n. 3, p. 207–218, 2019. DOI: 10.6008/CBPC2179-6858.2019.003.0018.

VAN DE VELDEN, M. et al. Fundamentals, kinetics and endothermicity of the biomass pyrolysis reaction. Renewable Energy, v. 35, n. 1, p. 232–242, 2010.

VON MÜHLEN, C. Índices de retenção em cromatografia gasosa bidimensional abrangente. Sci Chromatogr, v. 1, n. 3, p. 21–28, 2009.

ZHOU, Q. et al. Bioupgrading of the aqueous phase of pyrolysis oil from lignocellulosic biomass. Bioresources and Bioprocessing, v. 10, n. 34, 2023. DOI: 10.1186/s40643-023-00654-3.

CHAPTER 3:
PRODUCTION OF REDUCING SUGARS FROM THE LIGNOCELLULOSIC CONTENT OF ANNONI GRASS (*ERAGROSTIS PLANA NEES*)

Jander Luis Fernandes Monks, Mauricio Campesato Padilha, Daniela Härter Hörnke, Carlos Schaedler, Ricardo Peraça Toralles

ABSTRACT

Annoni grass (*Eragrostis plana Nees*) is a weed with high fiber content and invasive characteristics, limiting efficiency in livestock productivity. Previous studies show that lignocellulose-rich materials possess a highly rigid cell wall and low porosity, which limits their direct utilization in fermentation processes. The hypothesis to be tested is that these limitations can be overcome and reducing sugars can be obtained from Annoni grass leaves through a process combining hydrothermal pretreatment and enzymatic hydrolysis. Thus, the objective of this work was to optimize the extraction of reducing sugars from Annoni grass, aiming at the availability of a new organic feedstock for sustainable energy production. The experiment was conducted at the facilities of IFSul Pelotas, Brazil, where Annoni grass specimens were cultivated in a greenhouse under controlled conditions. Acid and alkaline pretreatment (1% w/w solutions) was performed on the dried samples in autoclave reactors containing ground Annoni grass leaves at a temperature of 165ºC for one hour, evaluating the difference in efficiency between crushed sample sizes. Subsequently, enzymatic hydrolysis was conducted with the material produced in the previous step, with the addition of a pH 4.89 buffer solution and enzyme extract under agitation of 150 rpm at 50°C for 168 hours. The results indicate a higher production of reducing sugars in finely ground leaves subjected to acid treatment and an optimal enzymatic hydrolysis time of 96 hours.

Keywords: Weed; Biomass; Cellulose; Sustainability.

1 INTRODUCTION

Annoni grass is a species native to Africa that was introduced to Brazil in the 1950s primarily identified as a low-quality forage (MEDEIROS et al., 2009; REIS, 1991), presenting high fiber content that often causes injuries to the mouths of grazing animals. As a weed, Annoni grass exhibits high seed production, which facilitates its spread and increases infestation levels in pasture areas. (MEDEIROS et al., 2007).

Lignocellulosic biomass pretreatment is a crucial step to render the cellulose structure more accessible to cellulolytic enzymes, facilitating the recovery of glucose monomers required for subsequent enzymatic hydrolysis. Enzymatic hydrolysis is generally preferred over chemical hydrolysis due to higher sugar yields, lower byproduct formation, and milder operating conditions (LEONEL, 2020).

However, lignocellulosic biomass hydrolysis, aiming at the production of fermentable sugars, presents very low yields, rendering pretreatment as an indispensable

method of modifying the lignocellulosic structure to facilitate the action of cellulolytic enzymes. Although widely used in the industry, enzymatic hydrolysis still faces challenges such as the high cost of enzymes and the difficulty regarding their recovery subsequently highlighting the need to investigate methods to reduce process costs and enhance economic viability (ROCHA, 2021).

Given the high availability of Annoni grass and the need to utilize cellulosic sources as an alternative for renewable energy production, this study is proposed of a process that combines pretreatment and enzymatic hydrolysis, aiming to the production of reducing sugars from the species *Eragrostis plana Nees*.

2 THEORETICAL FRAMEWORK

The Pampa is one of the six biomes or major natural regions of Brazil, being the only one restricted to a single state, occupying a surface of 178,000 km², which represents 63% of the territory of Rio Grande do Sul/Brazil and 2.1% of the national territory (CHOMENKO; BENCKE, 2016).

The Pampa also encompasses Uruguay, east-central Argentina, and the extreme southeast of Paraguay, representing the largest extension of temperate grassland ecosystems in South America. Historically, the Pampa fields have harbored diverse endemic plant and animal species, resulting in rich and abundant biodiversity. Furthermore, it provides a series of essential ecosystem services such as water purification, agricultural pest control, carbon storage (contributing to climate regulation), erosion control, and soil fertility replenishment. Additionally, the Pampa Biome is an important source of genetic resources, primarily forage and ornamental plants (CHOMENKO; BENCKE, 2016).

Throughout its evolution, the fields of the Pampa region were subject to natural disturbance regimes determined to be caused by factors such as spontaneous fires and grazing of native herbivores. Livestock farming is part of the Pampa Biome's history and has great economic and social importance for the state of Rio Grande do Sul. Currently, around 12 million heads of cattle in Rio Grande do Sul (IBGE, 2023) are managed amidst temporary summer crops, primarily soybeans, which expand rapidly over the same areas occupied by this herd.

In the period between 2004 and 2019, the land incorporated into agriculture increased by 808.5 thousand hectares (with soybeans accounting for 736 thousand hectares), allowing the inference that livestock activity is being replaced by agriculture (OLIVEIRA, 2021).

The use of natural pastures of the Pampa Biome for livestock is historic, but inadequate management has led to degradation. This degradation is amplified and favored by one of the major threats to biome biodiversity, which is the invasion by Annoni grass (*Eragrostis plana Nees*).

The invasive species originating from South Africa is recognized for its low forage quality (REIS, 1993), as such, it is frequently rejected by grazing cattle and sheep. Its character as an invasive plant was verified by its rapid proliferation, competition, and elimination of other species (REIS, 1993; REIS; COELHO, 2000).

Economic and environmental damages result from the presence and area expansion of Annoni grass over the 6.5 million hectares of native pasture where beef cattle fields in RS and remnants of grassland vegetation are located (HASENACK et al., 2007). This vegetation is typical of the Pampa Biome, which presents rich floristic diversity and forage value.

It is estimated that two million hectares of this area are already compromised by the presence of the invader (MEDEIROS et al., 2004), representing a major threat to local biodiversity. Annoni grass is mentioned among 1,214 exotic species established in Brazil, of which 460 were recognized as invasive over 35 analyzed years (ADELINO et al., 2021).

Currently, one of the major challenges faced by society is reconciling the growth of energy demand with the great need for sustainability, as the gradual depletion of fossil fuels and greenhouse gas emissions have stimulated the use of renewable, sustainable, and low-cost energy sources. In view of this, second-generation ethanol (bioethanol) has been gaining prominence as an alternative to petroleum-derived fuels, as it is generated from lignocellulosic biomass (SANTIAGO; RODRIGUES, 2017).

The utilization of lignocellulosic materials requires pretreatment steps due to their resistance to biological processing, thus enabling the fractionation of their main components (cellulose, hemicellulose, and lignin). The conditions and type of pretreatment used direct the subsequent steps of lignocellulosic biomass processing (CASTRO, 2016).

Cellulose is the most abundant renewable resource in our natural ecosystem. Furthermore, it has high potential for the mass production of biofuels and renewable chemicals. However, cellulose consists of linear chains of linked β-D-glucose units. This fact makes this structure highly ordered primarily due to strong hydrogen bonds and, as a result, it becomes very resistant to enzymatic and microbial attacks (KHODAVERDI et al., 2012).

Thus, in the economically viable production of fermentable sugars aiming at bioethanol, cellulose hydrolysis is a main and challenging part of the process. The cellulose hydrolysis process is generally performed by enzymes or chemicals. Enzymatic hydrolysis is preferred due to higher sugar yields, lower by-product formation, and milder operating conditions (LYND et al., 2002).

Since the sugar yield in the hydrolysis of native celluloses is very low, pretreatment of cellulose prior to enzymatic hydrolysis is necessary to modify the cellulose structure and enable its enzymatic conversion. Various pretreatments have been suggested and developed, including biological, physical, chemical, and physicochemical methods. Among these processes, pretreatment with cellulose solvents and acid treatment prove to be quite effective (CARVALHO, 2017).

Performing adequate pretreatment enables cellulolytic enzymes access to the cellulose structure and the recovery of glucose monomers composing cellulose for the subsequent steps of enzymatic hydrolysis and alcoholic fermentation for bioethanol production (HUANG et al., 2015; MADADI et al., 2017). Despite being widely used in the industry, the use of enzymes for cellulose hydrolysis presents some limitations, such as high cost and difficulty in enzymatic recovery, making it necessary in this context to investigate ways to reduce process costs (ROCHA, 2021).

Fermentable sugars obtained from pretreated and enzymatically hydrolyzed cellulose are the standard substrates for yeast action, which are the most important microorganisms in obtaining alcohol via fermentation (FERREIRA et al., 2016).

Due to the large production of plant biomass, weeds such as Annoni grass emerge as potential sugar sources to produce lignocellulosic ethanol and are categorized as second-generation biofuels for being produced from alternative inputs.

3 METHODOLOGY

The research utilized the invasive species Annoni grass (*Eragrostis plana Nees*) cultivated in the rural area of the IFSul Pelotas Visconde da Graça Campus/Brazil.

Samples were dried in an oven at 60ºC for 72 hours until they reached constant weight. For pretreatment, ground leaves were separated using a 16-mesh sieve into passing and retained fractions.

Hydrothermal pretreatment occurred in a 25 mL stainless steel autoclave reactor. Into it, 1g of dried Annoni grass, 15 mL of distilled water, and 0.15 mL of analytical grade sulfuric acid were added to test the acid catalyst. For the alkaline catalyst test, separately,

1g of dry Annoni grass and 15.15 mL of 1% w/w aqueous NaOH solution were added. The mixture was then subjected to a temperature of 165ºC in an oven for 60 minutes. Four batches of four reactors each were repeated, totaling 24 grams of treated grass samples.

For the enzymatic hydrolysis operation, the content of eight reactors (solid phase and liquid phase) used in the pretreatment was placed in an Erlenmeyer flask, then combined with 0.1488 grams of enzymatic concentrate Cellic CTec3 with 28.51 mL of pH 4.89 buffer solution. The solution present in the flask was placed in a Benchtop Incubator with Orbital Shaking (Q816M22, Quimis, Brazil) at 150 rpm and 50ºC for 168 hours. At each cited time, in the aqueous extract, the concentrations (g L^{-1}) of fermentable sugars were determined: glucose and total reducing sugars (RS).

To determine glucose concentration, the methodology described in the instruction manual for glucose determination using colorimetric enzymatic monoreagent (GOD-PAP) (Quibasa, Brazil) was adapted.

In each 0.10 mL aliquot of analyzed sample, 2.0 mL of the monoreagent was added. After a water bath at 37ºC for 10 min, 1.0 mL of distilled water was added at room temperature. The reading in a UV/VIS spectrophotometer (AJX-1000, AJMICRONAL) was taken at 505 nm.

The concentration of reducing sugars (RS) was determined using the method described by Pereira (2024) using 1 mL of 3,5-dinitrosalicylic acid (DNS, Sigma Aldrich Chemie GmbH, Germany), 1 mL of extract, and 1 mL of distilled water, followed by a water bath (JProlab Model 8370) at 100ºC for 5 min, with reading in a UV/VIS spectrophotometer (AJX-1000, AJMICRONAL) at 490 nm. The concentration of RS (g L^{-1}) in the reactive medium was determined through an external calibration curve, using glucose (Sigma Aldrich Chemie GmbH, Germany) as standard in concentrations from 0 to 1.0 g L^{-1}.

The data obtained were calculated as means and standard deviations of independent experiments, performed in triplicate, with means compared by Tukey's test at a 5% probability level using the Statistica 7.1 for Windows program (StatSoft Inc., USA).

4 RESULTS AND DISCUSSION

In this chapter, experimentally obtained data aiming at the maximum production of total reducing sugars and glucose from Annoni grass biomass are presented and discussed. The investigation was conducted in two main stages: optimization of acid pretreatment for the destructuration of the lignocellulosic matrix and subsequent enzymatic hydrolysis of

the remaining substrate that received hydrothermal-acid treatment under optimal pre-treatment conditions.

The results of pretreatments and enzymatic hydrolysis are analyzed from the perspective of the conversion efficiency of lignocellulosic material into glucose and RS. The discussion debates justifications for the concentration values obtained through physicochemical mechanisms governing the release of fermentable sugars in this specific biomass and compares results with relevant literature on the transformation of lignocellulosic biomass into sugars whenever possible.

4.1. OPTIMIZATION OF PRETREATMENT

The pretreatment is a determining step in the economic viability of the process employed for biomass conversion, with the main objective of removing the hemicellulose and lignin barrier, increasing the porosity and accessibility of cellulose, which reacts by adsorption with the enzymatic medium employed subsequently. Thus, the production of fermentable sugars in the pretreatment of Annoni grass was optimized by studying the influence of the type of catalyst (NaOH and H_2SO_4) and sample size on this process.

4.1.1. Effect of catalyst type

The choice of acid catalyst plays a fundamental role in the hydrolysis kinetics of lignocellulosic material. Two different agents were evaluated (H_2SO_4 e NaOH 1% w/w), in dry and crushed annoni grass passing through (<1.0 mm), while keeping temperature and residence time constant. Table 1 presents the sugar release profile obtained.

Table 1. Means and standard deviations of glucose and RS concentrations after acid hydrothermal pretreatment with different catalysts.

Treatments	Reducing Sugar (g L^{-1})	Glucose (g L^{-1})
H_2SO_4	$20.73 \pm 0.88^{a*}$	2.85 ± 0.06^{a}
NaOH	1.51 ± 0.32^{b}	0.19 ± 0.01^{b}

Results are expressed as mean ± standard deviation (n = 3); compared by Tukey's method at 5% significance level ($p \leq 0.05$)

*Values with distinct letters in the column differ significantly.

Tukey's test at 5% evidenced that sulfuric acid promoted the highest release of total reducing sugars (20,73 g L^{-1}) and glucose (2,85 g L^{-1}), significantly surpassing alkaline treatment with NaOH.

This behavior consolidates dilute acid pretreatment (DAP) as one of the most promising methods for biomass bioconversion, given its high efficiency in hemicellulose

depolymerization, an essential characteristic for the economic viability of second-generation ethanol production (PASQUIER, 2023).

The superiority of acid treatment over basic treatment can be explained by the acid-catalyzed chemical hydrolysis mechanism. Unlike alkaline treatment, which acts primarily on lignin solubilization, acid promotes protonation of glycosidic oxygen, forming conjugated acids. This step is followed by C-O bond cleavage and formation of a cyclic carbocation in which, after rapid water addition, results in the release of monomeric sugar units (CHAGAS, 2023; PAULA et al., 2009; PEREIRA, 2024). This mechanism justifies the higher concentration of sugars in the acid liquor, since the hemicellulosic fraction is converted mostly into soluble monosaccharides.

Literature corroborates the superiority of sulfuric acid in releasing reducing sugars (COSTA, 2022; PEREIRA, 2024; RODRIGUES, 2018). However, severe DAP conditions may induce the formation of inhibitors such as furfural and hidroximethylfurfural, demanding process optimization to avoid detriments to the subsequent fermentation step (CASTRO, 2016; CHEAH et al., 2020; SRIVASTAVA et al., 2023).

4.1.2. Effect of Annoni grass particle size

The influence of biomass granulometry on pretreatment efficiency was investigated by comparing fractions separated through a Tyler 16 sieve (approximate opening of 1.0 mm). Two distinct fractions were analyzed: the one that passed through the sieve (passing, < 1.0 mm) and the one retained (retained, > 1.0 mm).

The particle size of lignocellulosic biomass plays a crucial role in the efficiency of the hydrolysis and fermentation process, directly affecting reaction rate and mass transfer. Structural alterations promoted by milling or cutting increase enzyme-cellulose affinity and, consequently, hydrolysis rate.

According to Woźniak et al. (2025), particle size influences diffusion kinetics, pretreatment efficiency, sugar yield, and lignin removal because smaller particles possess a larger specific surface area, thereby facilitating reagent access; however, excessively fine particles may present handling difficulties. On the other hand, larger particles may not undergo complete pretreatment in their interior due to heat and mass transfer limitations which result in problems for the subsequent hydrolysis step. Therefore, granulometric optimization is essential to achieve high conversions with viable production costs.

Figure 1 illustrates the sugar release behavior for the two studied fractions. Detailed quantitative data, presented in Table 2, corroborate the significant influence of granulometry on the process.

Figure 1. Influence of sample size on sugar concentrations produced in the acid hydrothermal pretreatment step for retained and passing fractions.

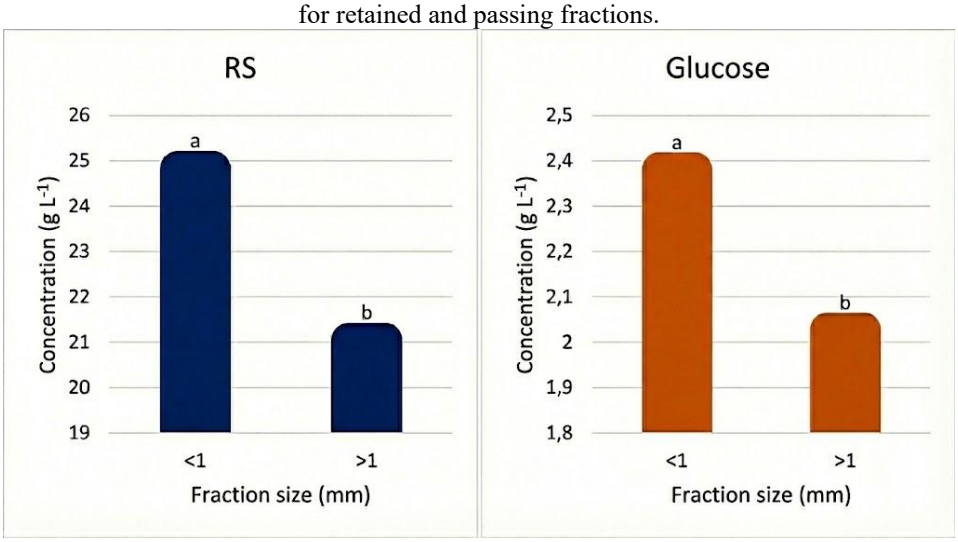

Table 2. Means and standard deviations of glucose and Reducing Sugar (RS) concentrations after acid hydrothermal pretreatment for different sample sizes.

Fraction	Reducing Sugar (g L^{-1})*	Glucose (g L^{-1})*
Retained	21.42 ± 1.66^{b}	2.06 ± 0.15^{b}
Passing	25.20 ± 1.45^{a}	2.42 ± 0.15^{a}

Results are expressed as mean ± standard deviation (n = 3); compared by Tukey's method at 5% significance level ($p \leq 0.05$)

*Values with distinct letters in the column differ significantly

Results demonstrate that the passing fraction in 16 mesh obtained significantly superior yields. The higher concentration of total reducing sugars (25.20 g L^{-1}) and glucose (2.42 g L^{-1}) in this fraction can be attributed to the larger accessible surface area and reduction of diffusion limitations, allowing more effective action of sulfuric acid throughout the particle structure. Conversely, in the retained fraction, reduced efficiency of catalyst penetration into the innermost biomass layers during the stipulated reaction time is observed.

4.2. ENZYMATIC HYDROLYSIS

After defining the best pretreatment conditions with use of sulfuric acid and smaller granulometry, the cellulose-rich biomass was then subjected to enzymatic hydrolysis. This

step aims to convert exposed cellulose into higher concentrations of fermentable sugars, using a commercial enzymatic concentrate on Cellic CTec3.

4.2.1. Reaction Time

Enzymatic hydrolysis kinetics were monitored for 168 hours to determine the point of maximum conversion and stabilization of sugar production. The release profile of reducing sugars (RS) and glucose is displayed in Figure 2 and detailed in Table 3.

Figure 2. Variation in the concentration of reducing sugars (RS) and glucose during 168 hours of enzymatic hydrolysis. The data points represent the mean concentrations with error bars corresponding to the 95% confidence interval.

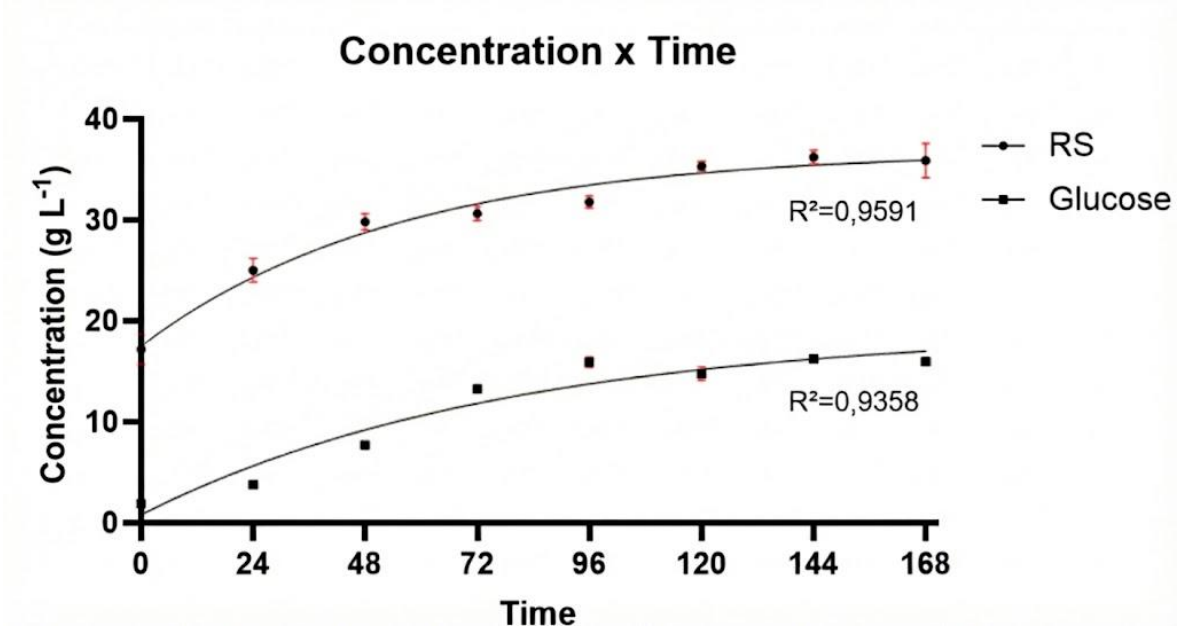

Regression analysis of kinetic data demonstrated that sugar release follows a characteristic asymptotic behavior, fitting precisely to the one-phase association model. The trend curves obtained presented high coefficients of determination (R^2), being 0.9358 for glucose and 0.9591 for reducing sugars. These values indicate that the mathematical model explains more than 93% of experimental data variability, confirming process robustness, and predictability of enzymatic saturation over time.

This behavior, characterized by a fast initial velocity followed by progressive deceleration until a plateau, is consistent with kinetic models reviewed by Pendse et al. (2023), who justify the hydrolysis rate reduction by diffusional resistances and enzymatic deactivation over the reaction course. Furthermore, Zhang et al. (2019) observed similar profiles in sugarcane bagasse hydrolysis, relating the initial fast phase to the degradation

of more accessible amorphous cellulose, while the subsequent slow phase reflects the difficulty in hydrolyzing the remaining crystalline fraction.

Table 3. Means and standard deviations of glucose and reducing sugar concentrations before, during, and after enzymatic hydrolysis of lignocellulosic substrate.

Time (h)	Reducing Sugar (g L^{-1})*	Glucose (g L^{-1})*
0	17.13 ± 1.47^{d}	1.95 ± 0.07^{e}
24	24.97 ± 1.18^{c}	3.80 ± 0.32^{d}
48	29.79 ± 0.79^{b}	7.71 ± 0.02^{c}
72	30.61 ± 0.72^{b}	13.25 ± 0.28^{b}
96	33.75 ± 0.59^{a}	15.87 ± 0.74^{a}
120	35.28 ± 0.52^{a}	14.51 ± 0.79^{a}
144	36.21 ± 0.67^{a}	16.22 ± 0.45^{a}
168	35.86 ± 1.70^{a}	15.94 ± 0.37^{a}

Results are expressed as mean ± standard deviation (n = 3); compared by Tukey's method at 5% significance level ($p \leq 0.05$)

*Values with different letters in the same column differ significantly.

The experiment performed reveals similar kinetic behavior for both glucose and total reducing sugars. It is observed that the concentration of fermentable sugars increases progressively, reaching a peak of 15.87 g L^{-1} for glucose and 33.75 g L^{-1} for RS at 96 hours. Statistical analysis (Tukey, $p \leq 0.05$) indicates no significant difference between the concentration obtained at 96h and subsequent times, suggesting that the system reaches an equilibrium plateau close to this period. Pereira (2024), who reported stabilization close to 120 hours for similar substrates, corroborates this stabilization profile. The fact that this study reaches the plateau early at 96 hours may represent an industrial energy advantage.

The deceleration observed after 96 hours can be explained not only by crystalline cellulose recalcitrance but also by unproductive adsorption of cellulases onto residual lignin, as reported by Xu et al. (2023). Lignin acts as a physical barrier and adsorbent, reducing the availability of free enzymes to act on the cellulosic substrate, a critical phenomenon justifying the observed plateau even with the presence of residual substrate (SANTIAGO; RODRIGUES, 2017).

For industrial optimization purposes, the time of 96 hours presents itself as the ideal cutoff point, balancing yield and operational cost.

4.2.2. Final yield

To quantify the real biomass transformation efficiency, mass yield was calculated, defined as the amount of sugars recovered per unit of processed raw material, considering the total reducing sugars and glucose production peaks at 96 hours.

Table 4. Mass yield of glucose and reducing sugars in Annoni Grass during conversion peak in enzymatic hydrolysis

	Reducing Sugar	Glucose
Mass Yield (%w/w)	66.02	29.70

5 FINAL CONSIDERATIONS

The present study investigated the technical viability of utilizing Annoni grass (*Eragrostis plana Nees*) as lignocellulosic feedstock to produce fermentable sugars, systematically analyzing pretreatment and enzymatic hydrolysis steps.

In the pretreatment stage, acid catalysis (1% w/w H_2SO_4) demonstrated statistical superiority over the alkaline method, evidencing efficacy in hemicellulosic solubilization, crucial for increasing porosity and exposing cellulose. Additionally, granulometric reduction proved critical: the use of the < 1.0 mm fraction resulted in significantly superior yields, confirming that increased surface area and reduced diffusional limitations are essential to optimize reagent-matrix interaction.

Enzymatic hydrolysis kinetics revealed asymptotic behavior, with total reducing sugars and glucose stabilizing after 96 hours (maximum concentration of 36.21 g L^{-1}, 16.22 g L^{-1}; yield of 66.02% w/w, 29.70% w/w, respectively). This profile, even with residual substrate, suggests limitations such as crystalline cellulose recalcitrance and unproductive enzyme adsorption on lignin, factors to be mitigated in future studies.

In summary, this work concludes that Annoni grass possesses promising potential as a substrate for second-generation ethanol production. The integrated route, combining acid pretreatment, adequate milling, and 96 to 120 hours enzymatic hydrolysis, allowed achieving competitive conversion yields that not only valorize this invasive species but also open opportunities for controlling its spread through sustainable economic utilization.

REFERENCES

ADELINO, J.R.P. et al. The economic costs of biological invasions in Brazil: a first assessment. NeoBiota, v.67, p.349-374, 2021. doi: 10.3897/neobiota.67.59185.

BARROCAS, Gustavo Eugenio Gerhard; TANURE, Janaína Paula Marques; GOMES, Rodrigo da Costa. Análises bromatológicas para determinação da qualidade nutricional de forrageiras: compêndio de POPs. Brasília, DF: Embrapa, 2017. (Documentos 306).

CARATTI, F.C. Capim-annoni: germinação, caracterização morfoanatômica, genética e absorção de herbicidas. 2019. Tese (Programa de Pós-Graduação em Fitossanidade) – Universidade Federal de Pelotas.

CARVALHO, J. A. et al. Efeito do pré-tratamento corona em materiais lignocelulósicos. For Science: Revista Científica do IFMG, Formiga, v. 5, n. 2, p. 281, out. 2017.

CASTRO, R. C. A. Produção de etanol a partir da palha de arroz por sacarificação e fermentação simultânea empregando um reator agitado não convencional. 2016. 223p. Tese (Doutorado em Ciências) - Programa de Pós-Graduação em Biotecnologia Industrial na área de Conversão de biomassa, Universidade de São Paulo, Lorena, 2016.

CHOMENKO, L.; BENCKE, G.A (Org). Nosso Pampa desconhecido. Porto Alegre: Fundação Zoobotânica do Rio Grande do Sul, 2016. 208p.

FAVARETTO, A. et al. New Cassane-like diterpenoids from Eragrostis plana. Journal of Agricultural Food Chemistry, v.67, p.1973-1981, 2019. https://doi.org/10.1021/acs.jafc.8b06832

FAVARETTO, A. et al. Pattern of allelochemical distribution in leaves and roots of tough lovegrass (Eragrostis plana Nees, Poaceae). Australian Journal of Crop Science, v.9, p.1119-1125, 2015.

FERREIRA, M.V. et al. Identifying yeast isolated from spoiled peach puree and assessment of its batch culture for invertase production. Food Science and Technology, New York, v.36, n.4, p.701–708, 2016.

HASENACK, H.; CORDEIRO, J.L.P.; COSTA, B.S.C da. Cobertura Vegetal Atual do Rio Grande do Sul. In: Simpósio de Forrageiras E PRODUÇÃO ANIMAL, 2., 2007, Porto Alegre. Anais... Porto Alegre: UFRGS - Departamento de Forrageiras e Agrometeorologia, 2007. p.15-21.

HUANG, Y. et al. Steam explosion distinctively enhances biomass enzymatic saccharification of cotton stalks by largely reducing cellulose polymerization degree in G. barbadense and G. hirsutum. Bioresource Technology, v. 181, p. 224–230, 2015.

IBGE - INSTITUTO BRASILEIRO DE GEOGRAFIA E ESTATÍSTICA. Rebanho de Bovinos (Bois e Vacas) - Pesquisa da Agropecuária Municipal. IBGE, 2023. Disponível em: https://www.ibge.gov.br/explica/producao-agropecuaria/bovinos/rs. Acesso em 31 out. 2024.

KHODAVERDI, M. et al. Kinetic modeling of rapid enzymatic hydrolysis of crystalline cellulose after pretreatment by NMMO. Journal of Industrial Microbiology and Biotechnology, v.39, n.3, p.429–438, 2012.

LAMEGO, F.P. et al. Factors affecting seed germination of Eragrostis plana populations. Advances in Weed Science, v.41, n.1, 2023.

LEONEL, Lillian Vieira. Estratégias visando à melhoria da produção de etanol por Kluyveromyces marxianus pelo processo de sacarificação simultânea à fermentação de cascas de arroz. 2020. 102 f. Tese (Doutorado em Engenharia Agrícola) – Universidade Estadual do Oeste do Paraná, Cascavel - PR

LYND, L. R. et al. Microbial Cellulose Utilization: Fundamentals and Biotechnology. Microbiology and molecular biology reviews, v. 66, n. 3, p. 506-577, set., 2002.

MADADI, M. T. Y.; ABBAS, A. Pretreatment of Lignocelollusic Biomass Based on Improving Enzymatic Hydrolysis. Journal for Research in Applied Sciences and Biotechnology,, v. 5, n. 1, p. 1-11, 2017.

MEDEIROS, R. B. de; FOCHT, T.; SAIBRO, J. C. do. Invasão, prevenção, controle e utilização do capim-annoni-2 (Eragrostis plana Nees) no Rio Grande do Sul, Brasil. Pesquisa Agropecuária Gaúcha, Porto Alegre, v. 13, n. 1/2, p. 105–114, 2007. Disponível em: https://revistapag.agricultura.rs.gov.br/ojs/index.php/revistapag/article/view/259. Acesso em: 1 dez. 2025.

MEDEIROS, R.B. de; SAIBRO, J.C. de; FOCHT, T. Invasão de capim-annoni (Eragrostis plana Nees) no bioma Pampa do Rio Grande do Sul. In: CAMPOS SULINOS conservação e uso sustentável da biodiversidade. Valério De Patta Pillar (et al.). Editores. – Brasília: MMA, 2009.

MEDEIROS, R. B.; PILLAR, V. P.; REIS, J. C. L. Expansão de Eragrostis plana Ness (capim-annoni-2), no Rio Grande do Sul e Indicativos de Controle. In: (Grupo Campos, Org.) 2004, Salto. Reunión del grupo técnico regional del Cono Sur en mejoramiento y utilización de los recursos forrajeros del área tropical y subtropical, 20. Salto: [s. n.], 2004. p. 208–211.

PEREIRA, E. C. (2024). Hidrólise enzimática da celulose e da casca de arroz com pré-tratamento ácido: parâmetros, modelagem e simulação. 2024. 123 p. TCC (Graduação em Engenharia Química) – Curso Superior de Engenhria Química, IFSUL – Instituto Federal Sul-Rio-Grandense do campus Pelotas, Pelotas, 2024

OLIVEIRA, J. C. P. Revisão sobre o ambiente e a produção agropecuária no bioma Pampa do Brasil. Bagé: Embrapa Pecuária Sul, 2021. Disponível em: https://ainfo.cnptia.embrapa.br/digital/bitstream/item/224144/1/DT-167-online.pdf

REIS, J. C. L. Capim-annoni-2: origem, morfologia, características, disseminação. In: REUNIÃO REGIONAL DE AVALIAÇÃO DE PESQUISA COM ANNONI-2 , Bagé. Anais... Bagé: EMBRAPA-CPPSUL, p. 5-23, 1993. (Documentos, 7).

REIS, J.C.L.; COELHO, R.W. Controle do Capim-Annoni-2 em Campos Naturais e Pastagens. Pelotas: Embrapa Clima Temperado, 2000. 21p. embrapa Clima Temperado, Circular Técnica, 22.

ROCHA, M. A. Otimização computacional da hidrólise enzimática de amido da farinha de arroz cultivar BRS-AG. 2021. 63 p. Dissertação (Mestrado em Engenharia Química) – Programa de Pós-graduação em Engenharia Química, Universidade Federal do Rio Grande, Rio Grande, 2021.

SANTIAGO, B. L. S.; RODRIGUES, F. A. Processamento de biomassa lignocelulósica para produção de etanol: uma revisão. The Journal of Engineering and Exact Sciences- JCEC, v. 03, n. 07, p. 1011-1022, 2017.

CHAGAS, J. S. Estudo cinético do processo de extração sonoquímica de nanocristais de celulose em duas etapas a partir da celulose microcristalina (mcc). Dissertação (Mestrado em Engenharia de Materiais) - Universidade Federal da Paraíba, João Pessoa, 2022.

PAULA, M. P.; LACERDA, T. M.; ZAMBON, M. D.; FROLLINI, E. Hidrólise ácida de celulose de sisal: estudos visando obtenção de nanofibras e de bioetanol. In: 10° Congresso Brasileiro de Polímeros. Foz do Iguaçu, 2009.

PEREIRA, E. C. Enzymatic Hydrolysis of Cellulose and Rice Husk with Acid Pretreatment: Parameters, Modeling, and Simulation. Trabalho de Conclusão de Curso (Curso Superior de Engenharia Química) – Departamento de Graduação e Pós-Graduação, Instituto Federal Sul-rio-grandense – Câmpus Pelotas, Pelotas, 2024.

WOŹNIAK, Adrian et al. Review of Lignocellulosic Biomass Pretreatment Using Physical, Thermal and Chemical Methods for Higher Yields in Bioethanol Production. Sustainability, v. 17, n. 1, p. 287, 2025.

PENDSE, Dhanashri S.; DESHMUKH, Minal; PANDE, Ashwini. Different pre-treatments and kinetic models for bioethanol production from lignocellulosic biomass: A review. Heliyon, v. 9, n. 6, p. e16604, jun. 2023.

XU, Jingliang et al. Employing Cationic Kraft Lignin as Additive to Enhance Enzymatic Hydrolysis of Corn Stalk. Polymers, v. 15, n. 9, p. 1991, 23 abr. 2023.

ZHANG, Hongdan et al. Investigation of alkaline hydrogen peroxide pretreatment and Tween 80 to enhance enzymatic hydrolysis of sugarcane bagasse. Biotechnology for Biofuels, v. 12, n. 1, p. 107, dez. 2019.

CHAPTER 4:
WOOD PRESERVATION AND SOIL CONTAMINATION BY HEAVY METALS

Daniel Arsand, Susane Seus

ABSTRACT

This chapter discusses the environmental implications of wood preservation processes, particularly focusing on soil contamination caused by heavy metals derived from preservative chemicals. Wood preservation is widely used to extend the service life of timber and protect it from biological degradation caused by fungi, insects, and microorganisms. However, the use of chemical preservatives, especially chromated copper arsenate (CCA), has raised significant environmental and health concerns due to its high toxicity and potential for metal leaching. The chapter highlights that CCA-treated wood releases arsenic (As), copper (Cu), and chromium (Cr) into surrounding environments through leaching, volatilization, and improper disposal. These heavy metals may persist in soils for long periods, remaining bioavailable and capable of migrating into groundwater systems, thereby contaminating other environmental compartments. The industrial wood treatment process is also described, including vacuum-pressure impregnation in autoclaves, curing yards, and storage areas. These operational stages represent critical points for potential contamination, particularly when spills, leaks, or inadequate waste management occur. The chapter also reviews Brazilian environmental legislation related to contaminated soils, including guidelines from environmental agencies and regulations establishing soil quality reference values. Consequently, the chapter underscores the importance of environmental monitoring, proper waste management, and the development of safer preservation alternatives. In conclusion, while wood preservation is essential for industrial and infrastructure applications, the environmental risks associated with heavy-metal-based preservatives demand stricter management, monitoring, and sustainable technological solutions to minimize soil contamination and protect environmental and human health.

Keywords: Leaching; Bioavailability; Environmental liability.

1 INTRODUCTION

Due to the usefulness and durability of wood, treatment plants employ preservative products, which are toxic substances designed to inhibit the action of wood-degrading agents. The most widely used preservative is chromated copper arsenate, commonly known as CCA. However, its use is controversial because of its high toxicity and the gradual loss of its components through leaching or volatilization, resulting in risks to the environment and human health. This chapter addresses precisely the issue of soil contamination by heavy metal ions.

2 CONTEXTUALIZATION

Wood preservation aims to increase the service life of wood and wood-derived products by applying chemical agents that prevent attack by biodeteriorating organisms (MORESCHI, 2013). Wood preservation activities are regulated by specific legislation and guided by norms of the Brazilian Association of Technical Standards (ABRAF, 2013). According to the association, the main wood preservation plants are concentrated in the Southeast and South regions, where the largest reforested areas in the country are located.

In Brazil, the use of preservative-treated wood emerged alongside industrial development, which created demands for rapid transportation, new communication systems, and improved energy distribution. These advances required wood with high resistance to xylophagous organisms for use in railways, telegraph systems, telephone lines, and electrification infrastructure (VIDAL et al., 2015).

The Brazilian Institute of Environment and Renewable Natural Resources (IBAMA) authorizes the use of several preservatives, with the most commonly applied by industry being Chromated Copper Arsenate (CCA Type C) and Chromated Copper Borate (CCB) (VIDAL et al., 2015). Due to the extensive use of CCA-treated wood, an increase in residues is expected in the coming decades (CHOI et al., 2012). Mercer and Frostick (2012) reported that As, Cu, and Cr leached from CCA-treated wood residues appeared in the environment at concentrations exceeding permissible limits, posing risks to the environment and human health. Contamination at wood treatment plants has been investigated by several authors (ANDERSON et al., 1996; BHATTACHARYA et al., 2002; JANIN et al., 2009).

Domingos (2020) assessed the toxicological effects of fly ash resulting from the combustion of CCA-treated wood. Analyses of leachate samples revealed arsenic concentrations of 0.46 $mg.mL^{-1}$ and 0.11 $mg.mL^{-1}$. Toxicity tests indicated high levels of acute and subacute toxicity in Lactuca sativa, Allium cepa L., and the microcrustaceans Artemia spp. Takahashi et al. (2018) reported deleterious effects in multiple organs of rats exposed to CCA for 30 days. However, little attention has been given to the effects of CCA and its components on genotoxicity and cell cycle dynamics in exposed organisms.

In addition to their toxic properties, metals and their compounds may remain bioavailable for long periods or migrate into aquifers, spreading contamination to other environmental matrices (FERRUCCI et al., 2017). Reported effects of metal-contaminated soils include inhibition of enzymatic activities due to impaired self-purification capacity linked to biological regeneration processes; qualitative and quantitative reductions in

normal growth of microbial and soil fauna populations; decreased crop yields and altered product composition; and risks to consumer health due to metal incorporation into the food chain (CHEN et al., 2015). Toxic metals may remain bioavailable for extended periods and contaminate other environmental matrices (LI et al., 2014).

In response to these risks, the Brazilian National Environmental Council (CONAMA), through Resolution N°. 420 of December 28, 2009, establishes guidelines and reference values for soil quality regarding the presence of chemical substances, as well as directives for the environmental management of contaminated areas. In the state of Rio Grande do Sul, Technical Guideline N°. 003/2021 – DIRTEC of Environmental Protection Foundation (FEPAM) provides guidance for the environmental licensing of suspect, potentially contaminated, contaminated, or degraded areas due to improper disposal of solid waste.

FEPAM Ordinance N°. 85/2014 establishes Reference Quality Values (RQV) for soils for nine chemical elements naturally present in the different geomorphological and geological provinces of the state, recognizing the importance of determining natural background concentrations and the need to manage contaminated areas resulting from anthropogenic activities.

The State Environmental Code of Rio Grande do Sul, established by State Law N°. 15,434 of January 9, 2020, determines in Article 4 that all individuals are responsible for maintaining a healthy environment that ensures quality of life for present and future generations. It further establishes that individuals and legal entities are responsible for fully repairing environmental damage they cause and for correcting or covering the costs of corrective actions.

Soil contamination resulting from industrial activities or waste disposal constitutes one of the most significant forms of environmental liability (FOGAÇA; CORREA, 2017).

3 WOOD PRESERVATION

Wood has physical–mechanical and anatomical characteristics that make it a highly versatile renewable resource. Among its advantages are thermal insulation, ease of workability, mechanical strength, and low energy consumption during processing. However, its disadvantages include low natural durability, susceptibility to cracking, and combustibility (VIDAL et al., 2015).

In Brazil, the use of preservative-treated wood emerged alongside industrial development, which created demands for rapid transportation, new communication

systems, and improved energy sources. These technological advancements required wood with high resistance to xylophagous organisms for application in railways, telephone lines, and electrification infrastructure (VIDAL et al., 2015). The main biological agents responsible for structural damage and wood deterioration include insects, fungi, mollusks, crustaceans, and bacteria (REMADE, 2013).

The wood industry encompasses the production and harvesting of trees for diverse applications, such as civil construction, shipbuilding, and furniture manufacturing. This sector includes processes for converting wood into sawn timber, pulp and paper, chemical products, and other derivatives, involving extraction, storage, chemical treatment, and final distribution for use (SINDIMADE, 2018).

The natural durability and service life of wood are negatively affected when exposed to environmental factors such as moisture, temperature fluctuations, and light (DHILLON et al., 2017; BOTOMÉ et al., 2017). Eucalyptus and pine species also exhibit low resistance to deterioration caused by insects, bacteria, and fungi when left untreated, making the application of chemical preservatives essential to prolong their durability (MATOS et al., 2020; DHILLON et al., 2017; FERRARINI et al., 2016).

The treatment process begins with the arrival of timber in the form of logs, sawn wood, sleepers, and other products. The wood is placed inside an autoclave, where its moisture is removed under vacuum, and the preservative is subsequently forced into the empty cell spaces. After treatment, the material is transferred to the curing yard, where it remains for approximately 10 days on a concrete surface in an open area. Once curing is complete, the treated wood is sent to the storage yard (MORESCHI, 2013). Currently, Chromated Copper Arsenate (CCA) is the most widely used wood preservative worldwide (ABPM, 2017; FERRARINI et al., 2016; FERRARINI et al., 2015). Figure 1 shows the industrial process for treating wood.

Figure 1. Flowchart about the industrial process for treating wood.

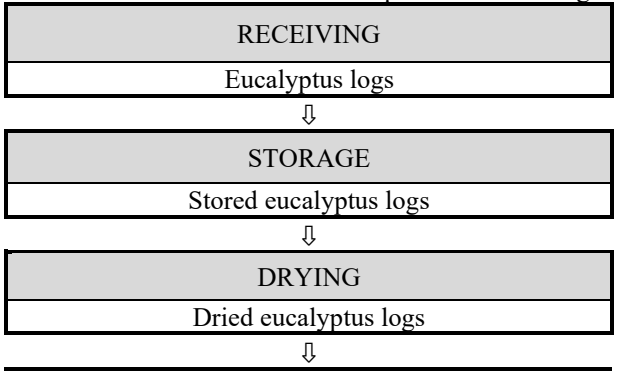

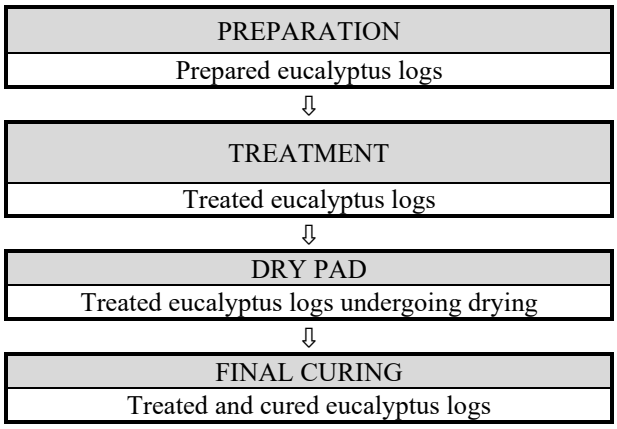

In Brazil, wood treatment methods using pressure in autoclaves are commonly employed, including the Bethell process, developed by John Bethell in 1838 in England. This method consists of an initial vacuum stage, followed by the introduction of the preservative without allowing air to enter the autoclave cylinder, proceeding to the pressure stage in which the product is impregnated into the wood. Subsequently, the preservative is drained, and a final vacuum is applied. While oily preservatives were originally used, water-soluble preservatives are currently predominant. The main preservatives used to prevent biological degradation of wood include creosote and chromated copper arsenate (CCA), which is available in three formulations (Types A, B, and C), as well as chromated copper borate (CCB). Creosote is classified as an oil-soluble preservative, whereas CCA and CCB formulations are water-soluble (VIDAL et al., 2015).

CCB emerged around 1960 as a response to concerns regarding the toxicity of arsenic in CCA, differing from it by replacing arsenic with boron or boric acid (MORESCHI, 2011). Table 1 presents the composition of CCB.

Table 1. Composition of CCB preservative.

COMPOUND	COMPOSITION (%)
CuO	26
B	10.5
CrO_3	63.5

In Brazil, the Brazilian Institute of Environment and Renewable Natural Resources (IBAMA) authorizes the use of several preservatives, with CCA Type C being the most commonly used in industry (VIDAL et al., 2015). Table 2 presents the composition of the different CCA types.

Table 2. Composition of CCA types.

COMPONENT	COMPOSIÇÃO (%)		
	TYPE A	TYPE B	TYPE C
CrO_3	65.5	35.3	47.5
CuO	18.1	19.6	18.5
As_2O_5	16.4	45.1	34.0

Source: Moreschi (2011)

Figure 2 illustrates the molecular structure of CCA.

Figure 2. Molecular structure of CCA

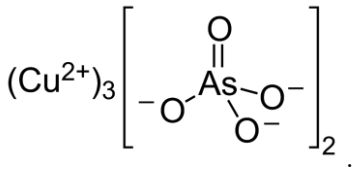

CCA is highly effective as a wood preservative and economically viable compared to other treatments, such as natural preservative oils, thermal modification, and alternative chemical treatments (KIMA; OHB; PARK, 2020; MOHAJERANI et al., 2018; FERRARINI et al., 2016).

When applied to wood under pressure, chromium triggers the precipitation of large amounts of copper and arsenic and reacts with the wood structure, making the preservative components practically insoluble. The fixation reaction induced by chromium enables arsenic to act as an insecticide, while copper functions as a fungicide, adhering to the cellular structures (SILVA, 2006). According to Freitas (2002), CCA is used in three different formulations - Types A, B, and C - all containing approximately 19% copper oxide.

Due to the extensive use of CCA-treated wood, an increase in residues is expected in the coming decades (CHOI et al., 2012; MERCER & FROSTICK, 2012). According to Lebow et al. (2004), the degree of preservative leaching into the environment depends on several factors, including retention level, wood species and age, moisture content, treatment process, weathering, and exposure conditions. Mercer and Frostick (2012) reported that As, Cu, and Cr leached from CCA-treated wood residues appear in the environment at concentrations exceeding permitted limits, posing risks to both the environment and human health.

The Brazilian Association of Technical Standards (ABNT) 16,202 establishes acceptable compositional ranges for the CCA-C preservative (Table 3).

Table 3. Limits established by ABNT 16,202/2013.

COMPOUND	Minimum [%]	Maximum [%]
CuO	17.0	21.0
CrO_3	44.5	50.5
As_2O_5	30.0	38.0

Based on the values presented in Table 3, relationships between the maximum and minimum proportions of the preservative components can be established, as shown in Table 4.

Table 4. Ratio between maximum and minimum component values.

Ratio	Minimum	Maximum
As/Cu	1.765	1.817
As/Cr	0.674	0.752

4 WOOD PRESERVATION AND ENVIRONMENTAL IMPACT

Industrial activities and inadequate management practices have introduced numerous contaminants into soils, including toxic metals and aggressive chemical compounds. Metals naturally participate in biological and geological cycles and are essential for the growth of organisms - from bacteria to humans - yet they are required only in trace concentrations, as excess levels can damage biological systems (FERRUCCI et al., 2017).

Soil contamination by toxic metals is particularly harmful because these elements are persistent, non-degradable, teratogenic, mutagenic, and carcinogenic (ALLOWAY, 2010). Arsenic and chromium are metals that do not naturally occur in any organism and do not perform nutritional or biochemical functions in microorganisms, plants, or animals.

Metals frequently associated with toxicity include arsenic, aluminum, lead, mercury, cadmium, manganese, copper, and iron. The accumulation of these substances in soil or biological systems occurs because they are not biodegradable, and their ingestion can have severe consequences for human and animal health, causing renal, pulmonary, cardiac, neurological, and gastrointestinal disorders, skin irritation, and various cancers, among other effects (MOSCHEM & GONÇALVES, 2020). Chromium and arsenic are known to be potent carcinogens (OHGAMI et al., 2015). Their release from CCA-treated residential structures - including stairs and outdoor installations in apartment complexes in Florida - has prompted extensive research (GRESS et al., 2016).

Among the effects of heavy-metal contamination in soils are the inhibition of enzymatic activities due to the destruction of self-purification capacity via biological regeneration processes, as well as qualitative and quantitative reductions in the natural growth of soil microbial communities. Additional impacts include decreased crop yields and alterations in product composition, posing risks to consumer health due to metal incorporation into the food chain (CHEN et al., 2015).

Arsenic is a significant chemical substance present in air, soil, water, and food. It may occur naturally or as a result of pollution from human activities (FSANZ, 2017). The main pathways of arsenic intoxication involve contaminated water and contact with polluted soil (USEPA, 2000). Tang (2015) reported the persistence of arsenic in soils surrounding playground structures, representing a contamination source for children through dermal contact and ingestion of contaminated soil. Additionally, elevated arsenic concentrations in groundwater are a frequent consequence of the use of CCA-treated wood (ROBINSON et al., 2004; SOUTH et al., 2007).

The most common industrial use of Cr(VI) in recent decades has been chromated copper arsenate (CCA), a water-based wood preservative widely applied in the United States during the 1980s, 1990s, and early 2000s (AWPI, 1999). Since 2003, the U.S. Environmental Protection Agency (EPA) has restricted the use of CCA-treated wood for residential purposes, permitting it only for industrial applications. Countries such as Germany, Australia, and Japan have implemented partial or total restrictions on CCA use. Even after EPA restrictions in 2003, Jambeck et al. (2007) estimated that approximately 9.7 million cubic meters of CCA-treated wood were discarded in the United States in 2008.

In China, such restrictions have not yet been implemented, and CCA-treated wood remains widely used in public parks (TANG et al., 2015). Recently, arsenic concentrations of up to 110 $mg.kg^{-1}$ have been reported in soils adjacent to CCA-treated wood structures (GRESS et al., 2016).

King et al. (2019) also documented the persistence of arsenic in soils surrounding old playground structures as an exposure pathway for children through dermal contact and ingestion of contaminated soil. Takahashi et al. (2018) reported deleterious effects in multiple organs of rats exposed to CCA for one month. However, limited attention has been given to the effects of CCA and its components on genotoxicity and cell-cycle dynamics in exposed organisms.

5 SOIL

Soil is the layer of organic and inorganic material that covers the rocky surface of the Earth. The organic fraction derives from the decomposition of plants and animals and is concentrated in the upper portion of the soil. The inorganic fraction consists of rock fragments. Other components of soil include water and air, whose proportions vary according to rainfall events (MENEZES, 2017). Soil is a rich natural system composed of minerals, organic matter, gases, liquids, and organisms engaged in dynamic interactions (YU et al., 2019). Industrialization and urbanization have resulted in widespread soil contamination by several toxic metals, including Cr, As, Cd, Hg, Pb, Se, Zn, and Ni (GONG et al., 2018).

When contaminants reach the soil through leaks or spills, they undergo geochemical and biological processes and distribute among different phases: vapor phase, residual or adsorbed phase, free phase, and dissolved phase. The distribution of the contaminant depends on its physicochemical characteristics and the type of soil (POLICARPO, 2008). Among the main contaminants are toxic metals, which are considered a major source of soil pollution because they are stable in the environment and cannot be degraded (BORGES, 2007).

Resolution N°. 420 of the National Environmental Council (CONAMA, 2009) establishes criteria and guideline values for soil quality concerning the presence of chemical substances and sets forth directives for the environmental management of areas contaminated by anthropogenic activities. According to CONAMA, prevention values (PV) represent the threshold concentrations below which soil is capable of sustaining its main ecological functions. Investigation values (IV) represent concentrations above which potential risks - direct or indirect - to human health exist.

The quality reference value (QRV) corresponds to the concentration of a given substance that defines the natural quality of the soil and is determined through statistical interpretation of physicochemical analyses of diverse soil types, as recommended by CONAMA Resolution N°. 460/2013. CONAMA established classes to define soil quality according to the concentration of chemical substances:

Class 1 – soils with concentrations of chemical substances less than or equal to the QRV;

Class 2 – soils with concentrations of at least one chemical substance greater than the QRV and less than or equal to the PV;

Class 3 – soils with concentrations of at least one chemical substance greater than the VP and less than or equal to the IV;

Class 4 – soils with concentrations of at least one chemical substance greater than the IV.

Table 5 presents the guideline values for soils according to CONAMA Resolution N°. 420/2009.

Table 5. Guideline values for soils (mg.kg^{-1} dry weight).

Substances	PV[1]	QRV	IV		
			Agricultural	Residential	Industrial
Arsenic	15	0.60	35	55	150
Barium	150	84	300	500	750
Cadmium	1.3	0.5	3	8	20
Lead	72	13	180	300	900
Cobalt	25	4	35	65	90
Copper	60	5	200	400	600
Chromium	75	35	150	300	400
Mercury	0.5	0.1	12	36	70
Nickel	30	9	70	100	130
Vanadium	-	24	-	-	1000
Zinc	300	35	450	1000	2000

Source: Adapted from CONAMA, 2009

[1] Prevention values established in CONAMA Resolution N°. 420/2009.

Ordinance FEPAM N°. 85/2014 establishes RQV for soils for nine chemical elements naturally present in the geomorphological/geological provinces of the state of Rio Grande do Sul (RS). The regulation addresses the importance of determining natural background concentrations to define the intrinsic quality of RS soils and to support proper environmental management of areas contaminated by these substances due to anthropogenic activities. Table 6 presents the reference values (90th percentile) for metals according to different soil groups.

Table 6. QRV (90th percentile) by soil group based on geomorphological/geological provinces of Rio Grande do Sul.

Elementos (mg.kg^{-1})	Grupos de solos originados das províncias geomorfológicas/geológicas do RS				
	(1)	(2)	(3)	(4)	(5)
Zn	120	31	31	29	33
Cu	203	9	13	11	37
Cr	94	40	25	21	27
Ni	47	12	10	7	11
Pb	36	18	19	16	27
Cd	0.59	0.40	0.38	0.42	0.36
Co	75	13	8	7	29
V	567	48	56	76	177
Hg	0.073	0.034	0.043	0.015	0.105

Source: Adapted from Ordinance FEPAM N°. 85/2014.

The mobility and retention of toxic metals in soil vary according to their properties, such as pH, cation-exchange capacity, organic matter content, quantity and type of clay fraction, and ionic competition (CETESB, 2001). Regarding the incorporation of non-hazardous industrial biosolids into agricultural soils, Ordinance FEPAM N°. 80/2020 specifies that the application of biosolids is prohibited in agricultural areas that exhibit metal concentrations within the investigation-level thresholds of CONAMA Resolution 420/2009.

6 MONITORING OF METALS IN SOILS

The determination of metals in soil samples and the evaluation of their concentrations are generally performed using atomic absorption spectrophotometry. The analytical digestion method most commonly employed for soil samples is that of the United States Environmental Protection Agency (USEPA), known as EPA 3052, whose purpose is the complete decomposition of the sample matrix.

According to this method, representative samples of 0.5 g are digested in 9 mL of concentrated nitric acid and 3 mL of hydrofluoric acid for 15 minutes using microwave-assisted heating. The sample and acids are placed into inert digestion vessels. The vessel is then sealed and heated in a microwave digestion system. After cooling, the vessel contents are filtered, centrifuged, decanted, diluted, and subsequently analyzed using the selected instrumentation.

REFERENCES

ASSOCIAÇÃO BRASILEIRA DE PRODUTORES DE FLORESTAS PLANTADAS (ABRAF). Anuário estatístico da ABRAF: ano base 2012. Brasília, 2013.

ALLOWAY, B.J. Heavy metals in soils: trace metals and metalloids in soils and their bioavailability. 3. ed. Ontario: Springer, 613 p.,2010.

ASSOCIAÇÃO BRASILEIRA DE NORMAS TÉCNICAS – ABNT. (2004b). NBR 10005: Procedimento para Obtenção de Extrato Lixiviado de Resíduos Sólidos (3 p.). Rio de Janeiro: ABNT. Associação Brasileira de Produtores de Florestas Plantadas – ABRAF. (2012). Anuário estatístico da ABRAF 2012: ano base 2011 (150 p.). Brasília: ABRAF.

ASSOCIAÇÃO BRASILEIRA DE PRESERVADORES DE MADEIRA. ABNT publica duas normas técnicas que marcam o início de nova fase do setor de madeira tratada no país, ABPM, São Paulo. 2017. Disponível em: http://www.abpm.com.br/noticia. Acesso em: 02 fevereiro 2023.

ASSOCIAÇÃO BRASILEIRA DOS PRESERVADORES DE MADEIRA – ABPM. (2016). Boletim Eletrônico Quinzenal, 14(659). Recuperado em 3 de outubro de 2016, de http://www.abpm.com.br.

ASSOCIAÇÃO BRASILEIRA DE NORMAS TÉCNICAS – ABNT. NBR-9480: Moirões de madeiras preservada para cercas. Rio de Janeiro, 1986.

ASSOCIAÇÃO BRASILEIRA DE NORMAS TÉCNICAS – ABNT. NBR 16202: Postes de Eucalipto Preservados para Redes de Distribuição. Rio de Janeiro, 2013.65 p.

BHATTACHARYA P, MUKHERJEE AB, JACKS G, NORDQVIST S. Metal contamination at a wood preservation site: characterisation and experimental studies on remediation. Sci Total Environ. 2002 May 6;290(1-3):165-80. doi: 10.1016/s0048-9697(01)01073-7. PMID: 12083708.

BOTOMÉ, M. L.; POLETTO, P.; JUNGES, J.; PERONDI, D.; DETTMER, A.; GODINHO, M. Preparation and characterization of a metal-rich activated carbon from CCA-treated wood for CO2 capture. Chemical Engineering Journal, v. 321, p. 614-621, 2017.

BORGES, R.C. Aplicação de resíduo URA na remediação química de solos contaminados por Cd, Pb e Zn. 2007, 95f. Dissertação (Mestrado em Ciência do Solo), Universidade Federal Rural do Rio de Janeiro, Seropédica, 2007.

BRASIL. MINISTÉRIO DO MEIO AMBIENTE – Conselho Nacional de Meio Ambiente. Resolução CONAMA n° 420/2009. Dispõe sobre critérios e valores orientadores de qualidade do solo quanto à presença de substâncias químicas e estabelece diretrizes para o gerenciamento ambiental de áreas contaminadas por essas substâncias em decorrência de atividades antrópicas. Diário Oficial da União, 30 de dezembro de 2009.

BRASIL. MINISTÉRIO DO MEIO AMBIENTE – Conselho Nacional de Meio Ambiente. Resolução CONAMA n° 460/2013. Altera a Resolução CONAMA no 420, de 28 de dezembro de 2009, que dispõe sobre critérios e valores orientadores de qualidade do solo quanto à presença de substâncias químicas e dá outras providências.

CHEN, H; TENG, Y; LU, S; WANG, Y; WANG, J. Contamination features and health risk of soil heavy metals in China. Elsevier Science of the total Environment, v. 512-513, p. 143-153, 2015.

CHOI, Y.S; BYOUNG, J. A; KIM.G.H. Extraction of chromium, copper, and arsenic from CCA – treated wood by using wood vinegar. Elsevier, Bioresource Technology 120, 328-331, 2012.

DHILLON, G. S.; ROSINE, G. M. L.; KAUR, S.; HEGDE, K.; BRAR, S. K.; DROGUI, P.; VERMA, M. Novel biomaterials from citric acid fermentation as biosorbents for removal of metals from waste chromated copper arsenate wood leachates. International Biodeterioration & Biodegradation, v. 119, p. 147-154, 2017.

EPA - ENVIRONMENTAL PROTECTION AGENCY. Method 3052: microwave assisted acid digestion of siliceous and organically based matrices. United States, 1996.

FEPAM - Fundação Estadual de Proteção Ambiental Henrique Luiz Roessler/RS. Portaria n.º 85 de 05 de setembro de 2014. Dispõe sobre o estabelecimento de Valores de Referência de Qualidade (VRQ) dos solos para 09 (nove) elementos químicos naturalmente presentes nas diferentes províncias geomorfológicas/geológicas do Estado do Rio Grande do Sul, Porto Alegre, 2014.

FERRARINI, S. F.; DOS SANTOS, H. S.; MIRANDA, L. G.; AZEVEDO, C. M. N.; MAIA, S. M.; PIRES, M. Descontamination of CCA-treated eucalyptus wood waste by acid leaching. Waste Management, v. 49, p. 253-262, 2016.

FERRARINI, S. F.; MIRANDA, L. G.; MAIA, S. M.; PIRES, M. Madeira tratada com arseniato de cobre cromatado (CCA): opções de destino para os resíduos gerados e perspectivas no desenvolvimento de metodologias para a remoção de elementos tóxicos. Periódico Tchê Química, v. 12, p. 7-21, 2015.

FERRUCCI, A.; VOCCIANTE, M.; BAGATIN, R.; FERRO, S. Electrokinetic remediation of soils contaminated by potentially toxic metals: Dedicated analytical tools for assessing the contamination baseline in a complex scenario. Journal of Environmental Managemet, v. 2003, p. 1163-1168, 2017.

FOGAÇA, A. T. P.; CORREA, C. C.; Investigação Ambiental e suas Etapas: um Estudo de Caso para Locação de Imóvel. INOVAE - ISSN: 2357-7797, São Paulo, v. 5, n. 2, p. 96-107, 2017.

FREITAS, V. P. Variações na retenção do CCA-A em estacas de Pinus após 21 anos de exposição em campo de apodrecimento. 2002. 76 f. Dissertação (Mestrado em Recursos Florestais). Universidade de São Paulo, São Paulo, 2002.

FSANZ - FOOD STANDARDS AUSTRALIA NEW ZELAND. Austrália and New Zealand Food Standard Code – Schedule 19 – Maximum levels of contaminants and natural toxicants, Austrália e Nova Zelândia: Fsanz, 2017.

GONG, Y., ZHAO, D., & WANG, Q."An overview of field-scale studies on remediation of soil contaminated with heavy metals and metalloids: Technical progress over the last decade". Water Research, v. 147, p. 440–460, 2018.

GRESS, J.; SILVA, E.B.; OLIVEIRA, L.M.; ZHAO, D.; ANDERSON, G.; HEARD, D.; STUCHAL, L.D.; MA, L.Q. Potencial arsenic exposures in 25 species of zoo animals living in CCA-wood enclosures. Science of the total Environment, Elsevier, v. 551-552, p. 614-621, 2016.

JANIN, A; BLAIS, J. F; MERCIER, G; DROGUI, P. Selective recovery of Cr and Cu in leachate from chromated copper arsenate treated wood using chelating and acidic ion exchange resins. Journal of Hazardous Materials, v. 169, p. 1099-1105, 2009.

JAMBECK, J. et al. CCA-Treated wood disposed in landfills and life-cycle trade-offs with waste-to-energy and MSW landfill disposal. Waste Management, v. 27, n. 8, p. 21–28, 2007.

KIMA, J. Y.; OHB, S.; PARKC, Y. K. Overview of biochar production from preservative-treated wood with detailed analysis of biochar characteristics, heavy metals behaviors, and their ecotoxicity. Journal of Hazardous Materials, v. 384, n. 121356, 2020.

KING, C.M.D.; DOZIER, C.S.; CAMPBELL, J.L.; CURRY, E.D.; Godri Pollitt, K.J. Long-term leaching of arsenic from pressure-treated playground structures in the northeastern United States. Science of The Total Environment, Volume 656, 2019, 834-842. https://doi.org/10.1016/j.scitotenv.2018.11.315.

LEBOW, S.; COOPER, P.; LEBOW, P. Variability in evaluating environmental impacts of treated wood. Madison, USA: U.S. Department of Agriculture, Forest Service, Forest Products Laboratory. 10 p, 2004.

LI, Z.; MA, Z.; KUIJP, VAN DER. J. T.; YUAN. Z.; HUANG, L. A review of soil heavy metal pollution from mines in China: Pollution and health risk assessment. Science of the Total Environment, Elsevier, v. 468–469, p. 843–853, 2014.

MATOS, R. C.; OLIVEIRA, H.; FONSECA, H. M. A. C.; MOARIS, S.; SHARMA, B.; SANTOS, C.; PEREIRA, M. L. Comparative Cr, As and CCA induced Cytostaticity in mice kidney: A contribution to assess CCA toxicity. Environmental Toxicolog y and Pharmacolog y, v. 73, 2020.

MENEZES, P. M. Tratamento de solo contaminado com petróleo utilizando processos eletroquímicos. Dissertação (Mestrado em Ciência e Engenharia de Petróleo), Centro de Ciências Exatas e da Terra, Universidade Federal do Rio Grande do Norte, Natal, 2017.

MORESCHI, J.C. Biodegradação e preservação da madeira. Métodos de tratamento da madeira. 4º edição, vol III, 2013.

MERCER. T. G; FROSTICK. L. E. Leaching characteristics of CCA-treated wood waste: A UK study. Science of the Environment. Elsevier, p. 427-428, 2012.

MOSCHEM, J. C; GONÇALVES, P. R. Impacto Toxicológico de Metais Pesados: Uma Análise de Efeitos Bioquímicos e Celulares. Health And Biosciences, São Mateus, v. 1, n. 2, p. 88-100, 2020.

OHGAMI, N; YAMANOSHITA, O; THANG, N. D; YAJIMA, I; NAKANO, C; WENTING, W; OHNUMA, S. Carcinogenic risk of chromium, copper and arsenic in CCA-treated wood. Elsevier Environmental Pollution, v. 206, p.456-460, 2015.

POLICARPO, N.A. Tratamento de solos contaminados com bifenilas policloradas (PCBs). 2008. 75p. Dissertação (Mestrado em Engenharia). Universidade Federal de São Paulo, 2008.

REVISTA DA MADEIRA. Madeira: tendências internacionais na preservação de madeiras. Revista da madeira. 2008.

SILVA, J.C. Madeira preservada – Os impactos ambientais. Revista da Madeira. Viçosa: UFV. 100 ed. 2006.

TAKAHASHI, N., YOSHIDA, T., KOJIMA, S., YAMAGUCHI, S., OHTSUKA, R., TAKEDA, M., KOSAKA, T., HARADA T. Pathological and clinical pathological changes induced by fourweek, repeated-dose, oral administration of the wood preservative chromated copper arsenate in wistar rats. Toxicol. Pathol. Toxicologic Pathology, vol. 46 (3) 312-323, 2018.

TANG, Y; GAO, W; WANG, X; DING, S; AN, T; XIAO, W; WONG, M.H; ZHANG C; 2015. Variation of arsenic concentration on surfaces of in-service CCA-treated wood planks in a park and its influencing field factors. Environm. Monitor. Assess 187, 4214. Disponível em: < https://iehpc.gdut.edu.cn/2015-30.pdf>. Acesso em: 25 mar. 2021.

USEPA. National Primary Drinking Water Regulations, Arsenic and Clarifications to Compliance and New Source Contaminants Monitoring; Proposed Rule. Federal Register, v. 65, n. 121, p.38888-38983, June 22, 2000.

VIDAL. M.; EVANGELISTA, W. V.; SILVA, J. C. & JANKOWSKI, I. P. Preservação de madeiras no Brasil: histórico, cenário atual e tendências. Ciência Florestal, v. 25, n. 1, p. 257-271, 2015.

CHAPTER 5:
LOW-COST METHOD FOR THE EXTRACTION OF BISPHENOL-A IN GOLDEN MUSSEL (*LIMNOPERNA FORTUNEI*) FOR ENVIRONMENTAL ANALYSIS

Bernardo dos Santos Vaz, Suzana de Moura Pereira, Aleccia Rodrigues Macedo

ABSTRACT

Bisphenol A (BPA) is a widely distributed micropollutant and endocrine-disrupting compound with weak estrogenic activity. This study aimed to develop a low-cost and environmentally friendly analytical method for the identification and quantification of BPA in golden mussel tissues. Samples were pre-concentrated by freeze-drying and subjected to solvent extraction (80% methanol and 20% water) under sonication. Extracts were analyzed by high-performance liquid chromatography (HPLC). Three drying approaches—nitrogen flow, a 40°C laboratory oven, and a glass desiccator with silica gel—were evaluated to reduce operational costs. The glass desiccator provided the most efficient recovery with minimal maintenance requirements. The method achieved limits of detection and quantification of 0.0023 µg/mL and 0.0465 µg/mL, respectively. BPA levels quantified in mussel extracts reached 0.8365 µg/mL. Overall, the developed procedure constitutes a robust, cost-effective, and environmentally sustainable liquid–liquid extraction method suitable for BPA determination in biological matrices.

Keywords: Environmental analysis; Chromatography; HPLC; Endocrine disruptors; Mussel; Organic pollutants.

1 INTRODUCTION

Bisphenol A (2,2-bis(4-hydroxyphenyl)propane), or BPA, is a plasticizing chemical compound with endocrine-disrupting properties found worldwide. It is one of the most important synthetic products, manufactured on a large scale since the 1960s (STAPLES et al., 1998). Due to its phenolic molecular structure, BPA can interact with estrogen receptors and therefore exert estrogenic activity (KONIECZNA; RUTKOWSKA; RACHOŃ, 2015).

The harmful implications of BPA are not limited to humans. The homeostasis of aquatic ecosystems can be disrupted in several ways, including feminization of wildlife species and developmental or behavioral alterations (BHANDARI et al., 2015).

Due to the high production volumes and disposal of products synthesized from BPA—such as polycarbonate plastics, epoxy resins, flame retardants, and other materials—its presence has been widely detected in environmental matrices (BOLZ; HAGENMAIER; KÖRNER, 2001). Wastewater discharges and plastic debris constitute the main pathways of BPA contamination in aquatic environments (PHILBERT et al., 2008; IM; LÖFFLER, 2016; ARAKAWA, 2020).

The incorporation of BPA into food webs and the contamination of ecosystems have increasingly drawn scientific attention, given its capacity to interfere with growth physiology, lipid accumulation, reproduction, and the endocrine system, as well as to induce hypothyroidism in mammals (ZAFRA-GÓMEZ et al., 2008; AHMED; WALAA; ASMAA, 2018). BPA exhibits weak estrogenic properties and is commonly detected at concentrations ranging from $\mu g \cdot L^{-1}$ to $ng \cdot L^{-1}$, thereby being classified as a micropollutant (OEHLMANN et al., 2009).

Monitoring pollutants such as BPA in biological matrices is challenging, particularly due to the difficulty of obtaining reliable analytical methods for detecting the low concentrations present in environmental samples. Several sensitive and selective analytical techniques are available for the determination of organic micropollutants—such as gas chromatography and liquid chromatography—and are widely used for separation, identification, and quantification (GIBSON et al., 2007). However, additional challenges arise with plasticizers, as many laboratory consumables (e.g., syringes, filters, pipettes) are composed of similar materials. Furthermore, due to trace-level concentrations, multiple extraction procedures are often required for quantification.

In this context, the present study proposes analytical procedures to develop a simple, low-cost, and environmentally friendly methodology for extracting and determining BPA in the golden mussel Limnoperna fortunei. The method is based on high-performance liquid chromatography with a diode-array detector (DAD), combined with ultrasound-assisted liquid–liquid extraction for BPA determination in a biological matrix.

2 METHODOLOGY

2.1 MATERIALS AND STANDARDS

The analytical standard BPA 99% ($C_{15}H_{16}O_2$) (CAS 80-05-7) was purchased from Sigma-Aldrich (St. Louis, MO, USA). Methanol (CH_3OH) (CAS 67-56-1), previously distilled, was of HPLC grade. Acetonitrile (CH_3CN) (CAS 75-05-8), HPLC grade, was obtained from Merck. All reagents used were of analytical grade, and all aqueous solutions and washing water were prepared using deionized and double-distilled water in glassware.

2.2 CLEANING OF MATERIALS AND PREPARATION OF BPA-FREE SAMPLES

All materials used were washed with a 1% Extran solution (MA-02-neutral, Merck) and rinsed with ultrapure water (Milli-Q system, Micropore) distilled in glass. Drying was

carried out in an oven at 100 °C for non-volumetric glassware, and in a muffle furnace at 250 °C for ceramic and metal materials. Afterwards, all items were rinsed again with distilled methanol to remove potential traces of organic matter and BPA and then dried under the same conditions. All plastics used (microtubes, conical tubes, pipette tips) were high-quality polypropylene to avoid contamination of samples by BPA. Before the cleaning process, both water and solvents contained detectable BPA residues, but after cleaning, all were tested by HPLC to ensure BPA-free conditions.

2.3 COLLECTION AND STORAGE OF GOLDEN MUSSEL SAMPLES

Golden mussels were collected in the Pelotas Stream (31°45'37.9"S 52°16'29.9"W), located in the urban area of the municipality of Pelotas, Rio Grande do Sul, Brazil, in October 2017. All sampling procedures were carried out with precautions to minimize the risk of BPA contamination. Samples were stored and transported in amber glass bottles with aluminum caps and protected from light. Upon arrival at the laboratory, samples were frozen for storage.

Whole frozen mussels were placed in decontaminated containers and freeze-dried for 24 h. After lyophilization, samples were stored in amber glass flasks covered with aluminum foil to protect them from light and kept at –10 °C.

2.4 SAMPLE PREPARATION

Sample preparation was carried out under stringent contamination-control conditions. To extract analytes from mussel samples, a liquid–liquid extraction method was employed. A total of 100 mg of soft tissue was separated and homogenized. After maceration, 5 mL of extraction solvent (80% methanol and 20% water) was added. Samples were transferred to 15 mL conical tubes, vortexed for 2 minutes, and sonicated at room temperature for 60 minutes.

After ultrasonic treatment, samples were filtered using a Büchner funnel (50 mL) with a porous plate and cellulose acetate membrane (47 mm diameter, 0.45 µm pore size), aided by a vacuum pump (Pro-Tools model 131) and a Kitasato flask. The filtrates were then transferred to 2 mL microtubes and dried. Subsequently, 500 µL of methanol was added and samples were centrifuged in a MiniSpin centrifuge for 10 minutes. A total of 100 µL of the supernatant was transferred to amber HPLC vials for analysis.

2.5 DRYING TESTS FOR CONCENTRATION

A BPA stock solution (2.6 mg·mL⁻¹) was prepared to obtain a 9 µg·mL⁻¹ standard solution for drying tests, in order to assess potential analyte losses during solvent evaporation. The extraction solvent consisted of methanol and water (80:20%). Amber vials were filled with 1.5 mL of the solution and dried using the following methods:

- glass desiccator with silica under vacuum;
- oven at 40 °C;
- nitrogen stream.

After drying, 500 µL of methanol was added for HPLC analysis. All drying tests were performed in triplicate.

2.6 HPLC INSTRUMENTATION AND CONDITIONS

HPLC analyses were carried out using an Agilent 1260 Infinity High-Performance Liquid Chromatograph equipped with a diode-array detector (DAD, model G1315D), column housing (G1316A), autosampler (G1329B), and quaternary pump (G1311C). The analytical column used was a Phenomenex Kinetex Core-Shell C18 100 Å (4.6 × 250 mm, 5 µm). The mobile phase consisted of water (A) and acetonitrile (B) in a gradient: 15 min A:B 80:20%, 10 min A:B 50:50%, 10 min B 100%, 10 min A:B 80:20%. The total run time was 45 min per sample, with a flow rate of 0.5 mL·min⁻¹, column temperature of 24 °C, and injection volume of 10 µL. Detection was performed at 220 nm.

The linear correlation coefficient (r) was obtained from a BPA calibration curve (0.5, 1, 2, 4, and 8 µg·mL⁻¹). A stock solution of 5 mg·mL⁻¹ was prepared by weighing the analytical standard and diluting it in methanol. The limits of detection (LOD) and quantification (LOQ) were calculated using signal-to-noise ratios of 3:1 and 10:1, respectively.

BPA identification was based on spectral matching and retention time. Quantification followed the external calibration curve method, using linear regression of peak areas relative to standard concentrations. All calibration points and mussel extracts were analyzed in triplicate.

2.7 BLANK CONTROL TESTS

Blank control tests were performed during all experimental procedures to exclude potential analytical interferences or contamination during sample processing. Solvents were processed following the same sample preparation procedures. No BPA was detected in blank assays.

3 RESULTS AND DISCUSSION

3.1 PRELIMINARY STUDIES: CLEANING TEST RESULTS

One of the major challenges when working with a ubiquitously distributed compound such as BPA is obtaining standardized and contamination-free samples (CERKVENIK-FLAJS, 2020). There is a shortage of detailed standardized methodologies for glassware cleaning routines prior to BPA analysis, and the compound is frequently affected by blank contamination (SALGUEIRO-GONZÁLEZ et al., 2012). For the preparation of standards and samples, several BPA-free methods and materials were used, as described below.

Regarding materials, glass, ceramic, and stainless-steel items were selected because they are naturally BPA-free and resistant to high temperatures and organic solvents, both of which were necessary for the cleaning protocol. However, part of the extraction technique developed in this study required centrifugation. A market survey was performed to determine whether any manufacturer provided BPA-free conical tubes. Only the German laboratory brand Eppendorf® offered such products in Brazil, and these were scientifically verified to be BPA-free (GATIMEL et al., 2016).

Analysis of blank samples indicated that the cleaning protocol and the distillation of solvents and water were effective for eliminating BPA contamination. Several authors have reported methodological difficulties in achieving BPA-free samples (SALGUEIRO-GONZÁLEZ et al., 2012; CERKVENIK-FLAJS, 2020). Problems related to contaminated HPLC vial septa were resolved by adopting chemically inert alternatives, such as silicone/PTFE (CERKVENIK-FLAJS, 2020). Therefore, routine testing of laboratory consumables is advised to confirm the absence of BPA (CERKVENIK-FLAJS, 2020).

3.2 LYOPHILIZATION RESULTS: WET-TO-DRY MASS CONVERSION

The use of fresh mussels requires more labor compared with freeze-dried mussels. Fresh specimens must be externally cleaned, and the opening of valves and removal of soft tissues is more difficult and time-consuming than when using lyophilized individuals. On

average, mussel soft tissues consist of 83% water, 9% proteins, 4% carbohydrates, 2% ash, and 1% lipids (FURLAN et al., 2011). Lyophilization facilitates maceration and homogenization, enabling the processing of larger amounts of tissue and functioning as a pre-concentration method (RAJASÄRKKÄ; VIRTA, 2013). This technique generally provides satisfactory recovery (MARTÍNEZ-MORAL; TENA, 2011) and has been used in chromatographic analyses for determining multiple organic compounds in human milk (RODRÍGUEZ-GÓMEZ et al., 2014), BPA in zooplankton, poultry manure, the sea cucumber Holothuria tubulosa, and marine sediment (RODRÍGUEZ-GÓMEZ et al., 2014; STANISZEWSKA; NEHRING; MUDRAK-CEGIOŁKA, 2016; MARTÍN et al., 2017; AZNAR et al., 2018). In this study, lyophilization reduced sample volume by more than 80%.

3.3 DRYING TEST RESULTS

One of the most widely employed methods for drying BPA-containing samples is nitrogen (N_2) evaporation (ARAR; ALAWI, 2019; CERKVENIK-FLAJS, 2020; GUO et al., 2020; HERRERO et al., 2021; DE LEO et al., 2021; TRAN et al., 2021). In our experiments, drying 4.5 mL from three vials containing methanol/water (80:20%) required a 10 L cylinder of high-purity N_2 (99.99%), which costs approximately R$ 900. Industrial-grade N_2 (99.8%) costs around R$ 200.

Due to the high cost and large gas consumption required for sample concentration and drying, alternative methods were investigated to reduce expenses without compromising BPA recovery or causing contamination.

The drying test results for nitrogen flow, desiccator, and oven drying are shown in Table 1. According to the data obtained, no analyte loss occurred during any of the drying methods. Samples dried under nitrogen flow must be processed individually, require constant cylinder monitoring, and have an average drying time of approximately 6 hours per vial. For three vials totaling 4.5 mL, an entire 10 L cylinder was necessary.

Oven drying was the slowest technique (53 hours) and may increase the risk of contamination due to prolonged exposure. Samples dried in a desiccator required 48 hours and minimal handling, making this the preferred method, as it showed no significant variation compared with the control (Table 1).

Based on these results, the desiccator method was selected for sample drying and concentration due to its low maintenance cost and efficient analyte recovery.

Table 1. Drying tests to assess possible BPA losses.

Samples	Recovery (%)	%RSD
Control	100	0.77
N_2	106.12	1.62
Desiccator	106.18	1.08
Oven 40 ºC	112.90	11.05

3.4 ANALYTICAL PERFORMANCE

3.4.1 Linearity

For the construction of the analytical curve (Figure 1), the concentrations ranged from 0.5, 1, 2, 4, and 8 µg/mL. The calibration curve was obtained by plotting the peak areas (Y) against the analyte concentrations (X). A linear relationship was observed between the peak area and the standard BPA concentration. The regression line generated during calibration was described by $Y = 64.3X + 17.8$ ($r^2 = 0.994$) for BPA.

The linear correlation coefficient meets the requirement established by Anvisa, which must be equal to or greater than 0.99 (ANVISA, 2017), demonstrating that the tested concentration ranges indicate a linear method suitable for sample quantification.

Figure 1. Calibration curve of BPA.

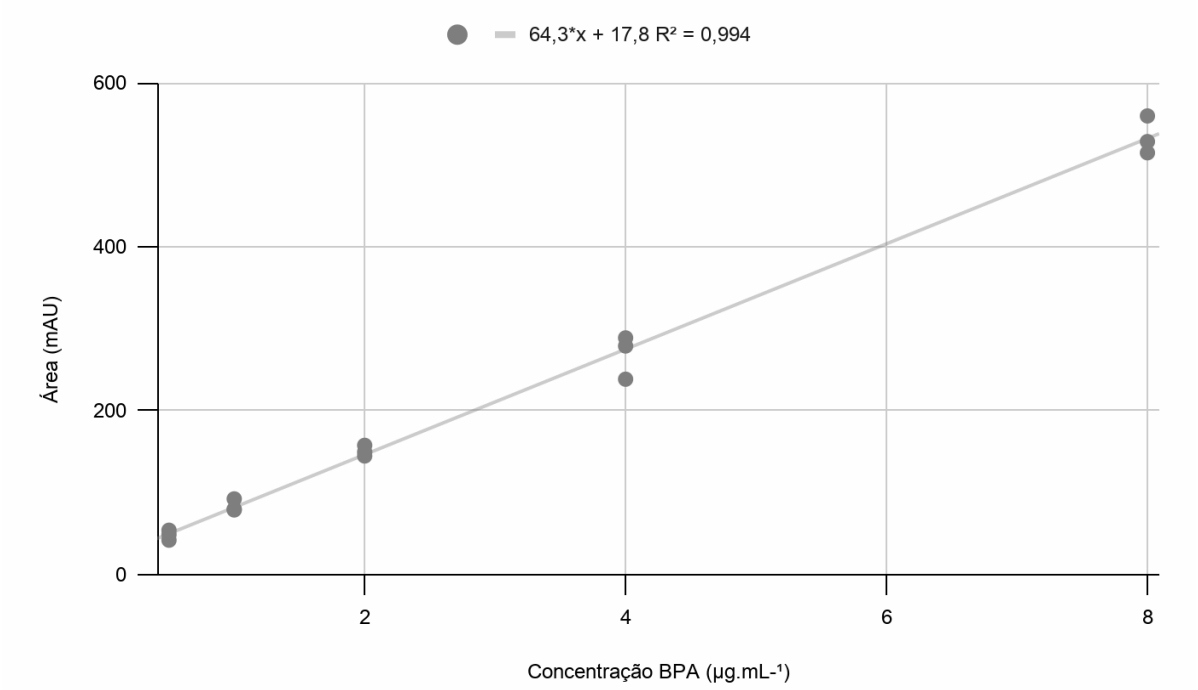

3.4.2 Sensitivity

The sensitivity of the method is demonstrated through the limits of detection and quantification. The limit of detection is the lowest analyte concentration identifiable in the blank, while the limit of quantification is the lowest analyte concentration that can be reliably quantified. The limit of detection was 0.0023 µg/mL, and the limit of quantification was 0.0465 µg/mL based on the signal-to-noise ratio for BPA.

3.4.3 Quantification of BPA in Golden Mussel Tissues

The developed method was applied to freeze-dried soft tissues of the golden mussel collected in the environment. BPA concentration in the mussel extracts (0.8365 µg/mL ± 0.0855) was above the limit of quantification (0.0465 µg/mL).

Figures 2 and 3 show the chromatogram of BPA (retention time: 13.519 min) extracted from the golden mussel (Limnoperna fortunei). The procedures adopted resulted in an average recovery of 83.65 ng/g of dry mussel tissue (8.365 ng/100 mg of dry tissue). Considering that each 100 mg of dry tissue contains 5.5 mussels (average adults ~15 mm), based on the extraction data, each individual contains approximately 1.5 ng of BPA in its tissues.

Figure 2. Chromatogram of a BPA sample (retention time: 13.519 min) extracted from the biological matrix (Limnoperna fortunei). Absorbance (mAU) is shown on the Y-axis and time (minutes) on the X-axis.

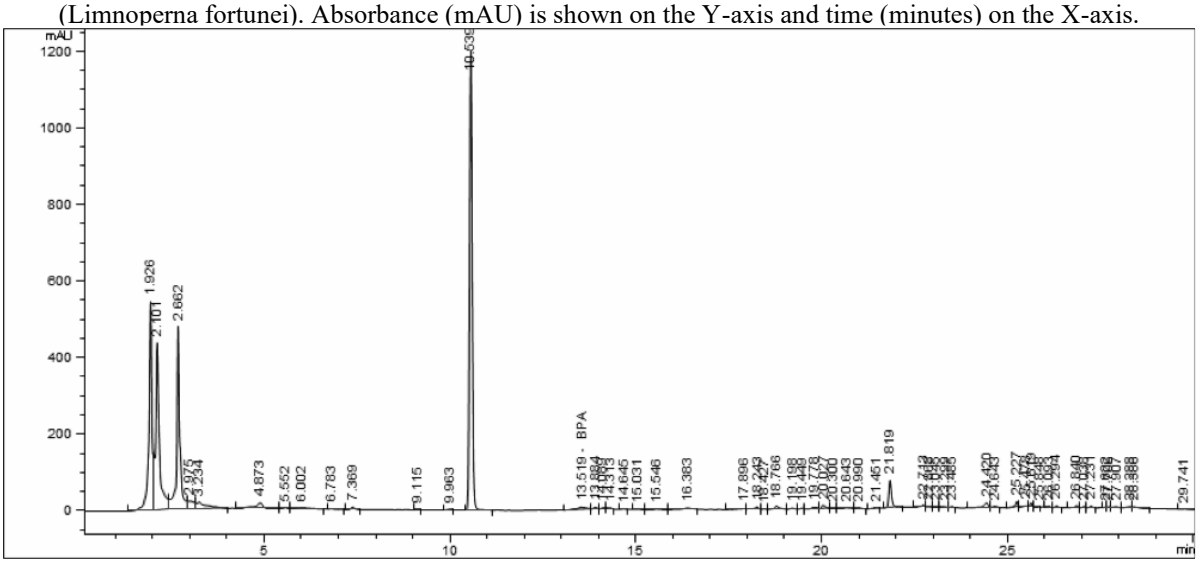

The method did not demonstrate selectivity between peaks, as interferents were observed at the analyte's retention time (Figure 3). However, the selectivity of an analytical method can be demonstrated through its ability to unequivocally identify or quantify the analyte of interest. In chromatographic methods, chromatographic purity of the analyte

must be verified (ANVISA, 2017). The result obtained indicated a high degree of purity, internally measured by the chromatograph (999.475 purity). Therefore, in addition to detecting and identifying the analyte, a degree of selectivity was achieved in the column, enabling the isolation of BPA during extraction from mussel tissues.

Figure 3: Detail of the chromatogram of a BPA sample (retention time: 13.519 min) extracted from the biological matrix (Limnoperna fortunei). Absorbance (mAU) on the Y-axis and time in minutes on the X-axis.

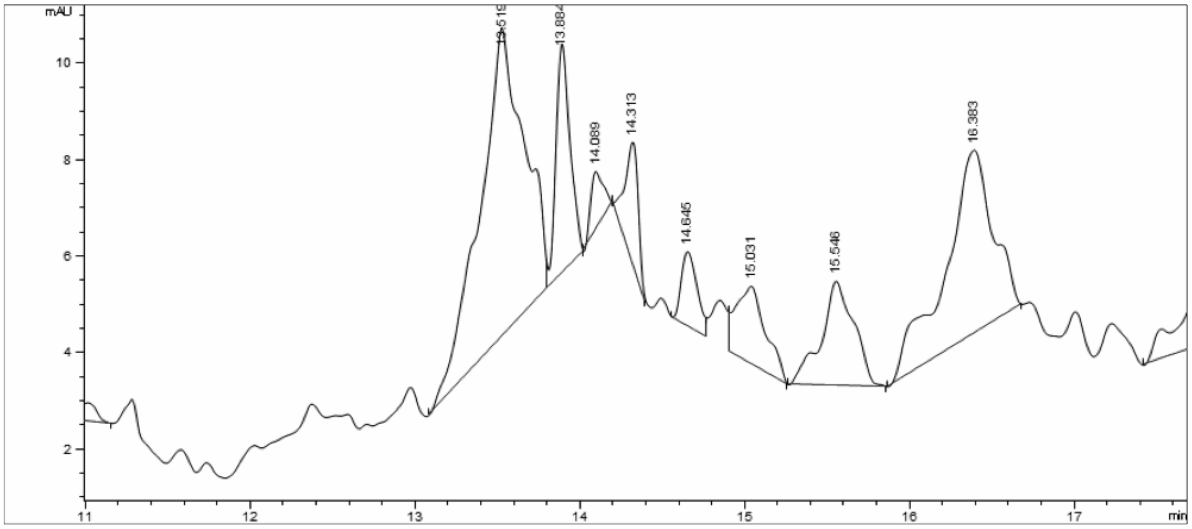

The confirmation of positive results for environmental pollutants has become a concern due to the negative effects associated with identification errors. Reliable analytical methods with accurate quantification of analytes must be developed, but the analyte must also be unequivocally identified at the concentration levels of interest (HERNÁNDEZ et al., 2007).

4 CONCLUSIONS

The pre-concentration method using freeze-drying followed by solvent extraction (methanol + water) and determination by HPLC proved suitable for the detection and quantification of BPA in soft tissues of the golden mussel. Analyses of mussel samples collected in Arroio Pelotas, RS, indicated contamination by BPA.

The development of fast, efficient, low-cost, and environmentally friendly methodologies for the detection and quantification of plasticizers in tissues and environmental samples is important due to the harmful effects of these pollutants on human and environmental health. The test results depend on the type of environmental matrix. The method was efficient, inexpensive, and environmentally sound for the determination and quantification of BPA in golden mussel tissues.

REFERENCES

AHMED, R. G.; WALAA, G. H.; ASMAA, F. S. Suppressive effects of neonatal bisphenol A on the neuroendocrine system. Toxicology and industrial health, v. 34, n. 6, 2018. p. 397–407.

ARAKAWA, K. Simultaneous Metabarcoding of Eukaryotes and Prokaryotes to Elucidate the Community Structures within Tardigrade Microhabitats. Diversity, v. 12(3) n. 110. 2020. p. 1-12.

ARAR, S.; ALAWI, M. A new solvent extraction method with gas chromatography–Mass spectrometry for bisphenol a determination in canned foods. Acta Chromatographica, 2019. v. 31 n. 1. p. 71–78.

AZNAR, R. ALBERTO, B. MARTIN, A. N. R. SÁNCHEZ-BRUNETE, C. Analysis of emerging organic contaminants in poultry manure by gas chromatography-tandem mass spectrometry. Journal of separation science, v. 41, n. 4, 2018. p. 940–947.

BHANDARI, R. K. DEEM, S. L. HOLLIDAY, D. K. JANDEGIAN, C. M. KASSOTIS, C. D. NAGEL, S. C. TILLITT, D. E. SAAL, F. S. V. RESENFILD. C. S. Effects of the environmental estrogenic contaminants bisphenol A and 17α-ethinyl estradiol on sexual development and adult behaviors in aquatic wildlife species. V. 14, 2015. p. 195–219.

BOLZ, U.; HAGENMAIER, H.; KÖRNER, W. Phenolic xenoestrogens in surface water, sediments, and sewage sludge from Baden-Württemberg, south-west Germany. Environmental pollution, v. 115, n. 2, 2001. p. 291–301.

CERKVENIK-FLAJS, V. Bisphenol A background contamination encountered during advanced blood sampling and laboratory analysis. International Journal of Environmental Analytical Chemistry 2020. p. 1–11

DE LEO, V. ; CASIELLO, M. DELUCA, G. COTUGNO, P. CATUCCI, L. NACCI, A. FUSCO, C.; D'ACCOLTI, L. Concerning Synthesis of New Biobased Polycarbonates with Curcumin in Replacement of Bisphenol A and Recycled Diphenyl Carbonate as Example of Circular Economy. Polymers, v. 13, n. 3, 2021 p. 361.

FURLAN, E. F., GALVÃO, J. A., SALÁN, E. O., OETTERER, M.. Composição centesimal e valor calórico de mexilhões Perna perna cultivados no litoral norte de São Paulo, Brasil. Boletim do Instituto de Pesca. , São Paulo, v. 37 n. 1. 2011, p. 85 – 93.

GATIMEL, N. LACROIX, Z. M. CHANTHAVISOUK, S. PICARD-HAGEN, N. V. GAYRARD, V. PARINAUD, J. LANDRI, R. D. Bisphenol A in culture media and plastic consumables used for ART. Human reproduction, v. 31, n. 7, 2016, p. 1436–1444.

GIBSON, R. BECCERRIL-BRAVO, E. SILVA-CASTRO, V. JIMÉNEZ, B. Determination of acidic pharmaceuticals and potential endocrine disrupting compounds in wastewaters and spring waters by selective elution and analysis by gas chromatography-mass spectrometry. Journal of chromatography. A, v. 1169, n. 1-2, 2007, p. 31–39.

GUO, M. HE, M. ZHONG, J. HE, Q. ISMAIL, B. B. CHEN, G. LIU, D. High-performance liquid chromatography (HPLC)-fluorescence method for determination of bisphenol A

diglycidyl ether (BADGE) and its derivatives in canned foods. The Science of the total environment, v. 710, 2020, p. 134975.

HERRERO, L. QUINTANILLA-LÓPEZ, J. E. FERNANDEZ, M. A. GÓMORA, B. Plasticisers and preservatives in commercial milk products: A comprehensive study on packages used in the Spanish market. Food Chemistry, 2021. 128031p.

IM, J.; LÖFFLER, F. E. Fate of Bisphenol A in Terrestrial and Aquatic Environments. Environmental science & technology, v. 50, n. 16, 2016, p. 8403–8416.

KONIECZNA, A.; RUTKOWSKA, A.; RACHOŃ, D. Health risk of exposure to Bisphenol A (BPA). Roczniki Panstwowego Zakladu Higieny, v. 66, n. 1, p. 5–11, mar. de 2015.

MARTÍNEZ-MORAL, M. P.; TENA, M. T. Focused ultrasound solid-liquid extraction and selective pressurised liquid extraction to determine bisphenol A and alkylphenols in sewage sludge by gas chromatography-mass spectrometry. Journal of separation science, v. 34, n. 18, 2011, p. 2513–2522.

MARTÍN, J. ZAFRA-GÓMEZ, A. IBANEZ-YUSTE, A. J. ALONZO, E. VILCHEZ, J. L. Multi-residue analysis of 36 priority and emerging pollutants in marine echinoderms (Holothuria tubulosa) and marine sediments by solid-liquid extraction followed by dispersive solid phase extraction and liquid chromatography-tandem mass spectrometry analysis. Talanta, v. 166, 2017, p. 336–348.

OEHLMANN, J. et al. A critical analysis of the biological impacts of plasticizers on wildlife. Philosophical transactions of the Royal Society of London. Series B, Biological sciences, v. 364, n. 1526, 2009, p. 2047–2062.

PHILBERT, M. A. et al. Scientific peer-review of the draft assessment of bisphenol A for use in food contact applications. jan. de 2008.

RAJASÄRKKÄ, J.; VIRTA, M. Characterization of a Bisphenol A Specific Yeast Bioreporter Utilizing the Bisphenol A-Targeted Receptor. 2013. 10067–10074p.

RODRÍGUEZ-GÓMEZ, R. et al. Stir-membrane solid-liquid-liquid microextraction for the determination of parabens in human breast milk samples by ultra high performance liquid chromatography-tandem mass spectrometry. Journal of chromatography. A, v. 1354, p. 26–33, ago. de 2014.

SALGUEIRO-GONZÁLEZ, N. et al. Blank and sample handling troubleshooting in ultratrace analysis of alkylphenols and bisphenol A by liquid chromatography tandem mass spectrometry. 2012. 413–419p.

STANISZEWSKA, M.; NEHRING, I.; MUDRAK-CEGIOŁKA, S. Changes of concentrations and possibility of accumulation of bisphenol A and alkylphenols, depending on biomass and composition, in zooplankton of the Southern Baltic (Gulf of Gdansk). Environmental pollution , v. 213, p. 489–501, jun. de 2016.

STAPLES, C. A. DORN, P. B. KLECKA, G. M. O'BLOCK, S. T. HARRIS, L. R. A review of the environmental fate, effects, and exposures of bisphenol A. Chemosphere, v. 36, n. 10, 1998, p. 2149–2173.

TRAN, T. M. TRAN-LAM, T. T. MAI, H. H. T. BACH, L. H. T. NGUYEN, H. M. N. TRINH, H. T. DANG, L. T. MINH, T. B. QUAN, T. C. HONG, A. Q. Parabens in personal care products and indoor dust from Hanoi, Vietnam: Temporal trends, emission sources, and non-dietary exposure through dust ingestion. The Science of the total environment, v. 761, 2021, p. 143274.

ZAFRA-GÓMEZ, A. BALESTEROS, O. NAVALÓN, A. VÍLCHEZ, J. L. Determination of some endocrine disrupter chemicals in urban wastewater samples using liquid chromatography–mass spectrometry. 2008. 87–94p.
How Tubes Can Affect Your Experiments | Lab Manager. Disponível em: <https://www.labmanager.com/white-papers-and-application-notes/2011/05/eppendorf-how-tubes-can-affect-your-experiments>. Acesso em: 22 nov. 2019.

CHAPTER 6:
EVALUATION OF PH CHANGE IN EVAPORATED LABORATORY CHEMICAL WASTE BY SOLAR EVAPORATION

Gladimir da Silva, Pablo Machado Mendes

ABSTRACT

Solar evaporation is a term commonly used when using equipment, often home-built, to evaporate water from chemical waste in order to reduce its volume. Condensed water is generally considered to be free of contaminants and is, in most cases, freely discarded. This study sought an empirical evaluation, considered as a preliminary test to verify the pH of the condensed fraction, as an initial assessment of a future solar distillation project for laboratory chemical waste, in which a single-effect solar evaporator the size of a computer case (deactivated, using only the casing) will be used and which will seek an alternative for reducing the volume of liquid chemical waste by increasing its useful life by reusing the drums in which they are discarded and stored in the building of the institution in question. The procedure is low cost, easy to perform and was based on the simple placement of petri dishes containing the liquid residue in the sun. After partial condensation on the upper inner part of the lid of the closed petri dish, the pH was measured and showed an improvement in relation to the initial pH of the residue, demonstrating a high potential for using this technology for the desired purpose. It is important to note that further studies are necessary to ensure that the condensate is not contaminated with possible chemical residues that may undergo the solar evaporation process and still remain above the required legal parameters.

Keywords: Effluent; Evapoirradiation; Refuse.

1 INTRODUCTION

Initially, chemical waste management consists of a hazardous waste management program that seeks to identify procedures to ensure the correct segregation, disposal, storage, transport, and final destination of these wastes, minimizing the environmental impact caused by the incorrect disposal of toxic waste. In this context, the disposal of chemical waste from laboratories is varied, both in terms of its origin and the chemical characteristics of the waste itself, as observed at the site under study. The minimum action required of the administration is to try to develop simple, inexpensive, and sustainable procedures to deal with this chemical asset and liability that plagues public entities. Specialized companies charge per liter of effluent received, and an alternative to reduce costs would be pre-treatment of the effluent to reduce volume (Souza, 2016). This work aligns with the need to reduce the volume of chemical waste generated in public and private technical and higher education institutions. These institutions must align with national government plans, as these plans demand environmentally sustainable conduct that is consistent with the educational objectives provided to the internal academic community

and other external stakeholders, such as regulatory environmental agencies and the wider community. Ideally, all institutions would strive for performance that is rigorously aligned with new global ESG (environmental, social, and governance) trends. However, in practice, institutions face structural problems and often struggle to adopt this type of proposal, which, apparently, suggests a more advanced management approach in most cases. The inclusion of didactic experimentation programs for the reuse of chemical waste, associated with effluent neutralization and evaporation processes, will bring a series of benefits to organizations and the environment, as it minimizes organizational costs, improves the community's quality of life, and preserves the natural ecosystem (Filho et al., 2019). Solar evaporation is a term commonly used when employing equipment, often homemade, to evaporate water from chemical waste in order to reduce the volume of waste. This methodology is perfectly suited for all institutions, as it offers a cheap alternative that can reuse materials for the construction of the solar evaporator. Therefore, this work proposed a simple pH verification, on a minimal scale, through the placement of chemical waste in a Petri dish in the sun in order to have a preliminary reflection on the condensates of some laboratory chemical waste. The average humidities of cities in Rio Grande do Sul were also initially observed, according to (VAGHETTI, 2025).

2 THEORETICAL FRAMEWORK

There are several technologies for producing potable water from saltwater, such as reverse osmosis, electrodialysis, multi-stage flash distillation, multi-effect distillation, and solar distillation. Among these technologies, solar distillation presents itself as an interesting alternative, since it uses a free and abundant energy source, is easy to operate, does not generate pollution, and is effective in water treatment, thus being an integrated solution for both the scarcity of potable water and the energy and environmental problems also faced (FARIA, 2015).

Compared to traditional methods, such as incineration or chemical treatments, evaporation is more economical and ecological, reducing the volume of effluents by up to 90%. This results in significant savings in operating costs, which can reach 30%, even considering the initial acquisition, electrical, maintenance, and evaporator cleaning costs. (FILHO, 2024).

Normally, the pH of distilled water is acidic. Water for human consumption is, in general terms, a solution, while distilled water is a pure substance; however, all water that

comes into contact with the atmosphere will dissolve carbon dioxide, which is why the pH is less than 7.0. (CARVALHO, 2015).

Regarding performance in solar stills, the maximization of performance in conical solar stills was achieved through various energy storage materials such as steel spheres, glass spheres (marbles), sand-colored stones, and black gravel, all 1.5 cm in diameter. BELLILA et al. (2024, p. 1).

3 METHODOLOGY

The experiment began with the arrangement of 10 types of waste from chemistry teaching laboratories (photo 1) in lidded Petri dishes, without hermetically sealing (external lid diameter: 9.5 cm; internal diameter: 9.0 cm and height: 2.0 cm), placed outdoors with the liquid waste (photos 2, 3 and 4). The dishes contained distilled water (the white), copper, chromium, iron, basic inorganic, carbonates, metallic organic, KMnO4, silver, alcohol, and inorganic acid waste. The external temperature was measured at 20°C at 10:10 am on a sunny morning in April, during the autumn season in the city of Pelotas-RS. Relative humidity: 73% and atmospheric pressure: 1016 mb. Subsequently, the container was exposed to sunlight for a period of 2 hours, from 9 to 11 am, so that the physical phenomenon of evaporation would occur naturally on the residue present. It is known from previous studies (Vasconcelos, 2015) that such evaporation can reach 95% of the total effluent volume in a common single-effect evaporator. The residues were poured into the petri dishes in a volume of 10 mL. The initial pHs of the liquid chemical residues in the containers were measured beforehand for later comparison with the pH measurements of the condensate in the petri dishes. The pH of the condensed liquid in the upper inner part of the dish was measured using Macherey-Nagel pH paper, Ref. 92110 (photo 5). Furthermore, the choice of solar evaporation was due to the use of free natural energy, since artificial heat sources demand high expenditure on electricity or gas. It must be considered that solar evaporation is not rapid and depends on sunny days for a continuous and fluid process, noting that very hot days impair evaporation due to the temperature that can rise on the glass surface. Also, the colligative effect (David, 2014), that is, the effect due to the gradual increase in solute concentration during solar evaporation, as condensate is produced.

Next, the most concentrated residue from the petri dish was transferred back to the original container, and the neutral pH evaporates were discarded. Table 1 shows the increase or decrease in pH values of each type of residue and its respective condensate..

Photo 1 – Chemical laboratory waste containers:

Source: by the author.

Photo 2 and 3 -Petri dishes exposed to sunlight in a preliminary test: distilled water (blank), solutions of copper, chromium, iron, inorganic bases and carbonate residues:

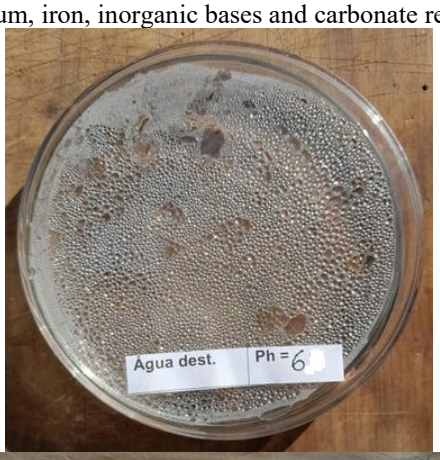

Source: by the author.

Photo 4 -Petri dishes exposed to sunlight in a preliminary test: solutions of organic metallic residue, KMnO4, silver, alcohol, and inorganic acids:

Source: by the author.

Photo 5 - pH strip brand Macherey-Nagel (Ref. 92110).

Source: by the author.

Table 1 – Laboratory waste solutions, pH of the waste and pH of its condensate:

Residue in solution	Initial pH of the residue	pH of the condensate on the lid of the petri dish
Cobre	12	10
Cromo	1	3
Ferro	1	4
Básico inorgânico	12	7
Carbonatos	8	7
Metálico orgânico	0	3
$KMnO_4$	1	6
Prata	5	5

Álcool	5	6
Inorgânico ácido	1	5
água destilada (branco)	6	6

4 RESULTS AND DISCUSSION

According to Table 1, two residues reached a neutral pH, while six improved their pH to near 7 compared to the original pH. Even so, 90% of the residues tested showed an improvement in pH. This highlights an opportunity to study the reduction of laboratory waste through solar evaporation. It was observed that the condensates of the chromium and iron waste solutions, with a pH of 1.0, increased to pH 3 and 4 respectively, still acidic, possibly due to contaminants, reflux caused by the condensate dripping back into the solute due to the very low height of the Petri dish lid. The same occurred with the organic metallic residue, with an increase in pH from 0 in the residue to pH 3 in the condensate. In the copper residue solution, the pH decreased from 12 in the residue to 10 in the condensate. The basic inorganic residue decreased in pH from 12 to 7, the KMnO4 residue increased from 1 to 6, and the acidic inorganic residue increased from 1 to 5 in the residue and condensate. The silver residue, with a pH of 5, remained constant in the condensate, while the alcohol residue went from pH 5 to 6. If these pH values are repeated in the single-effect evaporator, it would be advisable to re-evaporate the more acidic solutions in an attempt to equalize the pH values. The pH of the distilled water (blank) remained at 6. Regarding costs, it is important to report that the collection of the last batch of waste at the institution cost approximately R$30,000.00 for the disposal of 1200 liters of hazardous liquid laboratory waste. Analyzing the existing literature (Vasconcelos, 2015), it is possible to achieve a reduction of up to 95% in the volume of waste with this same technology, solar evaporation. Applying the simple calculation (0.95 x 1200 liters = 1140 liters evaporated), leaving 60 liters of waste to be disposed of (approximate price to dispose of 60 liters = R$ 1,500.00 reais), in the proper proportions and logistics, a more than significant, viable and necessary saving. As for the mass of dry residue at the bottom of the container, this can vary substantially, noting that the concentrations from one drum to another can also vary, possibly due to the diversity of procedures resulting from different dilutions of discarded waste. The final result was obtaining a clean condensate with a moderated pH. Even more important is to know, preliminarily, the behavior and pH values of the condensate, as it will be discarded if it shows an absence of contamination and has a pH close to neutral. The final result was obtaining a clean condensate with a moderated pH.

5 FINAL CONSIDERATIONS

Based on initial tests, it is suggested that further development of the study on evaporation and volume reduction of chemical waste generated in chemistry laboratories be pursued. It would be constructive to begin a feasibility study of economic and operational viability, aiming to reduce the volume of effluent requiring special management. It is also advised that the chemical waste evaporation strategy should complement other methodologies for minimizing, eliminating, and treating these effluents. Future work should involve verifying the concentration of the aforementioned waste condensates, which should be below the parameters monitored by environmental agencies. This establishes a more sustainable and economical approach to managing this type of environmental liability originating from public and private institutions. Article 225, "caput," of the Federal Constitution (BRAZIL, 2023) is explicit regarding the duty of the Public Authorities to defend and preserve an ecologically balanced environment. Also according to Law 6.938/1981, in its article 4 - The National Environmental Policy will aim: I - at the compatibility of socio-economic development with the preservation of environmental quality and ecological balance; And, thus, sustainable national development as one of the principles of Law 14.133/2021, the new law on bidding and administrative contracts.

6 CONCLUSION

Finally, this preliminary study, which verified pH equalization and improvement in 8 out of 10 samples, allowed us to foresee the viability of the evaporation process for chemical laboratory waste. Condensation was found in 8 types of waste, and we recommend that future work continue with studies investigating possible condensate contamination with greater precision, within or well below the inspection parameters, in order to guarantee its safe disposal.

REFERENCES

BELLILA, Abdelkader et al. Maximizing solar distillation performance for conical solar still through varied energy storage materials. Scientific Reports, v. 14, n. 29218. p. 1-18, 2024. DOI: https://doi.org/10.1038/s41598-024-79907-w. Disponível em:https://www.researchgate.net/publication/386104800_Maximizing_solar_distillation_performance_for_conical_solar_still_through_varied_energy_storage_materials. Acesso em: 16 jul. 2025.

BRASIL. Constituição da República Federativa do Brasil. Brasília: Senado Federal, 1988. Disponível em: http://www.planalto.gov.br/ccivil_03/constituicao/constituicao.htm. Acesso em: 14 ago. 2023.

BRASIL. Lei 6.938, de 31 de agosto de 1981. Dispõe sobre a Política Nacional do Meio Ambiente, seus fins e mecanismos de formulação e aplicação, e dá outras providências. Disponível em: https://www.planalto.gov.br/ccivil_03/leis/L6938compilada.htm. Acesso em: 15 ago. 2023.

BRASIL. Lei Nº 14.133, de 1º de abril de 2021. Lei de Licitações e Contratos Administrativos. Disponível em: https://www.planalto.gov.br/ccivil_03/_ato2019-2022/2021/lei/l14133.htm. Acesso em: 19 de ago. de 2024.

CARVALHO, Eyre Katrine Ferreira. Potabilização de Água Eutrofizada Utilizando Destilação Solar. 2015. Dissertação (Pós-Graduação em Ciência e Tecnologia Ambiental) – Universidade Estadual da Paraíba, Campina Grande, 2015. Disponível em:file:https://tede.bc.uepb.edu.br/jspui/handle/tede/2891#preview-link0. Acesso em: 28 ago. 2025.

DAVID, G. R.; SILVA2, J. P. S.; VIEIRA, L.G.M. Estudo e desenvolvimento de adimensional para análise de dados. 1. 2014, Rio de Janeiro. X Congresso Brasileiro de Engenharia Química Iniciação Científica. Rio de Janeiro: Blucher Chemical Engineering Proceedings, 2014. p. 1.

FARIA, E.V; ALVES, I. F. B; ARAÚJO, S.A; BONTEMPO, L. H.S; LIMA, M. N; OLIVEIRA, L.C.C. B. Desenvolvimento e construção de um destilador solar para dessalinização de água salgada em diferentes concentrações de sais. 1. 2015, São Paulo. Congresso Brasileiro de Sistemas Particulados. São Paulo: UFSP, 2015, p. 1-10.

FILHO, E. J. M. A. Projeto de um Evaporador Solar para a Redução do Volume de Efluentes Originados dos Laboratórios do LITPEG-UFPE. 117f. Trabalho de Conclusão de Curso (Bacharelado em Engenharia Mecânica) – Universidade Federal de Pernambuco, Recife, 2024.

FILHO, J.C.O; C. C. S. Oliveira; K. K. B. Rocha; A. B. Santos; V. S. C; S. C. S. O. Gerenciamento de resíduos: modelo experimental de reuso de substâncias químicas e evaporação de efluentes, 1. 2019, João Pessoa. Anais: 10º Fórum Internacional de Resíduos Sólidos. João Pessoa: IFPE, 2019. p. 1-8.

SOUZA, T.R. Utilização de um evaporador solar na redução do volume de um efluente laboratorial. Revista Brasileira de Energias Renováveis, v.5, n.4, p.490-503, 2016.

VAGHETTI, N.N; DINIZ, G.B; SILVA, J.B; Climatologia da umidade relativa média mensal em regiões homogêneas do estado do Rio Grande do Sul. Revista Científica Revista Multidisciplinar. V. 2, N. 9, 2019. Disponível em: https://show.scientificsociety.net/2019/10/climatologia-da-umidade-relativa-media-mensal-em-regioes-homogeneas-do-estado-do-rio-grande-do-sul/. Acesso em: 7 de abr, 2025.

VASCONCELOS A. B. Utilização de um destilador solar convencional para o tratamento de efluente de uma agroindústria. 2015. 57f. Trabalho de Conclusão de Curso (Bacharelado em Engenharia Ambiental) – Universidade Tecnológica Federal do Paraná, Curitiba, 2015.

CHAPTER 7:
PHYTOTOXICITY ASSESSMENT BY GERMINATION INDEX (GI) IN SOIL FROM A FISH WASTE DISPOSAL SITE ON THE SHORE OF A LAGOON

Gladimir da Silva, Daniela Harter Hornke, Thábata Bierhals Hartwig, Pablo Machado Mendes

ABSTRACT

It is known that fish processing waste is an environmental problem in Brazil and a challenge for managers and researchers nationwide. This situation prompted our objective to seek a phytotoxicological evaluation of a fraction of beach soil where fish waste is buried at shallow depths after evisceration and cleaning. This preliminary bioassay aims to learn more about the lagoon shore soil that receives this waste. The bioassay used the germination of lettuce seeds in a prepared medium originating from the soil to be analyzed. Using this method, consolidated in the technical literature, the phytotoxicity or non-phytotoxicity of the studied medium was qualitatively verified. The method used is simple, yet extremely relevant as a preliminary diagnosis, being economical, fast, and objective compared to other costly and time-consuming methodologies in obtaining results. The procedure is low-cost, easy to perform, based on the direct collection of possibly polluted soil, with its transport to the laboratory and subsequent execution of the analytical procedure. After analysis, toxicity was demonstrated by the germination index in lettuce seeds in the collected beach sample. The result showed that there was toxicity in the sample. It should be noted that to precisely quantify the degree of toxicity of the soil on the edge of the lagoon, further studies are needed with the association of other methodologies.

Keywords: Bioassay; Contamination; Toxicity.

1 INTRODUCTION

Initially, the management of fishing waste in riverside communities is precarious, and it is public knowledge that these animal-derived wastes are dumped directly into the water or on the shoreline, which has an ecosystem sensitive to changes in the natural environment caused by humans. In this context, the unregulated disposal of fishing waste can become a health risk for the local population. Generally, beachfront areas near processing plants are the sites where fish waste is disposed of. It is important to emphasize that fishing waste is classified as "other," in class 1 (hazardous) or class 2 (non-hazardous), and the classification will depend on the physicochemical or infectious characteristics, such as pathogenicity, reactivity, corrosiveness, and toxicity, according to the Brazilian Association of Technical Standards (ABNT) (2024), specifically, NBR 10.004/2024, as updated. As an expected ethical measure, we should attempt to develop simple, inexpensive, and sustainable procedures with research studies and alternatives to these anthropogenic liabilities that plague these locations, which are also tourist attractions.

Companies in the sector collect a portion of this byproduct after evisceration and cleaning, but residues still remain in the soil at the seashore and within the water bodies. This work aligns with the need for a rapid biotechnological investigation, with simple and economical identification, without complex quantifications, aligning with the current trend of sustainability and the integration of problems faced by local actors with government institutions. This work seeks to determine, preliminarily, whether a given deposition site is toxic or not, enabling future, more detailed and generally costly investigations to obtain more accurate results. In this sense, we seek to analyze quickly and effectively the environmental quality of a beach soil area located a few meters from fish processing plants where evisceration and cleaning of this product takes place. In the search for a practical, reliable, and economical procedure, we refer to the following method consolidated in the literature in line with ZUCCONI (1988): "phytotoxicity bioassay through germination index (GI)". It is also emphasized that the lower the GI, the greater the toxicity of the compound analyzed, precisely because it totally or partially inhibits the growth of seed roots, MENDES et al. (2020). Therefore, soil samples were collected from the shore of Lagoa dos Patos in order to determine the health of the soil receiving in natura fish waste buried in a specific location. It is necessary to adopt a national, viable, and low-cost method, consistent with the new global ESG (environmental, social, and governance) strategies, concerned with the environment and society, in this case, locally, and with the initiative of members of a public institution maintained by resources from the Union. Furthermore, this study aligns with Sustainable Development Goal number 14.1 of the United Nations Brazil, which states: By 2025, prevent and significantly reduce marine pollution of all kinds, especially from land-based activities, including marine debris and nutrient pollution. UNITED NATIONS BRAZIL, (2025).

2 THEORETICAL FRAMEWORK

Seed germination tests have been widely used in recent years to indicate the toxicity levels of samples of organic compounds, biosolids, residues, and effluents. Lactuca sativa L., commonly known as lettuce, has been one of the main indicator species for these tests due to its high sensitivity to low toxicity levels compared to other seeds, and also because it is cultivated worldwide (MENDES et al., 2021).

Regarding the ecological effect (toxicity) of the generated sludge, in terms of stimulating the growth of the bioindicator (lettuce), sludge from treatment with okra and Moringa oleifera, separately, showed superior results when compared to sludge from the

association of these plants, in the evaluation of the toxicity of sludge from water treatment with natural coagulants/flocculants (SANTOS et al., 2025).

Raw and treated effluents from pig slaughterhouses showed phytotoxicity to cucumber and lettuce seeds. The germination index of lettuce seeds showed a negative correlation with the levels of total Kjeldahl nitrogen (TKN) and surfactants in the raw effluent. Therefore, effluents from pig slaughterhouses cannot be used for agricultural purposes, as they remain potentially phytotoxic even after treatment, Gerber et al., (2017).

It has been demonstrated that plant biomonitoring tests using L. sativa are useful tools for evaluating and comparing the toxicity of industrial surface treatment effluents, showing trace metal polycontamination in the evaluation of the phytotoxicity of polycontaminated industrial effluents using lettuce (Lactuca sativa) as a bioindicator, Charles et al., (2011).

The particle size and functional groups of microplastics (MPs) present in the soil over long periods undergo changes, which affects their toxicity to plants. Our study confirmed that the original MPs inhibited lettuce growth, while aged MPs exerted an even more significant negative effect, LI et al., (2025).

In the evaluation of the phytotoxicity of treated wastewater using Lactuca sativa: focusing on germination and root elongation test parameters, it was demonstrated that, among the multiple variable parameters used in the germination and elongation tests, the quality of the control water and seed density did not affect the lettuce germination rate (GR), nor the root length or total length, PRIAC et al., (2017).

3 METHODOLOGY

The study began with the collection of a spot sample from a location where fish waste/by-products are disposed of on the beach, behind a residence where the owners are fishermen and clean their catch. Located on the main street of Colônia Z3, Avenida Pernambuco (house number not mentioned at their request), the beach area extends approximately 4 meters from the residence at low tide. The by-product consists of fish heads, scales, skin, spines, and tails. Near the back boundary of the house, at a distance of 1 meter, the fish remains are deposited, buried at a depth of 10 cm. The sample, containing a mixture of medium beach sand and fish remains, was collected with a shovel in a standard bucket and then quartered for better representation. Subsequently, the sample was stored in a refrigerator at 4 degrees Celsius in the laboratory. For preparation, a 10g portion of the sample was weighed into a 200mL beaker using a Marte brand semi-analytical balance

(Model AD2000 with a maximum capacity of 2000g). The weighed soil portion was then dissolved and diluted to 100 mL of distilled water, followed by stirring for 2 minutes and letting it rest for 1 minute. It was filtered through 80g filter paper with an 11 cm diameter in an analytical funnel into a 250 mL Erlenmeyer flask. Next, a 5 mL aliquot of the supernatant was extracted using a graduated pipette and this volume was slowly poured onto a Petri dish previously lined with ordinary filter paper containing commercial lettuce seeds (smooth lettuce, Feltrin brand, batch: 0013202110000020). After identifying the petri dishes, they were placed in the refrigerator for 48 hours, protected from light, inside a closed conventional styrofoam box. On the day of data collection, the length of the roots of commercial lettuce seeds was measured using a digital caliper (Mitutoyo brand). It is recommended to use seeds from the same package only once due to the high sensitivity of the method adopted. Next, readings, calculations, results, and discussions were carried out. To determine the germination index (GI), the following formula was adopted: **GI** = Ga/Gc x Aa/Ac x 100, according to Zucconi et al (1988), where:

GI = germination index;
Ga = number of seeds germinated in the sample;
Gc = number of seeds germinated in the control;
Aa = average root length of the sample (mm);
Ac = average root length of the control (mm).

4 RESULTS AND DISCUSSION

Photos 1 and 2 – Location on the beach where the soil sample was taken (white stripe obscures unauthorized address - photo 1 and photo 2 - disposal site):

Sources: Photo 1 Google Maps, Oct 2025, Photo 2 by the authors.

Photo 3 - The five (5) petri dishes with bioassays after resting for 48h protected from light, samples B1, B2, B3, B4 and B5.

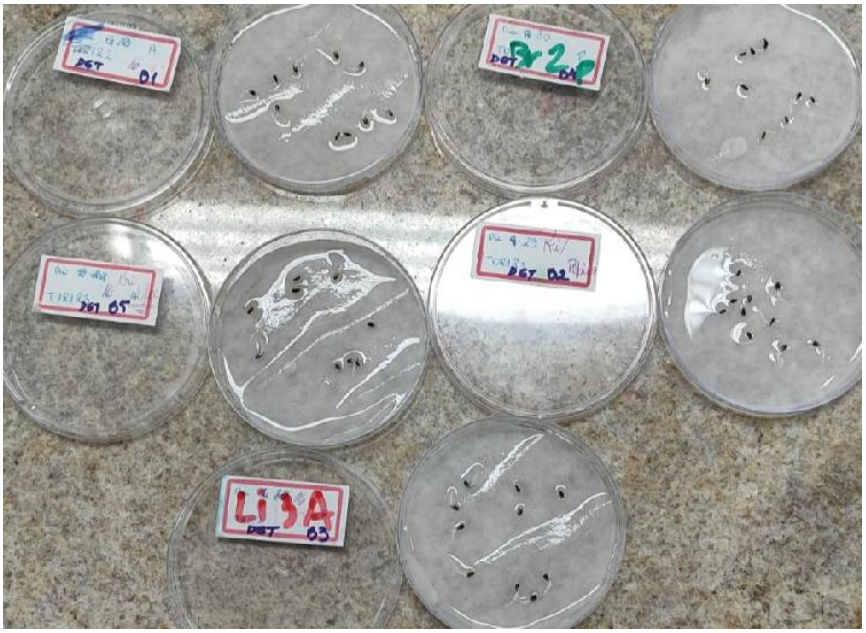

Source: by the authors.

Photo 4 - Zoom of the germination of sample B3:

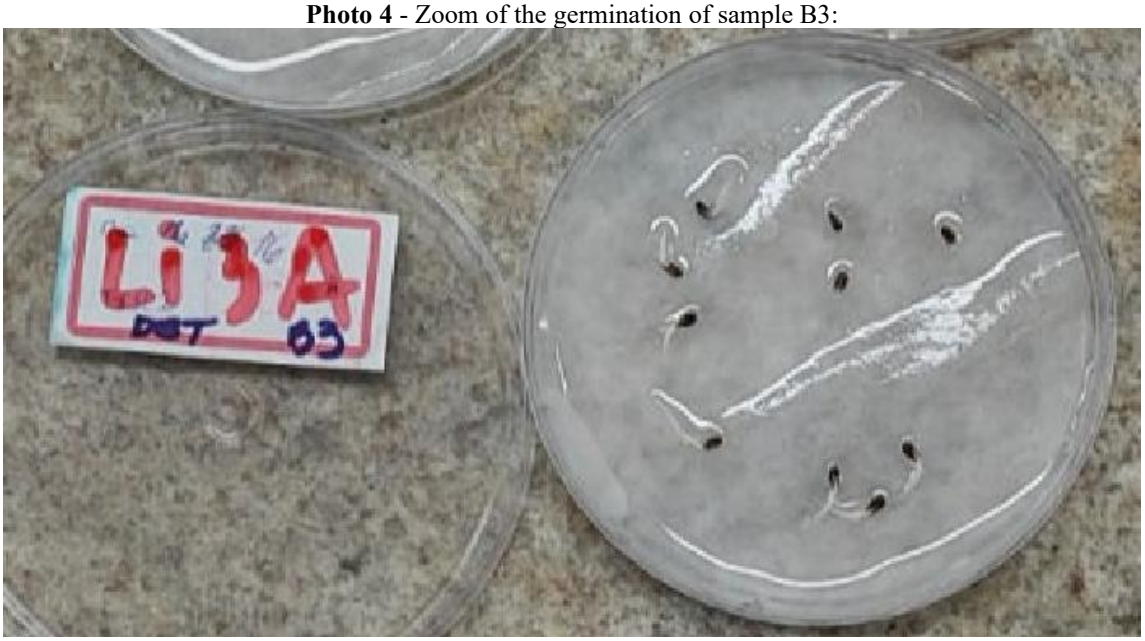

Source: by the authors.

According to the table below, samples B1 and B3 showed 100% germination, meaning that all 10 prepared samples germinated, with average elongation values of 5.47 and 5.42 mm, respectively. Three samples germinated partially: B2, B4, and B5, with average elongation values of 7.38, 4.03, and 4.01 mm, respectively. In sample B2, 5 petri dishes germinated, in sample B4, 8 samples germinated, and in B5, 7 samples germinated.

The control sample (blank), not shown in the table, showed an average elongation of 6.08 mm, with 9 samples germinating.

Table – Elongation of each sample, averages, and germination percentage:

A	Nº G	Al 1	Al 2	Al 3	Al 4	Al 5	Al 6	Al 7	Al 8	Al 9	A 10	Méd
B1	10	6,0	7,9	7,0	9,9	6,9	5,0	6,0	4,0	1,0	1,0	5,47
B2	5	7,0	9,0	8,9	7,1	4,9	-	-	-	-	-	7,38
B3	10	5,8	6,0	7,9	6,2	10,0	7,7	5,2	2,9	1,0	1,5	5,42
B4	8	3,1	5,0	8,5	3,1	2,0	2,2	1,8	6,5	-	-	4,03
B5	7	6,5	6,2	8,9	3,0	2,0	0,5	1,0	-	-	-	4,01

Legenda: A: sample, Nº G: number of germinations, Al.: elongation (mm), Méd.: average of elongations.

Formula: **GI** = Ga/Gc x Aa / Ac x 100 from Zucconi et al (1988), whereupon:

GI = germination index;

Ga = number of seeds germinated in the sample;

Gc = number of seeds germinated in the control;

Aa = average root length of the sample (mm);

Ac = average root length of the control (mm).

Ga = 8

Gc = 9

Aa = 5,262 mm

Ac = 6,08 mm

IG = 76,92%.

5 FINAL CONSIDERATIONS

Based on the bioassay tests performed, low phytotoxicity was found in the sample, which did not take into account the characteristics of the site, since there may be dissolution of soil portions due to the movement of the nearby tide, which may cause washing at certain times, and which were not the subject of this study. The determination of positive contamination is therefore noted. This establishes a more sustainable and economical approach to conducting research. The higher, lower, or non-existent toxicity at other sampling points should be investigated. Whether or not toxicity is present, it is suggested that this toxicity be quantified more precisely in order to obtain values to be compared to parameters of control and inspection standards, which can be carried out in subsequent work. Regarding expenses, the experiment is very low-cost, both in the acquisition of seeds and in laboratory supplies for its execution. Furthermore, art. Article 225, "caput," of the

Federal Constitution (BRAZIL, 2023) is explicit regarding the duty of the Public Authorities to defend and preserve an ecologically balanced environment. Also, according to Law 6.938/1981, in its article 4 - The National Environmental Policy will aim at: I - the compatibility of socio-economic development with the preservation of environmental quality and ecological balance;

It is concluded, therefore, that low phytotoxicity was detected in the soil sample from the edge of the lagoon with fish residues at the point considered.

REFERENCES

ASSOCIAÇÃO BRASILEIRA DE NORMAS TÉCNICAS (ABNT). NBR 10.004: Resíduos Sólidos - Classificação Parte 2: Sistema Geral de Classificação de Resíduos (SGCR). Rio de Janeiro, 2024. Disponível em: http://www.abnt.org.br/biblioteca/normas. Acesso em: 11 out. 2025.

BRASIL. Constituição da República Federativa do Brasil. Brasília: Senado Federal, 1988. Disponível em: http://www.planalto.gov.br/ccivil_03/constituicao/constituicao.htm. Acesso em: 14 ago. 2023.

BRASIL. Lei 6.938, DE 31 DE AGOSTO DE 1981. Dispõe sobre a Política Nacional do Meio Ambiente, seus fins e mecanismos de formulação e aplicação, e dá outras providências. Disponível em: https://www.planalto.gov.br/ccivil_03/leis/L6938compilada.htm. Acesso em: 15 ago. 2023.

CHARLES, J. et al. Evaluation of the phytotoxicity of polycontaminated industrial effluents using the lettuce plant (Lactuca sativa) as a bioindicator. Ecotoxicology and Environmental Safety. v. 74, n. 7, p. 2057-2064, oct 2011. https://doi.org/10.1016/j.ecoenv.2011.07.025. Disponível em: https://www.sciencedirect.com/science/article/pii/S0147651311002120. Acesso em: 25 nov 2025.

GERBER, M. D. et al. Phytotoxicity of effluents from swine slaughterhouses using lettuce and cucumber seeds as bioindicators. Science of The Total Environment. v. 592, n. 15, p. 86-90, aug. 2017. DOI: https://doi.org/10.1016/j.scitotenv.2017.03.075. Disponível em: https://www.sciencedirect.com/science/article/abs/pii/S0048969717305879. Acesso em: 25 nov 2025.

LI, X et al. Aging increases the phytotoxicity of polyethylene and polypropylene to Lactuca Sativa L. compared to original microplastics. Journal of Environmental Management, v. 383, 125423, may 2025. DOI: https://doi.org/10.1016/j.jenvman.2025.125423. Disponível em: https://www.sciencedirect.com/science/article/abs/pii/S0301479725013994. Acesso em: 25 nov. 2025.

MENDES, P. M. et al. Improvement of the phytotoxicity test with lettuce seed germination: reliability and accuracy of the method. Braz. J. of Develop. Curitiba, v.6, n.4 18178-18184, apr. 2020.

MENDES, P. M. et al. Phytotoxicity test in check: Proposition of methodology for comparison of different method adaptations usually used worldwide. Journal of Environmental Management, v. 291, 112698, 1 de aug. 2021. DOI: https://doi.org/10.1016/j.jenvman.2021.112698. Disponível em: https://www.sciencedirect.com/science/article/abs/pii/S030147972100760X. Acesso em: 25 nov. 2025.

NAÇÕES UNIDAS BRASIL. Objetivos de Desenvolvimento Sustentável.Brasília: ONU Brasil, [s.d.]. Disponível em:https://brasil.un.org/pt-br/sdgs/14. Acesso em: 13 out. 2025.

PRIAC, A. et al. Treated wastewater phytotoxicity assessment using Lactuca sativa: Focus on germination and root elongation test parameters. Comptes Rendus Biologies, v. 340, Issue 3, p.188-194, mar 2017. DOI: https://doi.org/10.1016/j.crvi.2017.01.002. Disponível em: https://www.sciencedirect.com/science/article/pii/S1631069117300033. Acesso em: 25 nov 2025.

SANTOS, A.L.A. et al. Toxicity of sludge from water treatment using natural coagulants/flocculants . Journal of Water Process Engineering, v. 77, 108644, sep. 2025. https://doi.org/10.1016/j.jwpe.2025.108644. Disponível em: https://www.sciencedirect.com/science/article/pii/S2214714425017179. Acesso em: 25 nov 2025.

ZUCCONI, F. et al. Evaluating toxicity in immature compost. Biocycle, Emmaus, v. 22, p.54-57, 1988.

CHAPTER 8:
INFLUENCE OF PARTIAL REPLACEMENT OF CEMENT BY GLASS POWDER ON MECHANICAL PROPERTIES OF CONCRETE

Gilberto Cardoso Xavier, João Pedro da Silva Viana, Juliana da Fonseca Teixeira, Ingrid Telles Moraes, Alessandra Buss Tessaro, Pablo Machado Mendes

ABSTRACT

This study investigated the influence of partially replacing Portland cement with glass powder of different granulometries and substitution levels on the mechanical properties of concrete. The glass powder was classified using 0.15 mm and 0.30 mm sieves, and granulometric analyses revealed a wide particle size distribution, with higher fineness and specific surface area in the material retained by the finer mesh. Five concrete mixes were produced and evaluated for axial compressive strength at 7 and 28 days. The results showed that the finer glass powder (0.15 mm) exhibited superior or equivalent performance compared to the reference concrete, particularly at the 5% replacement level, indicating potential benefits from the filler effect and the early onset of pozzolanic activity. In contrast, the coarser material (0.30 mm) led to reductions in strength, confirming its predominantly inert behavior. It is concluded that moderate replacement levels combined with finer granulometry represent a viable strategy for incorporating glass waste as a supplementary cementitious material, contributing to more sustainable practices in civil construction.

Keywords: Glass powder; Sustainable concrete; Mineral admixtures; Mechanical strength; Circular economy.

1 INTRODUCTION

Portland cement concrete is the most widely consumed building material globally, being fundamental to the development of modern infrastructure. According to Mehta and Monteiro (2014), this widespread use is directly related to its technical performance, although its consumption is associated with a significant environmental impact, mainly due to the cement manufacturing process. Cement production is one of the main industrial sources of carbon dioxide (CO_2) emissions, contributing approximately 5% to 8% of total global anthropogenic emissions. It is estimated that for every ton of cement produced, between 0.8 and 0.9 tons of CO_2 are released into the atmosphere, a direct byproduct of limestone decarbonation and the intensive consumption of fossil fuels in clinker kilns (Agência UFC, 2025).

Given the growing climate emergency, the search for more sustainable practices in civil construction has become imperative. In this context, the use of supplementary cementitious materials (SCMs) emerges as an effective strategy for the production of environmentally responsive concrete, according to Neville and Brooks (2013). These

materials, generally byproducts of industrial or agricultural processes, can partially replace Portland cement, promoting a double advantage: reduced clinker consumption and valorization of waste. As highlighted by Taylor (1997), this approach contributes to reducing the environmental impacts associated with the concrete production chain.

Glass represents a significant environmental challenge due to its non-biodegradable nature and low recycling rates in Brazil (25.8% in 2024), according to Cuesta et al. (2023). Grinding it into fine particles can activate pozzolanic reactivity, making it a viable candidate for cementitious replacement. Recent studies demonstrate that glass powder, although exhibiting a slower pozzolanic reaction compared to other materials, contributes to significant strength gains at advanced ages, highlighting its technical potential.

The effectiveness of glass powder is directly linked to its fineness: smaller particles increase the surface area available for reaction with calcium hydroxide, forming additional hydrated calcium silicates (C-S-H), according to Berodier and Scrivener (2014). In this sense, this study systematically investigates the influence of the partial replacement of Portland cement with glass powder at different proportions and particle sizes on the mechanical properties of concrete, aiming to contribute to the development of more sustainable concretes.

2 THEORETICAL FRAMEWORK

Supplementary cementitious materials (SCMs) are finely divided materials that can be added to concrete as a partial replacement for Portland cement. When properly selected and dosed, they are able to react with cement hydration products, modifying the microstructure of the paste and conferring significant improvements to the properties of the concrete. As highlighted by Mehta and Monteiro (2014), these materials play a relevant role in improving the mechanical performance and durability of concrete, since they contribute to the improvement of its microstructure.

The use of mixed concrete mixes (SCMs) has intensified in recent decades, driven by environmental, economic, and technical factors. The main mechanisms of action of mineral admixtures include the physical effect (filler and nucleation), the dilution effect, and the chemical effect (pozzolanic reaction). The filler effect refers to the physical role played by fine particles in filling voids between cement grains and aggregates, resulting in denser packing and reduced capillary porosity. According to Neville and Brooks (2013), this physical behavior is fundamental for improving the workability and mechanical performance of concretes containing admixtures.

Soda-lime glass, the most common type of glass produced, is composed predominantly of silica (SiO_2, approximately 70–75%), sodium oxide (Na_2O, 12–16%), and calcium oxide (CaO, 7–12%). The amorphous structure of the glass, combined with its high silica content, gives it the potential for pozzolanic reaction when finely ground. According to Sathiparan (2024), this composition and structure make glass powder a material capable of acting efficiently as a reactive mineral addition in cementitious matrices.

The pozzolanic activity of glass powder is directly related to its fineness. Smaller particles increase the specific surface area available for reaction with calcium hydroxide (CH) released during cement hydration. The pozzolanic reaction consists of the interaction between the amorphous silica present in the glass powder and CH, forming additional hydrated calcium silicates (C-S-H) that fill capillary pores, refining the microstructure. As highlighted by Zeybek et al. (2022), studies demonstrate that glass powder with a particle size smaller than 75 μm exhibits superior performance, resulting in compressive strength increases of up to 30% compared to the reference concrete, depending on the replacement content and curing age. These results reinforce the importance of fineness as a determinant of reactivity and performance gain.

The particle size distribution of glass powder is therefore a critical factor for its efficiency as a supplementary cementitious material. Scientific literature establishes that particles with a diameter smaller than 75 μm exhibit significant pozzolanic reactivity, while larger particles behave predominantly as an inert addition (filler effect). The specific surface area increases exponentially with the reduction in particle diameter; thus, for the same mass of material, smaller particles present a greater total surface area available for chemical reaction. According to Chen et al. (2025), this behavior explains why reducing the particle size enhances the material's performance when incorporated into cementitious mixtures.

Extremely fine particles (below 10 μm) can exhibit pozzolanic reactivity comparable to that of silica fume, one of the most reactive mineral admixtures available. However, very fine particles also increase the water demand of mixtures due to their larger surface area, requiring the use of superplasticizing admixtures to maintain workability, according to Muhedin and Shibeshi (2023). This balance between reactivity and rheological requirements shows that particle size optimization is essential to ensure performance without compromising properties in the fresh state.

The interfacial transition zone (ITZ) is a region approximately 50 μm thick located at the interface between aggregates and cement paste. This region exhibits a microstructure distinct from the paste in volume, characterized by higher porosity, a higher concentration of portlandite, and a lower density of C-S-H. The ITZ constitutes the weakest link in concrete, being the preferred location for the initiation and propagation of microcracks under loading. According to Mehta and Monteiro (2014), understanding this region is fundamental to understanding the mechanical behavior and durability of cementitious structures.

High-fineness mineral additions, such as glass powder with appropriate particle size distribution, can significantly improve the ITZ (Incremental Temperature Zone). Fine particles fill the voids near the aggregates, reducing local porosity. Furthermore, the pozzolanic reaction consumes the portlandite concentrated in the ITZ, replacing it with denser, stronger C-S-H (cement-sulfur-hydrogen), as highlighted by Knight et al. (2023). These combined effects contribute to the formation of a denser, more cohesive, and stronger ITZ, resulting in concrete with better overall performance.

3 METHODOLOGY

The cement used was CP V – HES (High Early Strength), according to the requirements of NBR 16697 (ABNT, 2018). The glass powder used was obtained from post-consumer colorless soda-lime glass, subsequently ground in a ball mill and sieved into two distinct particle sizes: 0.15 mm mesh and 0.30 mm mesh. The fine aggregates, consisting of natural quartz sand, and coarse aggregates, composed of basaltic crushed stone, were characterized according to the procedures of NBR NM 248 (ABNT, 2003). To ensure the workability of the mixtures, a superplasticizer additive based on polycarboxylates was used.

Five concrete mixes were produced: a reference mix, composed of 100% cement, and four mixes containing partial replacement of cement with glass powder in the following combinations:

PV 5% – 0.15 mm mesh;

PV 10% – 0.15 mm mesh;

PV 5% – 0.30 mm mesh;

PV 10% – 0.30 mm mesh.

The water/binder ratio was kept constant at 0.50 for all mixes, while the mortar content was fixed at 53%, ensuring comparability between the mixtures. The slump test of

the fresh concrete was monitored according to NBR 16889 (ABNT, 2020), remaining between 90 and 110 mm by adjusting the superplasticizer dosage.

The cylindrical specimens, with dimensions of 100 mm × 200 mm, were molded according to the procedures of NBR 5738 (ABNT, 2015). After molding, they remained in moist curing for 14 days in a climate-controlled chamber at 23 ± 2°C and a minimum relative humidity of 90%. Then, the specimens were transferred to air curing until they completed 28 days.

Axial compressive strength was determined according to NBR 5739 (ABNT, 2018), at 7 and 28 days, using a hydraulic press with a capacity of 300 kN and a loading rate of 0.45 ± 0.15 MPa/s. For each age and each mix design, three specimens were tested, and the result was expressed as the arithmetic mean, discarding outliers according to the normative criterion.

4 RESULTS AND DISCUSSION

The physicochemical characterization performed by nitrogen (N_2) adsorption shows relevant differences between the glass powder samples with distinct particle sizes. BET analysis revealed that the PV 150 μm sample had a specific surface area of 0.1394 m^2/g, while the PV 300 μm sample had a slightly higher surface area of 0.1561 m^2/g. Although both values are low—expected behavior for vitreous materials—it is noted that the finer sample (150 μm) did not generate a larger surface area, indicating possible particle agglomeration or low microtexture generation after grinding.

The Langmuir model showed a similar trend, with sample PV 150 registering 0.2204 m^2/g and sample PV 300 0.2431 m^2/g, reinforcing that the granulometric difference did not result in a significant increase in active surface area. The proximity between the values obtained by BET and Langmuir suggests that the surface is predominantly non-porous, a typical characteristic of amorphous vitreous materials.

The total pore volume was also very low for both samples. Sample PV 150 had a volume of 0.000392 cm^3/g, while sample PV 300 had 0.000375 cm^3/g, indicating a practically solid structure, without a significant presence of micropores or mesopores. As a result, the average pore width (calculated by 4V/A BET) remained high, being 112.5 Å for sample PV 150 and 96.1 Å for sample PV 300, values consistent with a low-porosity structure.

The evaluation of adsorption isotherms showed type IIB curves, typical of non-porous or macroporous solids, with low adsorption across the entire range of relative

pressures. The maximum amounts adsorbed were 0.2534 cm^3/g for sample PV 150 and 0.2425 cm^3/g for sample PV 300, reinforcing the low surface area of the material.

In general, the results show that there are no significant differences between the two particle sizes analyzed, either in specific surface area, pore volume, or adsorption behavior. Both samples have a poorly developed surface, low porosity, and an essentially non-porous character, indicating that the milling used did not produce highly reactive particles from the point of view of specific area. This means that pozzolanicity will not depend on pore development, but rather mainly on the vitreous composition and the presence of amorphous silica, in addition to factors such as alkalinity of the medium and actual fineness of the particles.

The particle size analysis of the glass powder revealed clear differences between the two groups evaluated, corresponding to the 0.30 mm sieves (GLASS POWDER 03 Group) and 0.15 mm sieves (GLASS POWDER 015 Group). In both cases, a wide distribution of particle sizes was observed, but with distinct behaviors in terms of fineness and homogeneity, directly reflecting the level of grinding and the fractionation adopted.

In the GLASS POWDER 03 group, corresponding to the powder retained or classified around the 0.30 mm mesh, the three tests showed very similar characteristics. The D50 values remained between 501.3 μm, 517.7 μm and 536.4 μm, indicating a predominance of coarse particles, with half of the sample having dimensions greater than 0.5 mm. The amplitude of the distribution was also high, as demonstrated by the D90 values, which ranged from 850.4 μm to 901.4 μm, evidencing a significant presence of large particles. The coefficients of variation between 47% and 51% confirm high particle size dispersion, although with greater uniformity when compared to the finer particle size samples. Furthermore, the specific surface areas determined showed reduced values, between 341.6 and 374.5 cm^2/ml, consistent with predominantly coarse particles and low surface reactivity.

The GLASS POWDER 015 group, referring to the material sieved through a 0.15 mm mesh, showed distinct behavior, marked by significantly smaller particles. The D50 values were practically constant between the two samples (180.8 μm and 180.4 μm), indicating reasonable repeatability of the grinding process. The presence of very fine particles was also noted, with D10 around 21 μm, representing a significant fraction of the sample with micrometric dimensions. In contrast, the D90 values, close to 366–367 μm, show that there is still a considerable portion of relatively large particles, reinforcing the idea of a material with a wide particle size distribution. The coefficients of variation,

however, were even higher — 71.10% and 72.71% — evidencing a very intense particle size dispersion, typical of mechanically ground materials without a rigorous fine classification step. The estimated specific surface area, close to 1607 cm²/ml in both samples, was substantially higher than that observed in the GLASS POWDER 03 group, reinforcing that the 0.15 mm mesh material has greater fineness and, potentially, greater reactivity.

The comparison between the two groups shows that the laser granulometry process can, in fact, separate classes of particles with distinct granulometric behaviors. The GLASS POWDER 03 group is composed mainly of coarse particles, with low specific area and lower pozzolanic reaction potential. In contrast, the GLASS POWDER 015 group has finer particles, a larger surface area, and a higher proportion of micrometric fractions, indicating greater suitability to act as a supplementary cementitious material. Despite this, both groups have a wide distribution and high coefficients of variation, suggesting that the grinding process still generates significant dimensional heterogeneity.

In general, the results show that glass powder sieved through smaller meshes has a finer granulometry and a larger specific area, characteristics that favor reactivity. On the other hand, the material classified on the 0.30 mm mesh remains essentially coarse and poorly activated, playing a role closer to a filler than a pozzolanic addition. Thus, the particle size distribution of glass powder proves to be a determining factor for its potential efficiency when used as a partial replacement for Portland cement.

The axial compressive strength results obtained at 7 and 28 days for all mixes are presented in Figure 1. In general, it is observed that the partial replacement of cement with glass powder influenced the mechanical behavior of the concrete in a distinct way, depending on both the replacement content and the particle size used.

At 7 days, the concretes produced with 0.15 mm mesh glass powder exhibited superior performance to the reference mix. The mix with 5% replacement reached 39.92 MPa, while the mix with 10% reached 42.94 MPa, exceeding the mixture without replacement (37.52 MPa). This behavior suggests that, even at early ages, the finer particle size contributed to a denser microstructure, possibly due to the filler effect and an initial, albeit moderate, pozzolanic activity.

Figure 1 - Axial compressive strength obtained at 7 and 28 days

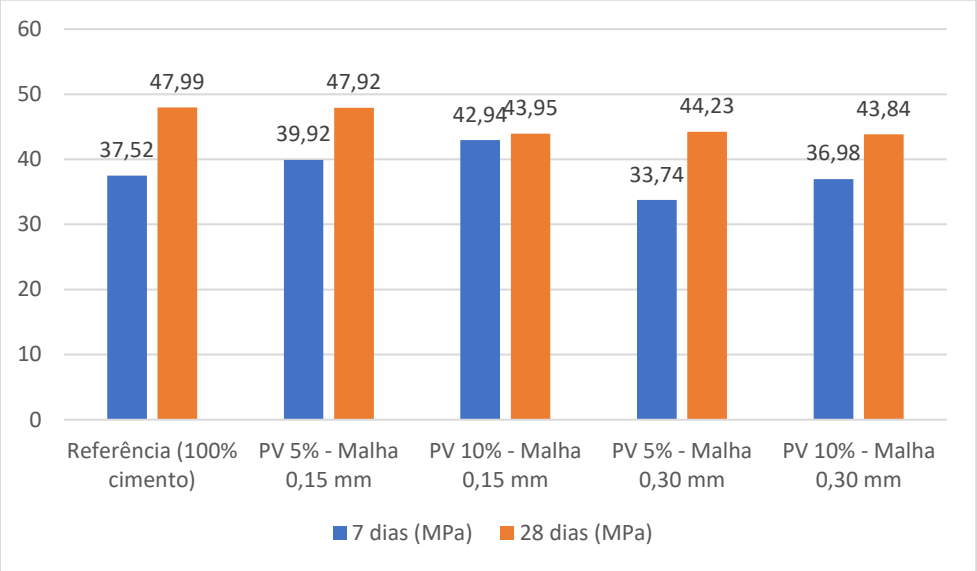

Source: Prepared by the authors (2025)

In contrast, the mixes produced with 0.30 mm mesh glass powder showed reductions in strength at 7 days. The 5% substitution resulted in 33.74 MPa, while the 10% substitution reached 36.98 MPa, both below the value obtained for the reference mix. This behavior is associated with the larger particle size, which acts predominantly as an inert addition, delaying the formation of hydrated products and reducing the packing of the cementitious matrix.

At 28 days, however, the behavior between the mixes showed a tendency to stabilize. The reference concrete reached 47.99 MPa, a value very close to that obtained by the mixes with glass powder substitution. The mix with 5% - 0.15 mm showed 47.92 MPa, practically the same as the reference, indicating that the presence of fine particles did not compromise the development of strength. The mixture with 10% - 0.15 mm, although it showed the greatest initial gain, reached 43.95 MPa, registering a slight reduction at 28 days, possibly associated with excess unreacted material, which tends to limit the continuity of hydration.

In the 0.30 mm mixes, both contents maintained similar performance at 28 days (44.23 MPa and 43.84 MPa, respectively), demonstrating that, despite the drop observed at 7 days, part of the initial deficit was recovered with age. Still, the values remain slightly lower than the reference mix, reinforcing the reactive limitation of the coarser particles.

In general, the results indicate that the finer glass powder (0.15 mm) exhibits more favorable behavior, either due to better particle packing or higher reactive potential, while the coarser particle size material (0.30 mm) acts essentially as a filler, without significantly

contributing to the formation of additional C-S-H. These findings reinforce the strong dependence between particle size and efficiency of glass powder as a supplementary cementitious material.

5 FINAL CONSIDERATIONS

The results obtained in this study demonstrate that the partial replacement of Portland cement with glass powder has potential for application as a supplementary cementitious material, provided that the determining influence of particle size on the mechanical properties of concrete is observed. Particle size analyses showed high dimensional heterogeneity in the ground particles, a typical characteristic of mechanical fragmentation processes, but revealed clear distinctions between the materials sieved through 0.15 mm and 0.30 mm meshes. While the powder classified at 0.30 mm remained essentially a low-fineness material, with particles larger than 500 μm predominating, the powder sieved at 0.15 mm showed a larger surface area and a significant presence of micrometric fractions, indicating more favorable conditions for pozzolanic reactions.

This particle size difference was directly reflected in the mechanical performance of the concretes. Mixes with finer glass powder (0.15 mm) showed increased strength at 7 days and performance equivalent to the reference concrete at 28 days, especially at a 5% replacement level, demonstrating good compatibility with the cementitious system. On the other hand, mixes produced with coarser glass powder (0.30 mm) showed reduced initial strength and lower values at 28 days, a behavior expected for materials that act predominantly as filler and do not have sufficient fineness to develop significant pozzolanic activity during the analyzed period.

The results indicate that moderate substitutions, especially on the order of 5% with finer-grained glass powder, can be incorporated into concrete without compromising mechanical properties and with potential benefits to the sustainability of civil construction. The fineness of the glass powder proved to be the key factor for its performance, being an indispensable condition for the material to effectively participate in hydration reactions and contribute to the refinement of the microstructure of the cementitious matrix.

Thus, it is concluded that glass powder has potential for use as a supplementary cementitious material, provided it is properly processed and classified. Additional studies involving older ages, direct evaluation of pozzolanicity, and microstructural analysis could complement and deepen the understanding of the mechanisms involved, contributing to the advancement of the sustainable use of glass waste in civil construction.

REFERENCES

ABNT – ASSOCIAÇÃO BRASILEIRA DE NORMAS TÉCNICAS. NBR 12653: Materiais pozolânicos – Requisitos. Rio de Janeiro, 2014.

ABNT – ASSOCIAÇÃO BRASILEIRA DE NORMAS TÉCNICAS. NBR NM 248: Agregados – Determinação da composição granulométrica. Rio de Janeiro, 2003.

ABNT – ASSOCIAÇÃO BRASILEIRA DE NORMAS TÉCNICAS. NBR 5738: Concreto – Procedimento para moldagem e cura de corpos de prova. Rio de Janeiro, 2015.

ABNT – ASSOCIAÇÃO BRASILEIRA DE NORMAS TÉCNICAS. NBR 5739: Concreto – Ensaio de compressão de corpos de prova cilíndricos. Rio de Janeiro, 2018.

ABNT – ASSOCIAÇÃO BRASILEIRA DE NORMAS TÉCNICAS. NBR 16697: Cimento Portland – Requisitos. Rio de Janeiro, 2018.

ABNT – ASSOCIAÇÃO BRASILEIRA DE NORMAS TÉCNICAS. NBR 16889: Concreto – Determinação da consistência pelo abatimento do tronco de cone. Rio de Janeiro, 2020.

AGÊNCIA UFC. Relatório de Impacto Ambiental da Produção de Cimento. Fortaleza: Universidade Federal do Ceará, 2025.

BERODIER, E.; SCRIVENER, K. Understanding the filler effect on the nucleation and growth of C-S-H. Journal of the American Ceramic Society, v. 97, n. 12, p. 3764–3773, 2014.

CHEN, Z.; ZHOU, Y.; HUANG, X.; LI, W. Improvement of interfacial transition zone between aggregate and paste through utilization of nano-materials. Journal of Sustainable Cement-Based Materials, v. 10, n. 3, p. 189–205, 2025.

CUESTA, A. et al. Local structure and Ca/Si ratio in C-S-H gels from hydration of blends of tricalcium silicate and silica fume. Cement and Concrete Research, v. 155, p. 106749, 2023.

KNIGHT, R.; MCDONALD, K.; SPAGNOLO, S. Sustainable concrete: A review of recent developments. Construction and Building Materials, v. 362, p. 129195, 2023.

MEHTA, P. K.; MONTEIRO, P. J. M. Concreto: Microestrutura, Propriedades e Materiais. 4. ed. São Paulo: IBRACON, 2014.

MUHEDIN, A.; SHIBESHI, K. Performance of concrete incorporating recycled glass powder and aggregate. Journal of Materials in Civil Engineering, v. 35, n. 4, 2023.

NEVILLE, A. M.; BROOKS, J. J. Tecnologia do Concreto. 2. ed. Porto Alegre: Bookman, 2013.

SATHIPARAN, N. Utilization of waste glass powder as supplementary cementitious material: A review. Construction and Building Materials, v. 401, p. 132847, 2024.

TAYLOR, H. F. W. Cement Chemistry. 2. ed. London: Thomas Telford, 1997.

ZEYBEK, Ö. et al. Influence of replacing cement with waste glass on mechanical properties of concrete. Materials, v. 15, n. 21, p. 7513, 2022.

CHAPTER 9:
BIOCHAR FROM GRAPE POMACE: PATHWAYS TO CIRCULAR ECONOMY AND SUSTAINABLE BIOENERGY

Rubinei de Servi Ferraz, Ricardo Lemos Sainz, Giani Mariza Britzius Barwald

ABSTRACT

This study examines the valorization of agro-industrial waste, focusing on grape pomace, a byproduct of wine production in Rio Grande do Sul, Brazil. Improper disposal of this material, which can represent up to 40% of the processed fruit mass, generates environmental impacts and additional costs for wineries. The research proposes slow pyrolysis as a sustainable alternative to transform pomace into biochar (BC), a carbon-rich material with environmental and energy applications. The process was carried out in a fixed-bed reactor at different temperatures (400°C, 450°C, and 500°C) after drying the material. Chemical and thermogravimetric analyses revealed the gradual decomposition of hemicellulose, cellulose, and lignin, highlighting the importance of lignin in producing stable, high-quality biochar. Results showed that the condition of 400°C and lower biomass mass (50 g) provided the highest biochar yield (89%). It is concluded that slow pyrolysis is a viable alternative for grape pomace utilization, aligned with circular economy principles and sustainability.

Keywords: Grape pomace; Pyrolysis; Biochar; Biomass; Sustainability.

1 INTRODUCTION

Climate change and its environmental impacts have demanded global efforts to reduce greenhouse gas emissions and promote sustainable energy alternatives. In this context, plant biomass emerges as a strategic resource, as plants, through photosynthesis, convert carbon dioxide into organic compounds that can be used for clean energy generation, thereby reducing dependence on fossil fuels and mitigating the effects of global warming (Ferraz, 2025, p. 13).

Brazil, as a major agro-industrial producer, faces significant challenges in managing solid waste generated from the processing of agricultural raw materials. These residues, often discarded without technical guidance, may cause soil and water pollution and represent additional costs for industries. In the wine sector, particularly in the state of Rio Grande do Sul, grape pomace is the main by-product of wine production, accounting for up to 40% of the weight of processed grapes (Licandro & Odio, 2021). The inadequate disposal of this material generates serious environmental and economic problems, exacerbated by the absence of specific national regulations for its valorization (Ferraz, 2025, p. 14).

Grape pomace—composed of skins, seeds, stems, and residual pulp—is produced in large quantities on a seasonal basis. Its accumulation and improper disposal pose environmental risks and increase management costs for wineries. Currently, part of this residue is directed to composting or simply abandoned in open areas, without technological utilization, which limits its valorization potential and reinforces the perception that it is merely an environmental liability (Ferraz, 2025, pp. 14–15).

In this context, slow pyrolysis emerges as a promising technological alternative for converting residual biomass into value-added products such as biochar, bio-oil, and non-condensable gases. Biochar, in particular, exhibits high thermal stability, porosity, and physicochemical properties that make it suitable for environmental and energy applications, including soil conditioning, pollutant adsorption, and energy generation (Belini, 2020; Costa, 2021).

The main objective of this study is to evaluate the feasibility of slow pyrolysis as a valorization technique for grape pomace, aiming at the production and physicochemical characterization of biochar. The specific objectives include the preliminary assessment of the physicochemical characteristics of grape pomace, the investigation of thermal conversion under different temperature and mass conditions, the characterization of the resulting biochar in terms of yield and properties, and the comparison of the obtained results with literature data to identify potential applications in sustainable practices.

The choice of slow pyrolysis as a technological route is justified by its ability to transform agro-industrial residues into value-added products, contributing to environmental impact mitigation, diversification of the energy matrix, and promotion of the circular economy. Furthermore, the valorization of grape pomace through pyrolysis aligns with the United Nations 2030 Agenda for Sustainable Development, particularly SDGs 7 (Affordable and Clean Energy), 12 (Responsible Consumption and Production), 13 (Climate Action), and 15 (Life on Land) (UN, 2020).

Thus, this chapter aims to demonstrate that the slow pyrolysis of grape pomace is a viable and sustainable alternative capable of transforming an environmental liability into a strategic input for agricultural and energy practices, strengthening the integration between science, innovation, and sustainability.

2 LITERATURE REWIEW

Plant biomass, as a renewable resource, is composed of different structural macromolecules and low-stability organic compounds that determine its behavior in energy

conversion processes. The main constituents of the plant cell wall are cellulose, hemicellulose, and lignin, in addition to cellular extractives such as sugars, proteins, and lipids. Cellulose, due to its linear and highly crystalline structure, provides mechanical strength to plants and exhibits low solubility in water, hindering microbial degradation. Hemicellulose, in contrast, is amorphous and heteropolysaccharidic, composed of pentoses and hexoses, and is more susceptible to thermal and chemical degradation. Lignin, an aromatic macromolecule, acts as a cementing matrix for cellulose and hemicellulose fibers, providing rigidity and protection against chemical and biological agents, and is responsible for the formation of more stable biochar during pyrolysis (Ferraz, 2025, pp. 16–17; Santos & Peres, 2012).

In the context of viticulture, grape pomace is the main solid residue generated, composed of skins, seeds, stems, and residual pulp. Its composition varies according to grape variety, vinification method, and edaphoclimatic conditions. White wine production results in pomace with higher residual pulp and sugar content, whereas red wine pomace exhibits lower mass due to alcoholic fermentation, which consumes part of the available sugars (Ferraz, 2025, pp. 19–20). Studies indicate that dried pomace may contain 38–52% seeds and 8–20% skins and stems, in addition to fibers and high-value phenolic compounds (Beres et al., 2017). These bioactive compounds—such as anthocyanins, tannins, and resveratrol—are relevant to the food, pharmaceutical, and cosmetic industries but are often wasted due to inadequate residue management (Christ & Burrit, 2013; Brenes et al., 2016).

The valorization of grape pomace can follow different technological routes. Integral utilization allows its use in composting, animal feed, or biochar production via pyrolysis. Seeds may be used for extracting oil rich in unsaturated fatty acids and antioxidants or for producing functional flour. Skins contain pigments and phenolic compounds that can be extracted for use as natural colorants or antioxidants in foods and supplements (Ferraz, 2025, p. 21). These routes demonstrate that grape pomace should not be treated merely as waste but as a raw material for value-added products.

Pyrolysis, a thermal process conducted in the absence of oxygen, converts biomass into three main products: biochar, bio-oil, and non-condensable gases. Slow pyrolysis, characterized by low heating rates and long residence times, favors the formation of the solid fraction (biochar). Lower temperatures, around 400 °C, tend to maximize biochar yield, whereas higher temperatures (500 °C or above) increase the production of bio-oil and gases due to greater degradation of volatile compounds (Bridgwater, 2012; Ferraz, 2025, pp. 22–24).

Thermogravimetric analysis (TGA) is frequently used to understand the gradual decomposition of biomass components, showing that hemicellulose, cellulose, and lignin degrade at distinct temperature ranges, which directly influences the quality and stability of the resulting biochar (Ferraz, 2025, Fig. 13, p. 42).

The resulting biochar exhibits physicochemical properties suitable for various applications. Its high porosity and thermal stability enable its use as a soil conditioner, adsorbent of organic and inorganic pollutants, and energy input. Recent studies highlight the potential of grape-pomace biochar for heavy-metal adsorption, soil fertility improvement, and mitigation of greenhouse gas emissions (Martins et al., 2020; Santos, 2022). Additionally, research indicates that biochar can serve as a precursor for activated carbon, increasing its industrial value (Belini, 2020).

From an environmental and economic perspective, the pyrolysis of grape pomace contributes to the circular economy by transforming a problematic residue into a strategic resource. This practice aligns with the United Nations Sustainable Development Goals, particularly SDGs 7, 12, 13, and 15 (UN, 2020). The adoption of agro-industrial residue valorization technologies, such as pyrolysis, strengthens the integration of science, innovation, and sustainability, offering solutions for environmental impact mitigation and diversification of the Brazilian energy matrix.

3 METHODOLOGY

This study was conducted using grape pomace obtained from wineries in the state of Rio Grande do Sul, Brazil, characterized as an agro-industrial residue of high availability and environmental relevance. The selection of this raw material is justified by its representativeness in the wine sector and its potential for valorization through thermochemical processes. Initially, the material was subjected to oven drying at 105 °C to reduce its moisture content, which was initially high (43.82%), as indicated by preliminary analyses (Ferraz, 2025). This step was essential to ensure greater efficiency in the pyrolysis process, as excessive moisture compromises thermal stability and the formation of solid products.

The proximate chemical characterization of the dried grape pomace (DGP) was performed by determining volatile matter, ash content, and fixed carbon. The average results obtained were 69.69% volatiles, 20.75% ash, and 9.56% fixed carbon, values that directly influence the efficiency of thermal conversion and the quality of the produced

biochar (Ferraz, 2025). These parameters were used as references for the experimental design and for comparison with literature data and are presented in Table 1 below.

Table 1 – Proximate Composition of Grape Pomace

Análise	Amostras BUS (%)			Média
	Amostra 1	Amostra 2	Amostra 3	
Umidade	43,44	43,77	44,24	43,82 ± 0,33
Voláteis	69,37	69,20	70,49	69,69 ± 0,32
Cinzas	22,31	18,51	21,43	20,75 ± 2,64
Carbono fixo	8,32	12,29	8,08	9,56 ± 3,73

The pyrolysis process was conducted in a fixed-bed reactor designed to operate under controlled temperature and residence-time conditions. The experiments were performed at three temperature ranges—400 °C, 450 °C, and 500 °C—using different biomass masses (50 g, 100 g, and 150 g), allowing the assessment of the influence of these variables on product yields.

To analyze the thermal decomposition of the main biomass components, thermogravimetric analysis (TGA) was performed, enabling the identification of the degradation ranges of hemicellulose, cellulose, and lignin. The resulting TGA curve revealed mass losses across distinct temperature intervals, confirming the contribution of lignin to the formation of more thermally stable biochar at temperatures above 400 °C (Ferraz, 2025).

The characterization of the produced biochar included physicochemical analyses such as porosity determination, thermal stability, and elemental composition, in addition to comparisons with literature data (Ferraz, 2025, Table 5, p. 45). These analyses were essential to validate the quality of the obtained product and to identify its potential applications in sectors such as agriculture, environmental remediation, and energy generation.

In summary, the adopted methodology integrated biomass preparation, preliminary analyses, fixed-bed reactor pyrolysis, experimental design, and product characterization. This systematic approach enabled not only the evaluation of the technical feasibility of slow pyrolysis of grape pomace but also provided a solid foundation for future industrial

and environmental applications aligned with circular-economy and sustainability principles.

4 RESULTS AND DISCUSSION

The results obtained from the slow pyrolysis of grape pomace demonstrate the direct influence of temperature and biomass mass on product yields. The proximate analysis of dried grape pomace (DGP) revealed average values of 69.69% volatile matter, 20.75% ash, and 9.56% fixed carbon, which are consistent with literature data and confirm the high presence of thermally degradable organic compounds (Ferraz, 2025). These parameters are critical for process efficiency, as the volatile fraction is directly associated with bio-oil and gas formation, while fixed carbon contributes to biochar stability.

Thermogravimetric analysis (TGA) provided insights into the gradual decomposition of the main biomass components. Hemicellulose degradation occurred between 200 °C and 300 °C, cellulose between 300 °C and 400 °C, and lignin above 400 °C, exhibiting slower and continuous decomposition. This characteristic of lignin explains the greater stability of biochar produced at lower temperatures, as its partial degradation favors carbon retention in the solid matrix (Ferraz, 2025, Figure 13, p. 42).

The pyrolysis experiments showed that the condition of 400 °C with 50 g of biomass yielded the highest biochar production, reaching 89%. Conversely, higher temperatures, such as 500 °C, favored the formation of bio-oil and non-condensable gases, reducing the solid fraction yield to approximately 70% (Ferraz, 2025). This behavior confirms that slow pyrolysis under moderate temperatures is more suitable for producing high-quality biochar, whereas higher temperatures may be explored to maximize bio-oil production.

Comparison with literature data reinforces the consistency of the results. Studies indicate that hemicellulose degradation contributes to the initial formation of bio-oil, while cellulose decomposition at intermediate temperatures increases gas release and reduces biochar yield. Lignin, due to its complex aromatic structure, is responsible for generating more stable biochar even at elevated temperatures (Martins et al., 2020; Oliveira et al., 2021). This comparative analysis demonstrates that the results obtained are in agreement with specialized literature (Ferraz, 2025).

From a physicochemical perspective, the produced biochar exhibited high porosity and thermal stability, characteristics that broaden its application potential. Environmentally, its capacity to adsorb organic and inorganic pollutants—such as heavy metals—stands out, as well as its use as a soil conditioner for degraded areas. In energy

applications, biochar can be incorporated into the energy matrix as a renewable input, partially replacing mineral coal and contributing to the reduction of greenhouse gas emissions (Santos, 2022).

The results also highlight the relevance of slow pyrolysis as a circular-economy strategy. By converting a problematic agro-industrial residue into a value-added resource, the process contributes to the sustainability of the wine sector and to environmental impact mitigation. This approach aligns with the United Nations Sustainable Development Goals, particularly those related to clean energy, responsible consumption and production, and climate action (UN, 2020).

In summary, the discussion confirms that slow pyrolysis of grape pomace is a viable and sustainable alternative capable of generating high-quality biochar and expanding the possibilities for agro-industrial residue utilization. Temperature and biomass mass are critical factors for process optimization, and the results demonstrate that moderate conditions favor the production of stable biochar with physicochemical properties suitable for environmental and energy applications.

5 CONCLUSION

Slow pyrolysis of grape pomace proved to be a viable and sustainable technological alternative for the valorization of agro-industrial residues, transforming an environmental liability into a strategic resource. The results showed that the condition of 400 °C with the lowest biomass mass (50 g) yielded the highest biochar production, reaching 89%, while higher temperatures favored the formation of bio-oil and non-condensable gases. This finding reinforces the importance of selecting appropriate operational conditions to optimize the process, enabling the production to be directed toward either maximizing the solid fraction or diversifying energy products.

From a physicochemical standpoint, the produced biochar exhibited high porosity and thermal stability, characteristics that expand its applicability across different sectors. Environmentally, its potential for pollutant adsorption and soil conditioning contributes to the recovery of impacted areas and to the mitigation of greenhouse gas emissions. In energy applications, biochar can be incorporated into the energy matrix as a renewable input, reducing dependence on mineral coal and supporting the transition to cleaner energy sources.

The research also highlights the relevance of pyrolysis as a circular-economy strategy, converting agro-industrial residues into value-added products. This practice

aligns with the United Nations Sustainable Development Goals, particularly those related to clean energy, sustainable production, and climate action. Additionally, it enhances the competitiveness of the wine sector by offering solutions for waste management and adding value to a subproduct often treated as a problem.

Among the study's limitations, the laboratory scale of the experiments stands out, as it does not yet allow a full assessment of the challenges associated with industrial-scale implementation. Issues such as collection logistics, transportation costs, and large-scale economic feasibility require further investigation. Another relevant point is the need for more detailed characterization of the chemical properties of biochar, including surface analyses and spectroscopy, to expand understanding of its specific applications.

Future research should include pilot- and industrial-scale studies focusing on integrating pyrolysis into grape-pomace waste-management systems. Investigating the potential of biochar as a precursor for activated carbon—thus increasing its industrial value—is also recommended, as well as exploring its application in environmental remediation systems and regenerative agriculture.

In summary, this work demonstrates that slow pyrolysis of grape pomace is a promising alternative for agro-industrial residue valorization, integrating science, innovation, and sustainability. By transforming a problematic residue into a strategic input, the process contributes to environmental impact mitigation, energy-matrix diversification, and the strengthening of the circular economy, establishing itself as a relevant solution for the wine sector and society.

REFERENCES

ALMEIDA, S. R. Pirólise de casca de arroz: estudo de parâmetros e caracterização de produtos. 2010. 74 f. Dissertação (Mestrado em Ciências dos Materiais) – Instituto de Química, Universidade Federal do Rio Grande do Sul, Porto Alegre, 2010.

ALVARES, J. S.; FERREIRA, A. P.; GONÇALVES, M. P. Caracterização do biocarvão produzido a partir do bagaço de uva via pirólise rápida: propriedades físicas e químicas. Journal of Biochar Science, v. 10, n. 3, p. 145–160, 2022.

ALVES, J. L. F. et al. Insights into the bioenergy potential of jackfruit wastes considering their physicochemical properties, bioenergy indicators, combustion behaviors, and emission characteristics. Renewable Energy, v. 155, p. 1328–1338, 2020.

ANEEL (Brasil). Atlas de energia elétrica. 2. ed. Brasília, DF: ANEEL, 2022. Disponível em: <http://www.aneel.gov.br/aplicacoes/Atlas/download.htm>. Acesso em: 10 set. 2023.

ANEEL (Brasil). Banco de informações de geração. Brasília, DF: ANEEL, 2023. Disponível em: <http://www.aneel.gov.br/aplicacoes/capacidadebrasil/capacidadebrasil.cfm>. Acesso em: 02 set. 2023.

BELINI, Rafael. Comparativo das propriedades do carvão ativado oriundo da semente da uva e carvão ativado produzido a partir do bagaço na clarificação de vinho. 2020. 59 p. Trabalho de Conclusão de Curso (Graduação em Engenharia Química) – Universidade Federal de Santa Catarina, Florianópolis, 2020.

BERES, C. et al. Grape pomace: chemical composition, biological properties, and potential applications. Food Research International, v. 99, p. 597–606, 2017.

BRIDGWATER, A. V. Review of fast pyrolysis of biomass and product upgrading. Biomass and Bioenergy, v. 38, p. 68–94, 2012.

CAPELETTO, G. J.; JOSÉ, G. Balanço Energético do Rio Grande do Sul 2019: ano base 2017. Porto Alegre: Grupo CEEE/Secretaria de Infraestrutura e Logística do Rio Grande do Sul, 2019.

COSTA, M. R. Caracterização do biocarvão produzido a partir da pirólise de resíduos agrícolas: estudo do bagaço de uva. 2021. 140 f. Dissertação (Mestrado em Engenharia Química) – Universidade Federal de Santa Catarina, Florianópolis, 2021.

EMBRAPA. Vitivinicultura Brasileira: panorama 2019. Brasília, DF: Embrapa, 2019. Disponível em: <http://ainfo.cnptia.embrapa.br/digital/bitstream/item/215377/1.pdf>. Acesso em: 10 fev. 2024.

FERRAZ, Rubinei de Servi. Da uva ao biocarvão: caracterização e propriedades após o processo de pirólise. 2025. 180 f. Dissertação (Mestrado em Engenharia e Ciências Ambientais) – Instituto Federal de Educação, Ciência e Tecnologia Sul-Rio-Grandense, Pelotas, 2025.

FERNANDES, F. S.; DOMENICO, M. D. Caracterização e cinética da pirólise do bagaço de uva. In: XI Seminário de Extensão e Inovação, UTFPR, Guarapuava, PR, 2021.

INSTITUTO BRASILEIRO DE BIOENERGIA. Produção e caracterização de biocarvão: aplicações sustentáveis. São Paulo: Editora Técnica, 2020.

LICANDRO, J.; ODIO, R. Resíduos da vitivinicultura e alternativas de aproveitamento. Porto Alegre: Editora Técnica, 2021.

LORA, E. E. S.; VENTURINI, O. J. Biocombustíveis. Rio de Janeiro: Interciência, 2018.

MARTINS, A. C.; FREITAS, M. M.; RODRIGUES, C. F. Potencial do biocarvão de bagaço de uva na adsorção de metais pesados: um estudo experimental. Journal of Applied Pyrolysis, v. 6, n. 1, p. 45–59, 2020.

OLIVEIRA, P. C.; SANTOS, L. M.; SILVA, R. F. Efeito da temperatura de pirólise nas propriedades físico-químicas do biocarvão produzido a partir do resíduo de uva. Renewable Energy Research Journal, v. 7, n. 2, p. 103–120, 2021.

ONU. Transformando nosso mundo: a Agenda 2030 para o Desenvolvimento Sustentável. Nova Iorque: Organização das Nações Unidas, 2020.

SANTOS, D. P. Avaliação das propriedades físico-químicas do biocarvão de bagaço de uva e suas aplicações na remediação de solos contaminados. 2022. 180 f. Tese (Doutorado em Engenharia Ambiental) – Universidade Estadual de Campinas, Campinas, 2022.

SANTOS, E.; PERES, J. Biomassa vegetal: composição e aplicações energéticas. Revista Brasileira de Energia Renovável, v. 2, n. 1, p. 45–60, 2012.

SOUZA, L. A.; COSTA, J. R.; MARTINS, D. C. Biocarvão do bagaço de uva: análise de espectroscopia FTIR e suas potenciais aplicações na agricultura. Journal of Environmental Technology, v. 8, n. 4, p. 221–234, 2023.

TELES, A. S. C. C. et al. Efeito da temperatura na degradação de compostos bioativos do bagaço de uva Pinot Noir durante a secagem. Revista Brasileira de Tecnologia de Alimentos, v. 21, 2018.

CHAPTER 10:
COMPETITIVENESS AND DIFFERENTIATION STRATEGIES IN THE GLOBAL OLIVE OIL MARKET: QUALITY, INNOVATION AND TERRITORIAL IDENTITY

Leonardo Betemps Kontz, Edi Ramson Bergmann

ABSTRACT

This study analyzes differentiation strategies and sources of competitive advantage in the global olive oil value chain, emphasizing the role of quality, technological innovation, and territorial identity. Traditionally dominated by Mediterranean countries, the olive oil market has undergone significant transformations with the emergence of new producers such as Brazil, which adopt value-based competitive models focused on premium market positioning. The research follows a qualitative, exploratory, and analytical approach, based on a systematized literature review and a comparative analysis of producing regions. The theoretical framework integrates competitive strategies, the Resource-Based View, dynamic capabilities, and territorial approaches. The results indicate that Brazil, particularly Rio Grande do Sul, demonstrates strong competitive potential supported by high levels of bioactive compounds, low acidity, superior sensory quality, and advanced production processes. It is concluded that contemporary competitiveness in the olive oil sector is increasingly driven by differentiation, innovation, and territorial embeddedness, positioning Brazil as an emerging player in high value-added markets.

Keywords: Olive oil; Competitive strategies; Differentiation; Competitive advantage.

1 INTRODUCTION

Olive oil has become one of the most symbolic products of contemporary gastronomy, associated with the Mediterranean diet as well as with healthy lifestyles, premium consumption, and differentiated gastronomic experiences. Over the last decades, the global olive oil market has undergone profound transformations involving the geographical expansion of production, the sophistication of quality standards, the emergence of new producing countries, and the reconfiguration of competitive strategies at the international scale (Anania & Pupo D'Andrea, 2008; IOC, 2019, 2023).

Traditionally, market leadership has been exercised by Mediterranean countries such as Spain, Italy, Greece, and Portugal, whose competitive advantage has been anchored in historical, institutional, and territorial factors, including climate, traditional cultivars, accumulated know-how, and consolidated systems of origin certification (Grigg, 2001; Vilar & Pereira, 2018).

However, the rise of producers from the so-called "New World of olive oil," such as Chile, Argentina, Uruguay, Australia, and more recently Brazil, has introduced new

competitive dynamics based on technological innovation, high quality standards, and strong origin-based positioning (Zago et al., 2021).

The combination of temperate climate, favorable thermal amplitudes, and investments in research and development has enabled Brazilian olive oils—particularly those produced in Rio Grande do Sul—to achieve sensory and physicochemical standards comparable to the best Mediterranean oils, receiving international awards and growing recognition (Embrapa, 2017; Zago et al., 2021).

In this context, the discussion on which competitive strategies and differentiation advantages sustain olive oil competitiveness in global markets becomes increasingly relevant, especially regarding how emerging countries such as Brazil can build solid positions in highly demanding markets. Classical competitiveness frameworks, such as those proposed by Porter (1980, 1985, 1998), and contemporary perspectives, including the Resource-Based View (Barney, 1991) and Dynamic Capabilities (Teece, Pisano & Shuen, 1997), offer a robust analytical foundation for interpreting these transformations.

The aim of this article is to analyze differentiation strategies and sources of competitive advantage in the global olive oil value chain, with particular attention to the role of quality, technological innovation, and territorial identity. As a reference case, the article examines the Brazilian olive-growing sector, especially in Rio Grande do Sul, as an example of an emerging trajectory that combines terroir, innovation, and sustainability to compete in premium markets.

2 COMPETITIVENESS AND DIFFERENTIATION

2.1 COMPETITIVENESS, COMPETITIVE ADVANTAGE AND AGRI-FOOD CHAINS

Competitiveness can be understood as the ability of a production system, firm, chain, or territory to sustain advantages that ensure its permanence and expansion in complex and constantly changing markets (Porter, 1985; Müller, 1994; Pagano, 2001). In this sense, competitiveness is not merely about competing in the short term, but about building relatively stable positions in contexts marked by globalization, fluctuating demand, technological innovations, and socio-environmental pressures.

From Porter's (1980, 1985) perspective, competitive advantage results from the way an organization performs its activities and positions itself in the market, whether through cost leadership, differentiation, or focus on specific niches. Sector structure analysis, based on the five competitive forces—rivalry among competitors, bargaining power of suppliers and buyers, threat of new entrants, and threat of substitute products—offers a framework

for understanding external pressures that shape strategic choices. D'Aveni (1994) and O'Shaughnessy (1995) emphasize the fluid and unstable nature of advantages in environments characterized by hypercompetition and temporary strategic positions.

In agri-food chains, competitiveness involves not only productive efficiency but also coordination among chain actors, quality attributes, sanitary standards, certifications, and the construction of collective reputation (Batalha & Silva, 1999, 2007). The literature indicates that competitive agri-industrial systems are those capable of aligning incentives, reducing transaction costs, and articulating joint strategies among producers, processors, distributors, and retailers (Zylbersztajn, 1995; Batalha & Silva, 2007).

In the Brazilian context, applied research in agri-industrial chains helps illustrate this logic. Kontz (2021), when analyzing competitive strategies in the beef industry of Rio Grande do Sul, demonstrates that sectoral competitiveness depends on the articulation between productive structures, consumption trends, and the ability to differentiate in high value-added niches. In a later study, Kontz and Antunes (2025) show that operating in specific niches-such as premium, certified, or sustainability-oriented meats, constitutes a relevant path to escape competition based solely on price, reinforcing the importance of differentiation in commodity-intensive food chains.

Kontz et al. (2014a, 2014b) and Hoffman et al. (2021) reinforce the idea that competitiveness, across different organizational contexts, is increasingly associated with the ability to generate perceived value for specific stakeholders. These contributions indicate that the logic of competitive advantage transcends the strictly productive domain and includes symbolic, relational, and institutional dimensions, highly relevant for agri-food chains such as olive oil.

In the olive oil sector, contemporary competitiveness is gradually shifting from a logic centered exclusively on volume and cost to one in which sensory quality, authenticity, and territorial origin become central elements of the value proposition (Vossen, 2013). The emergence of more informed consumers, concerned with health, sustainability, and food origin, leads extra virgin olive oil, particularly in premium segments, to be evaluated not only as an edible oil but as an identity product linked to territories, traditions, and narratives of quality. Table 1 summarizes the theoretical frameworks of competitiveness applied to olive oil.

Table 1 – Summary of theoretical frameworks of competitiveness applied to olive oil

Theoretical perspective	Key authors	Main focus	Application to olive oil
Generic strategies	Porter (1980, 1985, 1998); D'Aveni (1994)	Cost, differentiation, focus; hypercompetition	Differentiation through quality, terroir, premium branding; operation in specialized niches
Resource-Based View (RBV)	Barney (1991, 2020); Kontz (2021)	Rare and inimitable resources; strategic assets	Terroir, cultivars, reputation, know-how, reputational and socio-environmental assets
Dynamic capabilities	Teece, Pisano & Shuen (1997); Teece (2007, 2018)	Learning, innovation, reconfiguration	Adjusting to premium trends, climate change, and technological advances
Territory and identity	Ray (1998); Ilbery & Kneafsey (2000); Belletti et al. (2017)	Symbolic value, GIs, territorial branding	PDOs, PGIs, origin-based marketing, olive-oil tourism, regional brand building
Innovation, sustainability and value	Pascucci et al. (2021); Sachs et al. (2019); Machado et al. (2023); Kontz (2021); Kontz et al. (2025)	Innovation, digitalization, sustainability, consumer value	Traceable supply chains, circular economy, healthy and sustainable products, social legitimation

Source: Authors' elaboration.

2.2 TERRITORY, GEOGRAPHICAL INDICATIONS AND PRODUCT IDENTITY

Competitiveness in highly differentiated agri-food products is increasingly anchored in the ability to articulate territorial attributes with market strategies. Territory ceases to be merely a physical space and becomes a strategic resource, combining ecological conditions, socio-productive arrangements, and symbolic references that shape consumers' perception of value (Ray, 1998; Ilbery & Kneafsey, 2000).

From this perspective, the notion of *terroir*, traditionally associated with wine, has also gained centrality in olive oil, explaining how specific interactions among soil, climate, topography, agricultural practices, and local culture result in unique and inimitable sensory profiles. Likewise, Geographical Indications (GI), Protected Designations of Origin (PDO), and Protected Geographical Indications (PGI) operate as institutional mechanisms that translate and protect these territorial resources.

In addition to ensuring authenticity and preventing undue appropriation of collective reputation, such certifications strengthen the governance of the value chain, stimulate coordination among its segments, and promote rural development grounded in local knowledge (Belletti, Marescotti & Touzard, 2017; Tregear, Kuznesof & Moxey, 2007). In practice, they function as strategic instruments to escape price-based competition and consolidate differentiation based on origin, quality, and production heritage.

The consolidated experiences of Tuscany, Andalusia, Alentejo, Provence, and Crete demonstrate the strength of territorial identity in the construction of premium markets. In these regions, olive oil is closely associated with tourism experiences, terroir-based gastronomy, cultural routes, and centuries-old traditions (Muchnik & Sanz Cañada et al., 2010).

Thus, in the context of olive growing, territorial identity is not limited to landscape or tradition but incorporates contemporary values such as well-being, authenticity, sustainability, and traceability. The convergence of territory, quality, and sustainability therefore constitutes a strategic foundation for positioning olive oils, particularly those produced in emerging regions such as southern Brazil, within sophisticated global markets that are highly sensitive to origin.

2.3 GLOBAL DYNAMICS OF THE OLIVE OIL MARKET AND HEALTH CONSIDERATIONS

The international olive oil market is characterized by strong production concentration and significant geographical asymmetry. According to the International Olive Council (IOC, 2019; 2023) and recent Eurostat data (2023), more than 70% of global production is concentrated in a few Mediterranean countries, notably Spain, Italy, Greece, Turkey, and Portugal. Spain alone accounts for around 40–45% of all global production, exerting decisive influence over international prices, stocks, and market trends.

Despite this historical concentration, the emergence of new producing territories can be observed, such as Brazil, Uruguay, Argentina, the United States, Australia, and Chile. These countries, referred to as new olive-growing regions, are characterized by more technified production systems, intensive and super-intensive management models, and marketing strategies based on freshness, traceability, and territorial identity.

The expansion of olive cultivation into non-traditional areas is associated both with the genetic adaptation of cultivars and with the dynamics of the global market, which demands differentiated, sustainable, and high-quality olive oils.

From a consumption perspective, olive oil is no longer a product restricted to Mediterranean countries. Growth has been significant in middle- and high-income nations (López-Miranda et al., 2020). This movement is driven by three structuring vectors:

Scientific evidence on health benefits, especially regarding the prevention of cardiovascular diseases, antioxidant activity, and anti-inflammatory properties, has

reinforced the importance of olive oil consumption (Jimenez-Lopez et al., 2020; Romani et al., 2019).

Beauchamp et al. (2005), Cornwell and Ma (2008), and López-Miranda et al. (2020) recognize the relevance of the bioactive compounds in olive oil, including hydroxytyrosol, oleocanthal (with anti-inflammatory properties similar to ibuprofen), oleuropein, and tocopherols (vitamin E). These compounds consolidate olive oil as a functional food and drive its insertion into health and wellness niches.

3 DIFFERENTIATION AND COMPETITIVE ADVANTAGES: MEDITERRANEAN VERSUS BRAZIL

Recent studies show that Brazilian olive oils, especially those produced in temperate-climate regions with high thermal amplitude, such as Rio Grande do Sul, have reached chemical and sensory standards comparable to (and in some cases superior to) traditional Mediterranean oils (Embrapa, 2017; Zago et al., 2021). This finding breaks with the historical paradigm that excellence in olive oil would be restricted to the Mediterranean basin, revealing the competitive potential of new producing regions.

The performance of Brazilian olive oils can be explained by a unique combination of factors:

Scientific literature indicates that extra virgin olive oils produced in Brazil's temperate regions, particularly in Rio Grande do Sul, stand out due to their high levels of total polyphenols and bioactive compounds associated with sensory quality, oxidative stability, and health benefits (Embrapa, 2017; Zago et al., 2021). Phenolic compound levels frequently exceed 300 mg/kg, a value comparable to premium Mediterranean oils and superior to oils obtained from late harvesting or longer intervals between harvest and processing (Romani et al., 2019; Jimenez-Lopez et al., 2020).

Among the major phenols present in Brazilian olive oils are oleuropein, hydroxytyrosol, and oleocanthal, the latter widely studied for its anti-inflammatory activity similar to ibuprofen, as demonstrated by Beauchamp et al. (2005). These compounds act as powerful natural antioxidants, providing the oil with functional properties such as protection against oxidative damage, improvement of lipid profile, and reduction of inflammatory markers (Cornwell & Ma, 2008; López-Miranda et al., 2020).

The literature emphasizes that high concentrations of bioactive compounds are directly related to oxidative stability, a characteristic that determines the oil's shelf life and resistance to rancidity. Oils with higher phenolic content exhibit longer induction times

and greater resistance to degradation by light, oxygen, and temperature (Gargouri; Zribi; Bouaziz, 2015; Sanmartin et al., 2018).

Several agronomic and technological factors explain the superior performance of Brazilian olive oils. Studies conducted by Embrapa indicate that early harvesting, commonly practiced by producers in Rio Grande do Sul, promotes the formation of green, herbaceous oils naturally richer in phenolic compounds due to the lower degree of fruit maturation (Embrapa, 2017).

Likewise, low nighttime temperatures, typical of temperate climates, stimulate the accumulation of plant defense compounds, resulting in higher phenolic density in the fruit (Koutsaftakis et al., 2000).

Another determining factor is the short interval between harvest and extraction, often less than four hours in mills in Rio Grande do Sul. This reduced time minimizes respiration and enzymatic degradation processes, preserving volatile and bioactive compounds responsible for the freshness and sensory complexity of the oil (Zago et al., 2021; Pedan et al., 2019). This practice contrasts with more extensive and fragmented Mediterranean systems, in which the time between harvest and processing may exceed 24 hours.

Another point to consider is the extremely low acidity of the product produced in Rio Grande do Sul. Acidity levels in RS oils often range from 0.1% to 0.2%, well below the 0.8% limit for extra virgin oils established by the IOC. In some cases, batches display values of 0.08% or lower, indexes comparable to the finest oils from Tuscany and Alentejo.

Low acidity results from good orchard health, fast and clean harvesting, almost immediate transport to the mill, and extraction using modern systems with an inert atmosphere. This combination reduces hydrolysis and lipid oxidation processes, preserving the integrity of the oil.

Another factor that may constitute a point of differentiation is the sensory characterization of Brazilian olive oils, especially those from Rio Grande do Sul, evidencing the construction of an emerging sensory identity marked by positive attributes highly valued in traditional producing countries. Studies conducted by Embrapa and independent chemical-sensory analyses show that oils from the cultivars Arbequina, Arbosana, Koroneiki, and Picual exhibit consistent sensory profiles, with moderate to intense green fruitiness, herbaceous notes, and high harmony (Zago et al., 2021).

Among the most frequent descriptors are aromas of:

- fresh herbs

- green tomato
- green apple
- arugula
- green banana peel

Regarding freshness, resulting from the preservation of volatile and bioactive compounds immediately after extraction, it emerges as one of the main competitive advantages of Brazilian oils. Unlike what occurs in many traditional regions, where harvesting is carried out in large volumes and transported over long distances, Brazilian orchards are characterized by:

- small and medium-sized farms
- short logistics
- proximity between orchards and mills
- manual or semi-mechanized harvesting
- immediate processing, generally within less than 4 hours after harvest

This dynamic drastically reduces fruit respiration and the formation of sensory defects, especially those associated with fermentation, degradation, or excessive heating (Embrapa, 2017; Zago et al., 2021). In contrast, in Spain, Italy, and Greece, it is common for the interval between harvest and extraction to exceed 24-48 hours, especially in large-scale production regions where processing demand temporarily surpasses mill capacity.

Rapid processing results in:

- preservation of aromatic volatile compounds
- greater intensity of green fruitiness
- lower formation of defects
- brighter color and characteristic sheen
- preservation of phenols, positively impacting oxidative stability

Finally, producing regions in Brazil, particularly Campanha Gaúcha, Serra do Sudeste, Planalto das Araucárias, and parts of Serra da Mantiqueira, present a set of edaphoclimatic characteristics that favor the production of high-quality olive oils, even though they limit large-scale productivity. Climatic zoning studies (Wrege et al., 2009; Filippini Alba et al., 2013) indicate that these regions feature:

- temperate climate, with well-defined winters and moderate summers

- significant daily thermal amplitude, which stimulates the synthesis of phenolic compounds
- soils of moderate fertility, which reduce excessive vigor and favor greater concentration of bioactive compounds in the fruit
- well-distributed rainfall, reducing the need for intensive irrigation

These conditions contrast with the classic Mediterranean climate, characterized by:

- very hot and dry summers
- heavy dependence on irrigation
- severe water stress in many years
- higher occurrence of alternate bearing ("bienniality")

Although extreme water stress in the Mediterranean may favor phenolic levels in some cases, it also increases agronomic risks and production instability.

Brazil, particularly Rio Grande do Sul, presents a stable quality pattern, although with lower productivity due to insufficient winter chill in some years and variable climatic risks (rain during harvest, strong winds, late frosts). The "low scale with high quality" model therefore results from:

- climatic conditions favorable to phenolic accumulation
- lower pressure of Mediterranean-specific pests
- technical and careful harvesting
- accelerated modernization of Brazilian mills

Thus, while the Mediterranean retains the advantage of volume and tradition, Brazil stands out for its advantage in quality and innovation, positioning itself strategically in premium and gourmet niches.

4 METHODOLOGY

The present study adopted a qualitative approach, exploratory and analytical in nature, based on a systematized literature review and a comparative analysis between olive oil–producing regions.

The investigation was structured using national and international scientific sources, prioritizing peer-reviewed articles, technical reports, official regulations, and institutional documents relevant to the olive oil sector. Databases such as Scopus, Web of Science,

Scielo, Google Scholar, and repositories of specialized institutions, including Embrapa, the International Olive Council (IOC), Eurostat, and Brazilian governmental bodies (MAPA and Ibraoliva), were consulted, using descriptors related to competitiveness, olive oil quality, polyphenols, terroir, technological innovation, Brazilian olive growing, and differentiated agri-food markets.

The selection of materials followed criteria of thematic relevance, recency, methodological rigor, and alignment with the central objective of the study, covering publications produced primarily between 2000 and 2024. Classic studies on competitive advantage (Porter, 1980, 1985), strategic resources (Barney, 1991), dynamic capabilities (Teece, Pisano & Shuen, 1997), and agri-food territory and identity (Ray, 1998; Belletti et al., 2017) were included, as well as recent research on the chemical and sensory quality of Brazilian olive oils (Zago et al., 2021; Embrapa, 2017).

The methodology involved three integrated stages. The first consisted of the conceptual systematization of the main theories of competitiveness applied to agri-food chains, allowing the construction of the analytical framework used to interpret sectoral data. The second stage comprised a documentary analysis of chemical, sensory, and agronomic studies, with special attention to empirical results regarding polyphenol content, acidity, oxidative stability, sensory profiles, and the edaphoclimatic conditions of Brazilian and Mediterranean producing regions.

This analysis sought to identify factors that influence quality and differentiate products between traditional regions and new olive-growing frontiers. The third stage involved the construction of a comparative analysis between Brazil and the Mediterranean, integrating scientific evidence with the theoretical interpretation of differentiation strategies and competitive advantage.

Triangulation was also carried out between empirical studies, theoretical references, and sectoral data, ensuring greater interpretive consistency. The comparison was structured around key dimensions such as terroir, chemical characteristics, sensory profiles, technological practices, sectoral governance, and market strategies. This triangulation made it possible to identify convergent patterns, regional singularities, and strategic opportunities for Brazilian olive growing.

Finally, the results of the review and comparative analysis were integrated into an interpretative discussion, in light of contemporary theoretical frameworks of competitiveness, innovation, and territorial identity. The qualitative and analytical nature of the research enabled a deep understanding of how natural, technological, institutional,

and market factors combine to sustain the differentiation of Brazilian olive oils in premium markets.

5 DISCUSSION AND RESULTS

The analysis of the data and specialized literature reveals that Brazilian olive growing, especially that developed in Rio Grande do Sul, has reached a level of competitiveness that challenges the traditional perception of Mediterranean hegemony in the production of high-quality olive oils.

Studies by Embrapa (2017) and Zago et al. (2021) demonstrate that Brazilian olive oils frequently present polyphenol levels above 300 mg/kg, with high concentrations of compounds such as hydroxytyrosol, oleuropein, and oleocanthal. Beauchamp et al. (2005) had already highlighted oleocanthal as a potent anti-inflammatory agent, comparable to ibuprofen, reinforcing the functional appeal of Brazilian olive oils identified by Cornwell and Ma (2008), Romani et al. (2019), and López-Miranda et al. (2020).

The high density of phenols is directly related to oxidative stability, as pointed out by Sanmartin et al. (2018) and Gargouri, Zribi and Bouaziz (2015), indicating that oils produced in Rio Grande do Sul have longer shelf life and lower susceptibility to rancidity.

This remarkable chemical performance is favored by specific agronomic and technological factors. Early harvesting preserves the amount of bioactive compounds (Embrapa, 2017), while low nighttime temperatures, analyzed by Koutsaftakis et al. (2000), promote the accumulation of plant defense compounds, increasing phenolic content.

In addition, the short interval between harvest and extraction, generally less than four hours, reduces olive degradation and preserves volatiles responsible for freshness, as observed by Pedan et al. (2019). In comparison, Mediterranean systems, especially in Spain and Italy, may operate with 24- to 48-hour windows between harvest and processing, increasing the formation of defects such as “fusty” and “mustiness,” frequently noted as critical in the international literature (IOC, 2019; 2023).

In the sensory domain, the characterization of Brazilian olive oils stands out for harmony, green fruitiness, and aromatic complexity. Zago et al. (2021) demonstrate that the cultivars Arbequina, Arbosana, Koroneiki, and Picual, when cultivated in regions such as Campanha Gaúcha and Serra do Sudeste, exhibit sensory profiles with aromas of fresh herbs, green tomato, green apple, and arugula, sensory attributes widely valued in international competitions and aligned with the classifications established by the IOC

(2023). These profiles, as analyzed by Vossen (2013), are typical of premium olive oils and result from combinations of terroir, management practices, and efficient extraction.

Brazilian climatic conditions operate as a natural competitive advantage. Studies by Wrege et al. (2009) and Filippini Alba et al. (2013) show that the producing regions feature temperate climate, marked winters, and significant daily thermal amplitude that favor the synthesis of phenolic compounds and improvement of oxidative stability. The relatively uniform distribution of rainfall reduces extreme water stress, unlike the Mediterranean pattern, where severe droughts and heat waves affect not only volume but also quality, as analyzed by Yousfi et al. (2020). Although the classic Mediterranean climate may favor phenols in years of moderate drought, it also generates agronomic risks and production instability, highlighting the difference between a volume-based model and one structured for quality.

Brazil's performance is also associated with the technological modernization of mills. Nardella et al. (2021), Kalogianni et al. (2019), and Clodoveo (2013) highlight that advanced extraction technologies, controlled malaxation, and hermetic centrifugation systems have been rapidly incorporated into the Brazilian model, contributing to oils with greater freshness and fewer defects.

Brazilian competitiveness is also linked to territorial and institutional dimensions. Belletti, Marescotti and Touzard (2017), Tregear et al. (2007), Ray (1998), and Ilbery and Kneafsey (2000) demonstrate that the construction of territorial identity strengthens reputation and adds symbolic value to agri-food products.

The trajectory of olive growing in Rio Grande do Sul indicates strong potential for the consolidation of GIs in regions such as Campanha Gaúcha and Serra do Sudeste, a phenomenon comparable to well-established denominations in Tuscany, Andalusia, and Alentejo (Muchnik & Sanz Cañada et al., 2010).

This association between territory and product is aligned with analyses by Kontz, Palmeira and Zago (2014), Machado et al. (2023), and Kontz and Antunes (2025), who argue that socio-environmental reputation, legitimacy, and strategic positioning are central determinants of competitiveness in agri-food chains.

The set of results shows that Brazilian competitiveness does not derive from production scale but from qualitative excellence. This model reflects the logic described by Porter (1985; 1998), in which differentiation strategies, not cost leadership, sustain competitive positions in sophisticated markets.

Barney (1991) demonstrates that natural resources (terroir), organizational resources (innovation, governance), and relational resources (territorial identity) become valuable, rare, and difficult-to-imitate assets. Similarly, the rapid capacity for technological and agronomic adaptation in the Brazilian sector reflects the framework of dynamic capabilities discussed by Teece, Pisano and Shuen (1997), indicating that sustainable competitiveness depends on continuously learning, innovating, and reconfiguring productive practices.

The integration of terroir, qualified management, rapid extraction, technology, governance, and sustainability demonstrates that Brazil has structural and institutional conditions to consolidate itself in high value-added niches. While the Mediterranean maintains its historical leadership in volume, Brazil stands out as an emerging producer of exceptional olive oils, with a unique sensory identity, high phytochemical density, unmatched freshness, and growing international recognition.

6 CONCLUSIONS

The analysis carried out shows that the competitiveness of olive oil in the global scenario is no longer explained exclusively by traditional factors such as production scale, the age of the activity, or historical tradition, but now incorporates contemporary dimensions linked to quality, innovation, sustainability, and territorial identity. In this context, Brazilian olive growing, especially that developed in Rio Grande do Sul, emerges as an emblematic case of strategic repositioning within a highly concentrated sector dominated by Mediterranean countries.

The results demonstrate that Brazilian olive oils achieve physicochemical and sensory parameters equivalent to, and in many cases superior to, those of premium oils from renowned regions such as Tuscany, Andalusia, or Alentejo. The combination of early harvesting, rapid extraction, temperate climate, marked thermal amplitudes, and low pest pressure provides the country with intrinsic advantages that translate into high polyphenol content, low acidity, and balanced sensory profiles.

These attributes reinforce the argument that Brazilian competitiveness is based on strategic resources that are valuable, rare, and difficult to imitate, and that the rapid incorporation of advanced technologies and practices reveals the sector's capacity to develop dynamic capabilities.

In addition to natural and technological factors, sectoral governance plays a relevant role in the consolidation of the industry. The coordinated action between Embrapa,

universities, producers' associations, export support programs, and state public policies contributes to strengthening productive capacities, standardizing processes, and consolidating a culture of continuous innovation. This institutional environment fosters not only internal competitiveness but also the construction of external reputation, a central element in high value-added agri-food chains.

Another relevant aspect concerns the construction of territorial identity. Although still in its early stages, regions such as Campanha Gaúcha, Serra do Sudeste, and Mantiqueira exhibit consistent edaphoclimatic characteristics and emerging cultural narratives that reinforce a positioning based on origin, authenticity, and typicity.

The prospect of future Geographical Indications and the increasing linkage of olive oil to rural and gastronomic tourism suggest that Brazilian territory may consolidate strong regional brands in the medium term, provided that investments in coordination, certification, and quality communication are maintained.

In summary, the results point to a Brazilian model of competitiveness founded on excellence, innovation, and territoriality rather than volume. This represents a solid strategy for insertion into premium markets that value intrinsic product attributes and sustainable practices, increasing consumer perceived value and ensuring effective differentiation in highly competitive markets.

The trajectory of Brazilian olive growing demonstrates that it is possible to build sustainable competitive advantage even in sectors traditionally dominated by countries with centuries of tradition. Brazil, by articulating terroir, science, governance, and innovation, establishes itself as an emerging protagonist in the so-called "New World of olive oil," showing that contemporary competitiveness relies less on tradition and more on the capacity to generate authentic, consistent, and globally recognized value.

REFERENCES

ABUHABIB, M.M.; CAMPINS-MACHADO, F.M.; LOZANO-CASTELLÓN, J.; NINOT, A.; ROMERO-AROCA, A.; LAMUELA-RAVENTÓS, R.M.; PÉREZ, M.; VALLVERDÚ-QUERALT, A. (2025). Evaluation of Packaging Effects on the Phenolic Profile and Sensory Characteristics of Extra Virgin Olive Oil During Storage Using Liquid Chromatography Coupled with Mass Spectrometry. Foods, 14, 2532. https://doi.org/10.3390/foods14142532

ANANIA, G.; PUPO D'ANDREA, M. (2008). This document is discoverable and free to researchers across the globe due to the work of AgEcon Search. The global market for olive oil: policies, trends and challenges. Rome: FAO, 2008. Disponível em: https://www.fao.org.

BATALHA, M. O.; SILVA, A. L. Gerenciamento de sistemas agroindustriais. São Paulo: Atlas, 1999.

BATALHA, M. O.; SILVA, A. L. Gestão de cadeias produtivas agroindustriais. São Paulo: Atlas, 2007.

BARNEY, J. (1991). Firm resources and sustained competitive advantage. Journal of Management. DOI: 10.1177/014920639101700108.

BARNEY, J. Gaining and sustaining competitive advantage. New York: Pearson, 2020.

BEAUCHAMP, G. K., KEAST, R. S. J., MOREL, D., LIN, J., PIKA, J., HAN, Q., LEE, C.-H., SMITH, A. B., & BRESLIN, P. A. S. (2005). Ibuprofen-like activity in extra-virgin olive oil. Nature, 437(7055), 45–46. https://doi.org/10.1038/437045a

BELLETTI, G., MARESCOTTI, A., TOUZARD, J.-M. (2017). Geographical indications, public goods, and sustainable development: The roles of actors' strategies and public policies. World Development, 98, 45–57. https://doi.org/10.1016/j.worlddev.2015.05.004

CLODOVEO, M. L., DURANTE, V., & LA NOTTE, D. (2013). Working towards the development of innovative ultrasound equipment for the extraction of virgin olive oil. Journal of Agricultural Engineering, 44(s2), e60. https://doi.org/10.4081/jae.2013.s2.e60

COI- International Olive Council. (2023). Trade standard applying to olive oils and olive-pomace oils (COI/T.15/NC No. 3, Rev. 20). Madrid: International Olive Council.

D'AVENI, R. A. (1994). Hypercompetition: Managing the dynamics of strategic maneuvering. New York: Free Press.

EMBRAPA. (2017). Qualidade de azeites de oliva extra-virgem produzidos no Brasil. Embrapa Clima Temperado.

EUROSTAT. (2023). Olive oil statistics. European Commission. Retrieved from. Disponível em https://agriculture.ec.europa.eu/data-and-analysis/markets/price-data/price-monitoring-sector/olive-oil_en. Acesso em 07/12/2025

FILIPPINI ALBA, J. M., WREGE, M. S., COUTINHO, E. F., FLORES, C. A., & JORGE, R. O. (2013). Zoneamento edafoclimático da olivicultura para o Rio Grande do Sul. Brasília: EMBRAPA.

GARGOURI, B.; ZRIBI, A.; BOUAZIZ, M. Effect of containers on the quality of Chemlali olive oil during storage. Journal of Food Science and Technology, 52(4), 1948–1959, 2015. DOI: 10.1007/s13197-014-1273-2

GRIGG, D. (2001). Olive oil, the Mediterranean and the world. GeoJournal, 53, 163–172. https://doi.org/10.1023/A:1015702327546

HOFFMANN, R., CAVALHEIRO, E., KONTZ, L. B., & MARTINS, A. (2021). Satisfação e lealdade discente nas universidades públicas brasileiras. RACE - Revista de Administração, Contabilidade e Economia, 20(1), 133–152. https://doi.org/10.18593/race.20840

ILBERY, B., & KNEAFSEY, M. (2000). Producer constructions of quality in regional speciality food production: A case study from South West England. Journal of Rural Studies, 16(2), 217–230. https://doi.org/10.1016/S0743-0167(99)00041-8

IOC – International Olive Council. Market data. 2019; 2023.

JIMENEZ-LOPEZ, C., PEREIRA, A. G., & LOURENÇO-LOPES, C. (2020). Bioactive Compounds and Quality of Extra Virgin Olive Oil. Nutrients, 12(8), 2304. https://doi.org/10.3390/nu12082304

KONTZ, L. K.; PALMEIRA, E. M.; Zago, A. (2014 a). " A responsabilidade social como instrumento de marketing nas organizações ", Observatório da Economia Latinoamericana , Servicios Académicos Intercontinentales SL. Hasta 31/12/2022, edição 197, maio.

KONTZ, L. K.; PEIXOTO, L. T. Q; PALMEIRA, E. M. (2014 b). "Comportamento do consumidor no setor público: aspectos influenciadores da satisfação," Observatorio de la Economía Latinoamericana, Servicios Académicos Intercontinentales SL. Hasta 31/12/2022, issue 198, May. Handle: RePEc:erv:observ:y:2014:i:198:10

KONTZ, L. B., & ANTUNES JÚNIOR, J. A. V. (2025). Competitive Strategies and Differentiation in the Beef Industry: a Look at Market Niches. Revista De Gestão - RGSA, 19(6), e012377. https://doi.org/10.24857/rgsa.v19n6-021

KONTZ, L. B. (2021). Estratégias competitivas para a indústria da carne bovina do Estado do Rio Grande do Sul: Um estudo das tendências do mercado consumidor e produção [Tese de doutorado, Unisinos].

KOUTSAFTAKIS, A., KOTSIFAKIS, F., & STEFANOUDAKI, E. (2000). La caractérisation des huiles d'olive vierges extra-crétoises obtenues à partir de la variété Koroneiki: influence du site d'origine sur plusieurs paramètres chimiques. Olivae, (81), 20–25.

LÓPEZ-MIRANDA, J., YOUSFI, F., ROS, E., DE CATERINA, R., BADIMÓN, L., COVAS, M.-I., ESCRICH, E., ORDOVÁS, J. M., SORIGUER, F., ABIÁ, R., & OTHERS. (2010). Olive oil and health: Summary of the II International Conference on Olive Oil and Health consensus report. Nutrients, 2(8), 858–875. https://doi.org/10.3390/nu2080858

MAPA- MINISTÉRIO DA AGRICULTURA, PECUÁRIA E ABASTECIMENTO. (2017). Relatórios técnicos sobre fraudes em azeite de oliva no Brasil. Brasília: MAPA.

MUCHNIK, J., & SANZ CAÑADA, J. (2008). Food identity and territorial development: a theoretical contribution. Anthropology of Food, S3.

NARDELLA, M. (2021). A review on high-power ultrasound-assisted extraction of olive oils: Effect on oil yield, quality, chemical composition and consumer perception. Foods, 10(11), 2743. https://doi.org/10.3390/foods10112743

PEDAN, V., POPP, M., ROHN, S., NYFELER, M., & BONGARTZ, A. (2019). Characterization of phenolic compounds and their contribution to sensory properties of olive oil. Molecules, 24(11), 2041. https://doi.org/10.3390/molecules24112041

PORTER, M. Competitive Strategy. New York: Free Press, 1980.

PORTER, M. Competitive Advantage. New York: Free Press, 1985.

PORTER, M. On Competition. Harvard Business School Press, 1998.

PORTER, M. E., & HEPPELMANN, J. E. (2014). How smart, connected products are transforming competition. Harvard Business Review, 92(11), 64-88.

RAY, C. (1998). Culture, intellectual property and territorial rural development. Sociologia Ruralis, 38(1), 3-20. https://doi.org/10.1111/1467-9523.00060

ROMANI, A., IERI, F., URCIUOLI, S., NOCE, A., MARRONE, G., NEDIANI, C., & BERNINI, R. (2019). Health effects of phenolic compounds found in extra-virgin olive oil, by-products, and leaf of Olea europaea L. Nutrients, 11(8), 1776. https://doi.org/10.3390/nu11081776

SACHS, J. D., SCHMIDT-TRAUB, G., KROLL, C., LAFORTUNE, G., FULLER, G., & WOELM, F. (2019). Six transformations to achieve the Sustainable Development Goals. Nature Sustainability, 2(9), 805–814. https://doi.org/10.1038/s41893-019-0352-9

SANMARTIN, C., VENTURI, F., SGHERRI, C., NARI, A., MACALUSO, M., FLAMINI, G., QUARTACCI, M. F., TAGLIERI, I., ANDRICH, G., & ZINNAI, A. (2018). The effects of packaging and storage temperature on the shelf-life of extra virgin olive oil. Heliyon, 4(11), e00888. https://doi.org/10.1016/j.heliyon.2018.e00888

TEECE, D. J., PISANO, G., & SHUEN, A. (1997). Dynamic capabilities and strategic management. Strategic Management Journal, 18(7), 509–533. https://doi.org/10.1002/(SICI)1097-0266(199708)18:7

YOUSFI, K., CERT, R., GARCÍA, J. M., RAMOS, P., & MARZOUK, B. (2020). Influence of seasonal climate variability on olive oil composition. Food Chemistry, 310, 125803. https://doi.org/10.1016/j.foodchem.2019.125803

ZAGO, L., SQUEO, G., BERTONCINI, E. I., DIFONZO, G., & CAPONIO, F. (2019). Chemical and sensory characterization of Brazilian virgin olive oils. Food Research International, 126, 108588. https://doi.org/10.1016/j.foodres.2019.108588

REALIZAÇÃO:

SEVEN
publications company

ACESSE NOSSO CATÁLOGO!

WWW.SEVENPUBLI.COM

CONECTANDO O **PESQUISADOR** E A **CIÊNCIA** EM UM SÓ CLIQUE.